Phase Separation Phenomenon and Morphological Characteristics of PMMA/PCL Double Wall Microspheres

By

Min Sun Kim (Rosa Kim)

B.S., Columbia University, 2017

Thesis

Submitted in partial fulfillment of the requirements for Degree of Master of Science in the Department of Molecular Pharmacology, Physiology and Biotechnology, and the Center of Biomedical Engineering at Brown University

PROVIDENCE, RHODE ISLAND
MAY 2019

AUTHORIZATION TO LEND AND REPRODUCE THE THESIS

As the sole author of this thesis, I authorize Brown University to lend it to other institutions or individuals for the purpose of scholarly research.

Date: _____ Signature: _____

Min Sun Kim, Author

I further authorize Brown University to reproduce this thesis by photocopying or other means, in total or in part, at the request of other institutions or individuals for the purpose of scholarly research.

Date: _____ Signature: _____

Min Sun Kim, Author

This thesis by Min Sun Kim (Rosa Kim) is accepted in its present form by the Department of Biomedical Engineering as satisfying the thesis requirements for the degree of Master of Science.

Date: _____ Signature: _____

Dr. Edith Mathiowitz, Advisor

Date: _____ Signature: _____

Dr. Marissa Gray, Reader

Date: _____ Signature: _____

Dr. Celinda Kofron, Reader

Approved by the Graduate Council

Date: _____ Signature: _____

Andrew G. Campbell, Ph.D., Dean of the Graduate School

VITA

Min Sun (Rosa) Kim
Providence, Rhode Island
min_sun_kim@brown.edu | (646) – 832 – 6114

Education

Brown University
Providence, Rhode Island
September 2017 – Current
Major: Biomedical Engineering

Columbia University
New York, New York
September 2012 – May 2017
Major: Biomedical Engineering

Research

Brown University | Dr. Edith Mathiowitz Lab
Providence, Rhode Island
September 2019 – Current

- Phase separation phenomenon and characterization of internal morphologies of PMMA/PCL double wall microspheres.
- This research involved utilizing solvent evaporation process, cryotomy, light microscope use, and evaluating the internal morphologies and/or the states of phase separations of different PMMA/PCL double wall microspheres formed in different concentrations and ratios

Columbia University | Dr. Edward Guo (Bone Bioengineering) Lab
New York, New York
March 2016 – May 2017

- Regulation of sclerostin, OPG, and RANKL on differently aged bones.
- Responsibilities related to immunohistochemistry and microtomy.

Asan Institute for Life Sciences, Asan Medical Center | Dr. Nayoung Kim Lab
Seoul, South Korea
June 2015 – October 2015

- Independent project on miRNAs and cardiac allograft vasculopathy (CAV).
- This research involved extensive use of HUVEC culture, RNA quantification, Taqman qPCR, SYBR qPCR, Reverse Transcriptase, transfection, and more.

- Poster presentation in International Conference of the Korean Society for Molecular and Cellular Biology (KSMCB) with the title “Identification of Specific miRNAs involved in Cardiac Allograft Vasulopathy”.
- Participation in animal research regarding liver ischemia reperfusion injury (LIRI) and skin graft.

Konkuk University | Dr. Yeonhee Noh Lab
Seoul, South Korea
January 2010 – August 2012

- Study on effects of diets with various nutritional composition on energy balance in 90% pancreatectomized rats.
- Assisted with measuring daily diet, weekly weight, checking fasting blood glucose level, weighing organs, photo analysis on tissues taken at autopsy, western blots, and more.

Acknowledgements

I would like to thank Professor Edith Mathiowitz for her encouragement and guidance towards this research during my studies at Brown. She has guided and encouraged me on conducting this research with positive feedbacks and enthusiasms. She consistently showed enthusiasm towards my works, both in my research and my courseworks, encouraged me and provided a very educating environment. As a member of the Mathiowitz Lab, I have been able to develop confidence in studying polymer chemistry and to interact with a supportive and intelligent team.

I am grateful to all Mathiowitz Lab members, who willingly helped me throughout my academic years at Brown. I will miss working with all of them, who made my time a rewarding experience: Aharon Azagury, Stacia Furtado, Kosta Milovanovis, Cameron Baptista, Travis Nguyen, and Shiffoni Sukhlal. I could not have more enjoyed my time in lab without them.

Finally, I would like to thank my parents, Jung Ho Kim and Eun Jin Park, and my brother, Sung Hoon Kim, for their unconditional love and support throughout my whole academic career. I truly could not have done without them.

Table of Contents

Lists of Figures

List of Tables

1. Abstract

The main goal of this project is to examine the morphological characteristics on PMMA/PCL film casts and double walled microspheres formed in different ratios and concentrations. Double-walled microspheres are developed with two distinct layers of different polymers primarily to design a controlled drug delivery system utilizing a phenomenon called phase separation. There were many prior works done on formation of double wall microspheres with a wide range of different polymers and their drug encapsulation efficiency and release studies. Many of these investigations demonstrated that having an extra polymeric layer helps protect the encapsulated substances and allows controlled release and longer retention within the body. However, there had not been many studies on how different ratios of two polymers could influence the formation of double wall microspheres and specifically, their internal morphologies.

In the work presented here, PMMA/PCL double wall microspheres were formed using 1-step solvent evaporation process, which involves emulsification theory and phase separation phenomenon. In this thesis, how blends of different PMMA:PCL phase separate in the forms of film casts and microspheres would be addressed by investigating them with cross-polarized light, which helps distinguish the amorphous and the crystalline structures. Overall, depending on the polymer weight/volume concentrations (% w/v) and the ratios of the two polymers, internal morphologies of the film casts and the microspheres seem to differ. Yet, in all PMMA:PCL ratios, phase separation was observed in some degrees with PMMA:PCL = 1:1 microspheres exhibiting a few definite double walls. Understanding these morphological differences induced by different ratios of PMMA and PCL may be one of the key parameters in optimizing and forming efficient double wall microspheres to

carry drug, gene, and/or therapeutic molecules to the target site without degradation prior to reaching the target site.

2. Introduction

Effective delivery of therapeutic peptides/proteins or chemical drugs are rapidly being developed, but most administrations are oral and/or parenteral, which have poor stability or permeability in especially gastro-intestinal (GI) tract. [3, 5] Development of biocompatible and biodegradable polymeric microspheres/nanoparticles could overcome these limitations as they are known to improve sustained release and longer retention time. [5, 6] Specifically, double wall microspheres are important drug delivery carriers that could control and enhance the drug delivery. Currently, prevalent use of poly(D,L-lactic-co-glycolic acid) (PLGA) and poly(lactic acid) (PLA) which have been approved by the Food and Drug Administration (FDA) and the European Medicines Agency is largely because of the advantages of PLGA/PLA system for their biocompatibility, biodegradability, and controlled release of the encapsulated therapeutic agents. [6-8] In fact, PLGA/PLA particles were found to proficiently shield the drugs from immediate degradation. [32-34] And likely, double wall microspheres could be formulated to encapsulate drugs that have high solubility, shorter elimination half-life and low therapeutic efficacy for additional protection from degradation and for sustained release.

There have also been some researches on the use of poly(methyl methacrylate) (PMMA) microspheres in wide range of applications. PMMA is a non-biodegradable, amorphous polymer that is frequently used as bone cement. However, because of its non-biodegradability, there also could be bone weakening where the cement is placed since the cement would not allow space for new bones to grow. [9-12] Even so, PMMA

is still most widely used implant carrier for local sustained delivery of antibiotics, anti-fungal drugs, anti-inflammatory drugs, chemotherapeutic agents, and osteo-inductive agents. [11, 20-23] On the other hand, poly-ϵ-caprolactone (PCL) is a biodegradable, nontoxic and cheap crystalline polymer, but its degradation rate is slow due to its high degree of crystallinity and hydrophobicity. [13, 14-17] Depending on such properties as crystallinity, mechanical strengths, plasticity, and much more, all polymers have advantages and disadvantages in different biomedical applications and devices. To complement the abovementioned disadvantages of PMMA and PCL, Domingo et al. has analyzed *in vivo* behavior of micro-composites of PCL microdomains in PMMA matrix and discovered that PMMA/PCL micro-composites could be disintegrated into small enough fragments that could easily be cleared from the body. [13] Their experiments, to a great extent, confirmed the finding that blending PCL with other polymers generally improves the rate of biodegradation by allowing hydrophilicity without significantly affecting the mechanical integrity [13, 17, 18]. Although their PMMA/PCL blends were not in spherical forms, their *in vivo* behaviors validate the use of PMMA and PCL for double wall microspheres formation for this project. Despite the considerable amount of studies that approve the use of PMMA/PCL composites, there were not many analyses on the internal morphologies of PMMA/PCL microspheres, which might provide more insights to how the PMMA/PCL polymeric blends behave during phase separation, double wall microsphere formation and/or degradation.

Likewise, selecting appropriate materials for various biomedical applications depends on many properties and specifically, biocompatible and biodegradable polymers have been preferred materials of choice although they could be in complicated morphological structures with varying molecular composition, molecular

weight, and phase morphology. [24, 25] The polymers in biomedical applications and devices must not initiate any immune response, have appropriate mechanical properties for their intended use, be non-toxic to the body, and have appropriate permeability and processability. [26] These properties are significantly associated with structural morphology, so comprehensive understanding of morphology is essential in controlled use of polymers in biomedical applications. For this reason, it is of importance that this study mainly looks at the phase separation phenomenon and the internal morphological characteristics of PMMA/PCL double wall microspheres formed in different concentrations and ratios, which could evaluate the use of PMMA/PCL double wall microspheres as appropriate biomedical instruments.

2.1 Polymer Morphology

Polymer morphology refers to structural arrangement of the polymer chains and is largely classified into two types of polymers, amorphous and semi-crystalline. Amorphous polymers have randomly oriented isotropic structure and generally have glass transition temperature but no melting temperature. Semi-crystalline, on the other hand, have both regions of amorphous and crystalline structures with both glass transition temperature and a melting temperature. The crystalline regions of polymers are usually indicated with spherulites, which are polycrystalline structure composed of radially growing lamellar crystals connected by interlamellar amorphous phase (figure 1). [25] Throughout this study, the polarized light microscope is used to distinguish the amorphous and the crystalline regions as the darker areas represent more amorphous regions while the lighter, brighter spots represent more crystalline regions.

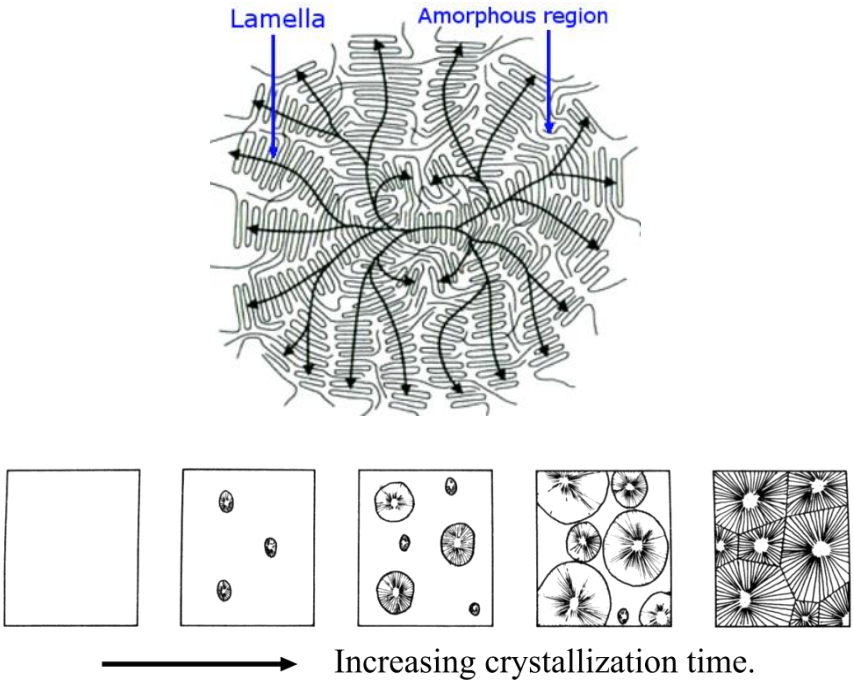

Figure 1. Schematic model of spherulite with black arrows indicating the direction of molecular alignment.[27]

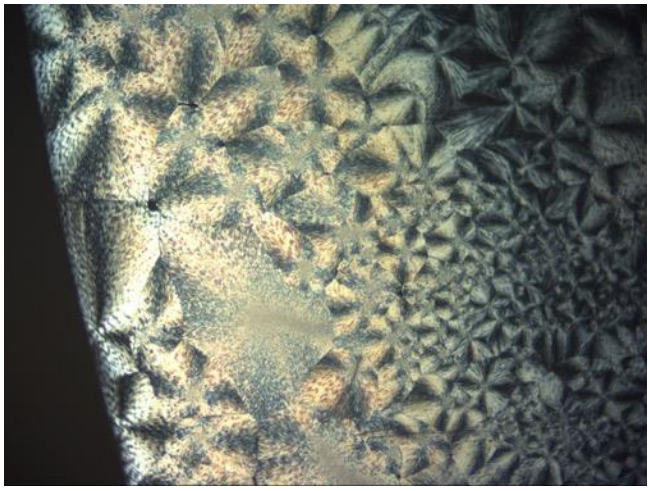
Figure 2. An example of spherulites formation.

The formation of spherulites, usually apparent in more crystalline polymers, is associated with crystallization of polymers and is dependent on various parameters; the number of nucleation sites, structure of polymer molecules, cooling rate and more.[27, 28] For instance, with rapid cooling rate, the spherulite molecules would not have sufficient time to orient themselves into ordered assembly, remaining in randomly aligned, disordered structures. Whereas, with slower cooling rate, some

polymer chains will take orderly configuration, aligning themselves in crystalline lamellae. And depending on the parameters, spherulites could be formed in various diameters ranging from micrometers to millimeters as spherulites grow in the direction of the crystalline lamella growth. Therefore, spherulites could result in higher density, hardness, and brittleness attributed to highly ordered crystalline lamellae and/or elasticity and impact resistance owing to the amorphous regions that connect the lamellae. Alignment of these polymer molecules to the lamellae could also result in birefringence producing a variety of colored patterns when spherulites are viewed with crossed polarizers in an optical microscope as shown in figure 2. [28] Birefringence could be explained by the anisotropic orientation of molecules in especially crystalline materials.

2.2 Phase Separation Phenomenon

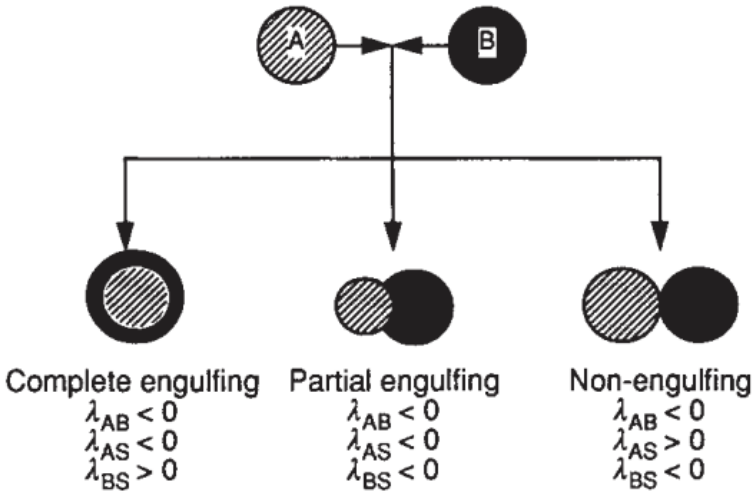

Figure 3. Three possible configurations for two-polymer system: complete engulfing, partial engulfing, and non-engulfing. The values of the three spreading coefficients (λ_{AB}, λ_{AS}, and λ_{BS}) for the system determine which configuration is most thermodynamically stable.[4]

Polymer blends could form either homogenous mixtures or experience a phenomenon called phase separations where two different phases are formed. By definition, phase separation phenomenon is the process during which a polymeric solution is separated into two immiscible liquids or two phases, and is frequently utilized to produce porous structures. [29-31] The technique used to create double wall microspheres in this project is called a solvent evaporation process, which involves this phase separation phenomenon and thus, understanding what and how phase separation works is very important. Phase separation phenomenon largely depends on a parameter called the spreading coefficient, which measures the tendency of one liquid phase to spread onto a second liquid phase. Depending on the spreading coefficients between two polymers and the solvent, the two polymers could configure themselves into three different configurations, complete engulfing, partial engulfing, and non-engulfing as shown in figure 3. [4] The most widely used model system is a solution composed by one or more polymers, a solvent and an aqueous non-solvent. In this study, there will be two different polymers, PMMA and PCL, blended in different ratios, dissolved in dichloromethane (DCM), which will be dispensed into the stirring aqueous solution of 1% PVA (figure 4). Another factor in polymeric microspheres configurations is evaporation rate and time. Assuming sufficient amount of time is provided before the microspheres precipitate, the two polymers will be able to phase separate completely during solvent evaporation process, which will be discussed later. By manipulating the evaporation rate of the solvent, DCM, amount of time for sufficient phase separation could be controlled.

$$\Delta G^{o} = \Delta H^{o} - T\Delta S^{o}$$

Equation1. Gibbs Free Energy

Whether two polymers are mutually miscible or immiscible also depends on the composition and the shape of Gibbs free energy curve (G). Gibbs free energy which depends on enthalpy, entropy, and temperature, is an important function in the study of phases ($\Delta G^o = \Delta H^o - T\Delta S^o$). Gibbs free energy of an enclosed system is defined as the energy available to do work and the reaction will be spontaneous when $\Delta G^o < 0$ and non-spontaneous when $\Delta G^o > 0$. Generally, polymeric mixtures are miscible when the free energy of mixing is negative ($\Delta G^o_{mix} < 0$) and immiscible when $\Delta G^o_{mix} > 0$. [29-31] Likewise, distinct phase separation behaviors depend on the shape of the Gibbs free energy curve and understanding how it affects the stability of the system needs to be well understood. [29-31] Temperature could also affect phase separation phenomenon because of the term $T\Delta S^o$ in calculating Gibbs free energy ($\Delta G^o = \Delta H^o - T\Delta S^o$). The higher the temperature, the lower the Gibbs free energy becomes, driving more miscibility of the polymers. By cooling, Gibbs free energy will be higher as $T\Delta S^o$ decreases, promoting phase separation phenomenon. Decreasing temperature also allows slower evaporation rate of DCM, which allows sufficient amount time for polymers to completely phase separate.

2.3 Solvent Evaporation

Microencapsulation by solvent evaporation technique is widely used in pharmaceutical industries and has received much attention due to enhanced effectiveness, bioavailability, and the dissolution rates. [25] It facilitates a controlled release of a drug, which has many clinical benefits. To construct viable PMMA/PCL double-walled polymeric microspheres, single-step solvent evaporation process developed in Mathiowitz Lab was used in this study. [4] Variations in weight/volume concentration (% w/v) of polymers in organic solvent, stirring rate, utilization of

homogenizer and more could result in a wide range of particle size and size distribution.

For single-step solvent evaporation, each polymer is dissolved in separate vials of 5mL of organic solvent, DCM, mixed together into 10mL of the two polymers and the organic solvent, which are then introduced into a stirring bath of 300mL of aqueous solution, 1% PVA (figure 4). As the 10mL solution of polymers and DCM are introduced into the stirring 300mL 1% PVA, emulsified droplets of PMMA, PCL, and DCM are immediately generated. As DCM evaporates from the droplets, the polymeric concentration within the droplets increases to the point where the two polymers become immiscible and begin to phase separate. Then, after 24 hours of stirring, final microspheres are collected, washed and lyophilized, during which extra liquid remaining in the polymeric microspheres are evaporated and solid polymeric spheres are formed. For internal morphologies, the lyophilized microspheres will be embedded in the embedding material called OCT, be frozen, and cryo-sectioned in thin slices to be observed with cross-polarized light.

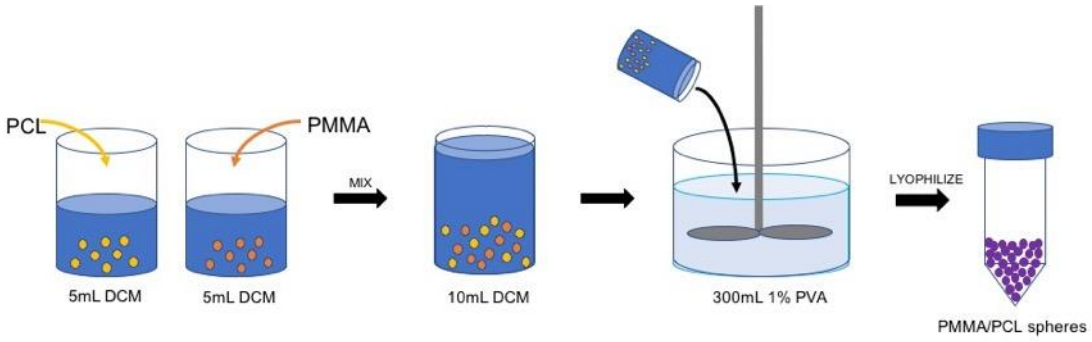

Figure 4. Schematic of Solvent Evaporation Process

3. Specific Aims

While there was some prior work with double wall microsphere formation and their encapsulation efficiency, there is currently insufficient data in literature characterizing different morphological structures of double wall microspheres formed with PMMA and PCL, which could enhance a controlled drug delivery. Having an extra polymeric layer in double wall microspheres seems to serve as a protective layer and allows longer retention within the body. [1,2] So the research presented here seeks to characterize the structural nature of the internal and surface morphology of PMMA-PCL film cast and double wall microspheres. This document provides an experimental study that examines the morphological behaviors of different rations of PMMA and PCL blends, investigated by observing both film casts and polymeric microspheres made up from the same blends.

Aim 1: Examine morphological characteristics of PMMA/PCL film casts to investigate how different blends of PMMA/PCL phase separate.

Aim 2: Fabricate PMMA/PCL double wall microspheres formed in different ratios using 1-step solvent evaporation process and determine the states of phase separation and their internal morphologies. The ratios between amorphous PMMA and crystalline PCL examined throughout this study are 1:9, 3:7, 1:1, 7:3, and 9:1 and the polymeric concentrations are 5% w/v and 20% w/v.

From this research, we could learn how blends of different PMMA:PCL phase separate in the forms of film casts and how different polymer concentrations and PMMA:PCL ratios determine the state of phase separation in the forms of microspheres. Especially, the questions to be answered from specific aim 2 are (1) if

any of the PMMA/PCL ratios formulate into double wall microspheres and (2) how internal structures of the microspheres differ by the varying ratios. These questions would be addressed as the phase separation features on the PMMA/PCL film casts and microspheres are investigated with cross-polarized light, which helps distinguish the amorphous and the crystalline structures.

4. Materials & Methods

4.1 Materials

Poly (methyl methacrylate) **(**PMMA), (M.W. 35 kDa) (Acros)

Polycaprolactone (PCL) (M.W. 50 kDa) (Durect Lactel)

Dichloromethane (DCM) (Fischer Chemical)

2% Polyvinyl alcohol (PVA)

Milli-Q H_2O

Optimal Cutting Temperature embedding compound (OCT)

Glass Slides

Polarized light microscope

Heidolph^{TM} overhead stirrer

4.2 Methods

The ratios between amorphous PMMA and crystalline PCL examined throughout this study are 1:9, 3:7, 1:1, 7:3, and 9:1 and the polymeric concentrations are 5% w/v and 20% w/v. These different ratios and concentrations were studied in the forms of film casts and microspheres.

4.2.1 Film cast of 20% w/v PMMA/PCL blends

Concentration of PMMA or PCL (w/v%)	PMMA (g) in 5mL DCM	PCL (g) in 5mL DCM
10	0.5 g	0.5 g
20	1.0 g	1.0 g
30	1.5 g	1.5 g
40	2.0 g	2.0 g
50	2.5 g	2.5 g

Table 1. Amount of PMMA, PCL added to 5mL DCM for 10~50% w/v concentration

Ratio of PMMA:PCL	PMMA (g) in 5mL DCM	PCL (g) in 5mL DCM
9:1	1.8 g	0.2 g
7:3	1.4 g	0.6 g
1:1	1.0 g	1.0 g
3:7	0.6 g	1.4 g
1:9	0.2 g	1.8 g

Table 2. Amount of PMMA and PCL added to total 10mL of DCM for 20% w/v concentration

In order to identify the morphological differences or phases between PMMA and PCL, morphologies of pure PMMA and pure PCL needed to be characterized first. In order to distinguish the amorphous PMMA and the crystalline PCL, 10 ~50% w/v pure PMMA and 10~50% w/v pure PCL were prepared in separate vials of 5mL DCM (table 1). Each solution was film casted onto ten separate petri dishes and examined with cross polarized light microscope in order to identify the different phases.

Then, to examine how film casts in different PMMA:PCL ratios phase separate, different amounts of PMMA and PCL were first dissolved in separate vials of 5mL DCM as shown in table 2. After 24 hours of dissolution, PMMA and PCL

were mixed and casted onto flat petri dishes for further examination with cross-polarized light.

4.2.2. Fabrication of double wall PMMA/PCL microspheres

4.2.2.1. Solvent evaporation for 20% w/v and 5% w/v PMMA/PCL microspheres

Microspheres were fabricated using a process called solvent evaporation (figure 4) and were formed in different polymeric concentrations (20% w/v and 5% w/v) and in different ratios.

As shown in table 2, different amounts of PMMA and PCL were dissolved separately in two glass vials with 5 mL of DCM. After PMMA and PCL were dissolved, they were mixed into one vial comprised of 10 mL DCM, PMMA, and PCL. Then, the combined polymeric solutions were dripped into a bath of 300mL 1% poly(vinyl alcohol) (PVA) stirred at approximately 1,300 rpm. 1% PVA acts an aqueous solution and/or surfactant for the emulsion during solvent evaporation process. The mechanism behind solvent evaporation is as organic solvent, DCM, evaporates, the polymer solution concentration increases to the point where the polymers are no longer soluble and began to separate (figure 4). The different amounts of polymers used for different PMMA/PCL ratios and polymer concentrations were as listed in table 2 for 20% w/v PMMA/PCL microspheres.

After the combined mixtures of PMMA/PCL were slowly poured into the beaker of stirring 1% PVA and stirred for at least 24 hours, the stirred solution was removed from the beaker into the centrifuging tube. For washing the microspheres, the solution was centrifuged under a preset condition, SLA-3000, which runs for 5 min at approximately 6,000~6,500 RPM. However, the rpm was increased to 8,000~9,000 rpm so that the microspheres were collected at the bottom more efficiently. Centrifugation

was performed three times and after each centrifugation, the supernatant was removed and filled with milliQ water for the consequent wash. The remaining supernatant should ideally be under 5 mL and be lyophilized for at least 24 hours. Once the microspheres were hardened after lyophilization, they were collected and stored for examination.

Ratio of PMMA:PCL	PMMA (g) in 5mL DCM	PCL (g) in 5mL DCM
9:1	0.45 g	0.05 g
7:3	0.35 g	0.15 g
1:1	0.25 g	0.25 g
3:7	0.15 g	0.35 g
1:9	0.05 g	0.45 g

Table 3. Amount of PMMA and PCL added to total 10mL of DCM for 5% w/v concentration

For 5% w/v PMMA/PCL microspheres, same procedure as mentioned above were performed with different amounts of PMMA and PCL as shown in table 3.

4.2.2.2. Solvent evaporation for 5% w/v PMMA/PCL with homogenizer

A few problems from previous formation method were the large variability in particle sizes and the diameters of some spheres that were measured to be larger than 100 um. Initial plan was to achieve PMMA/PCL spheres in the nanoscale since nanoparticles are more preferable especially as drug carriers for their high stability, high carrier capacity, improved bioavailability, feasibility of incorporating both hydrophilic and hydrophobic substances, and feasibility of diverse routes of administration. [49]

To solve this issue, physical methods including homogenization and sonication could be used, which allows faster stirring rate and homogenously sized particles. Homogenizer is an instrumentation shaped as a rod of equally sized holes,

through which the polymeric solution would first break up to small particle size before solidification occurs (figure 25). Therefore, homogenizer was used in the process of solvent evaporation at an rpm of 5,000 for 15 minutes. Depending on the molecular weights and the ratios of the PMMA/PCL blend, if homogenization is operated for long, the polymers could rupture even before precipitation, thereby not yielding microspheres. The PMMA/PCL solutions were prepared just as they were prepared for 20% w/v and 5% w/v film casts and microspheres created solely with the overhead stirrer (4.2.1. and 4.2.2.1.). Instead of the overhead stirrer, homogenizer was operated for 15 minutes in the aqueous solution to which solutions of DCM, PMMA, and PCL were introduced. After 15 minutes, the remaining solution will be stirred at a slower rate without the homogenizer for further DCM evaporation. However, these 5% w/v microspheres created with homogenizer have not yet been cryo-sectioned for further assessment.

4.2.3 Morphological Characterization with Polarized Light Microscopy

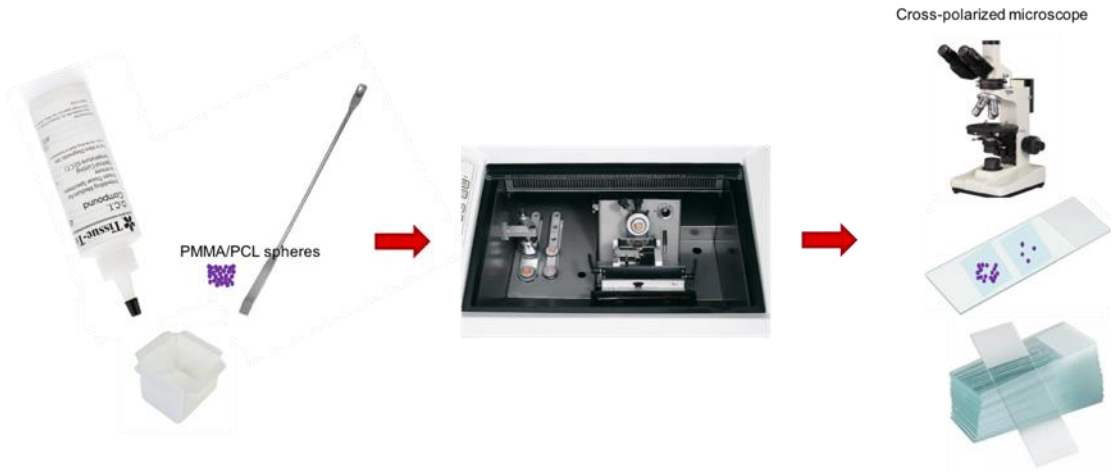

Figure 5. Schematic of microsphere embedding preparation for cryo-sections

In order to characterize the internal layers of the double wall microspheres, the microspheres were embedded in cryo-mold with OCT embedding material and were

frozen. Then, the embedded microspheres were sectioned by the cryotome in 16 – 20 um and placed onto the glass slides. The microspheres on the slides were examined by optical microscopy (with or without cross-polarized light) in order to distinguish the areas of the amorphous and the crystalline as amorphous regions are presented darker and crystalline regions are presented brighter, often with spherulite formations.

5. Results and Discussion

5.1. Film Casts Morphology

5.1.1. Film casts of PCL and PMMA

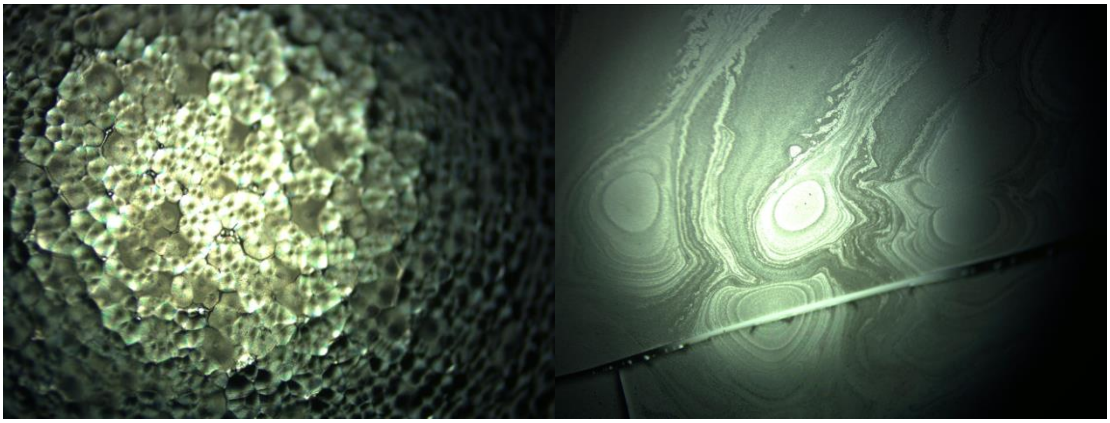

Figure 6**.** Film cast of (left) PCL and (right) PMMA. Un-defined magnification and concentration. Without cross-polarized light.

The main difference between semi-crystalline and amorphous polymers is depicted in figure 6. The left micrograph in figure 6 shows a film cast of pure PCL, semi-crystalline polymer with distinct ordered structures called spherulites that are bright and tends to reflect the light. Spherulites are composite structure made of both the crystalline and amorphous regions in which the crystalline regions are arranged in an essential radial fashion. On the other hand, amorphous polymers are shown to be more transparent without definite orders (right, figure 6) and with cross-polarized light, they would simply be dark regions, undistinguishable from the background.

Most importantly, although there were mostly crystalline spherulites present, there were still dark, rounds regions in the middle of the spherulites, indicating relatively amorphous regions. This implies that even in one type of polymer, there are some degree of phase separation exhibiting both crystalline and amorphous structures.

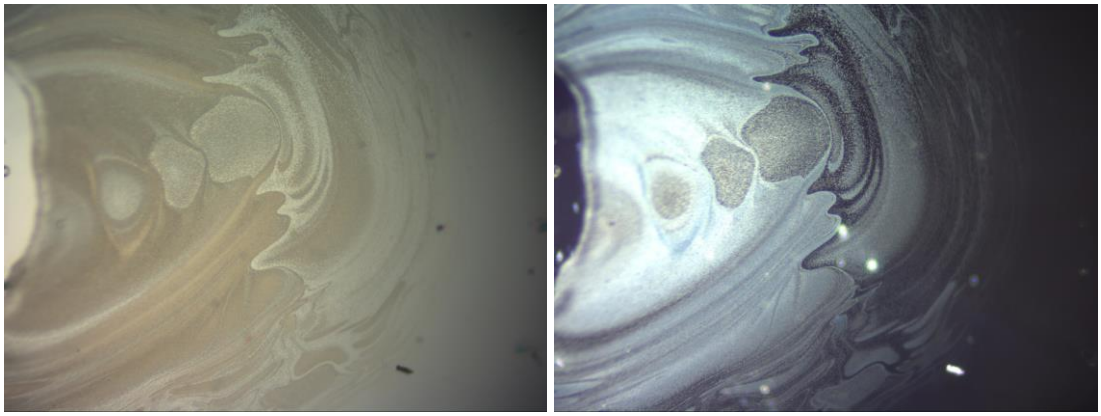

Figure 7. Film casts of 20% w/v PMMA at 10x magnification (left) without polarized light and (right) with polarized light

Similarly, there were phase separation occurring in film casts of pure amorphous polymer, PMMA as shown in figure 7. Figure 7 compares the amorphous states of PMMA without and with polarized light. Similar to the representation of darker amorphous spots present in pure crystalline PCL film (figure 6), there were both the lighter regions indicative of the relatively crystalline states and the darker regions indicative of the amorphous states, clearly distinguished as shown on the right micrograph in figure 7. These different regions demonstrate phases within amorphous polymer yet in different polymer concentration in each phase.

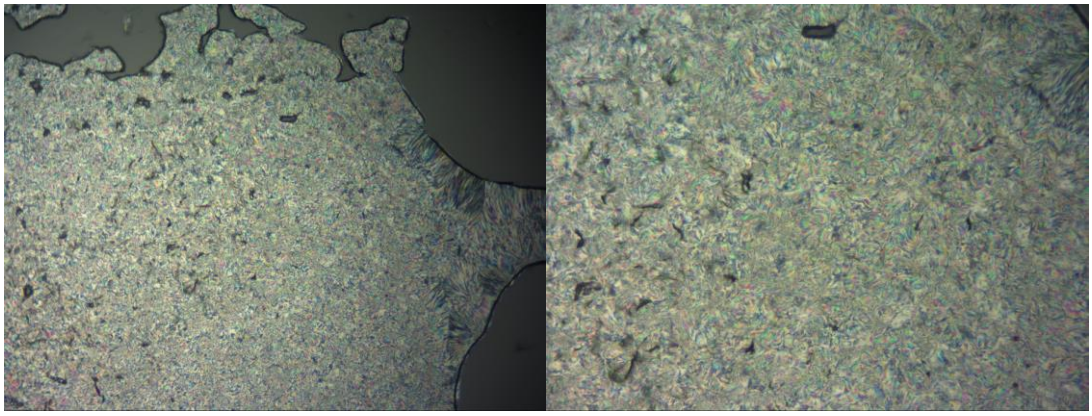

Figure 8. Film Casts of 50% w/v PCL at (left)10x and (right)20x magnification without polarized light

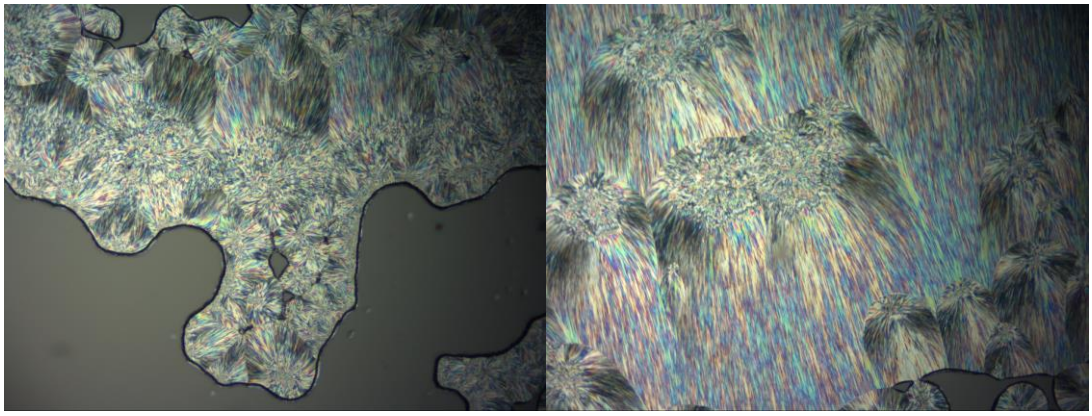

Figure 9. Film Casts of 50% w/v PCL at (left)10x and (right)20x magnification without polarized light

Figure 8 and 9 show clearer representations of spherulites formation in 50% w/v PCL film cast. Their formation is associated with crystallization of polymers and is controlled by numerous parameters including nucleation sites, structure of polymer molecules, cooling rate, viscosity, and more. Specifically, viscosity is known to control the crystallization and the rotation of crystal orientation, encouraging spherulite growth. [50] Likewise, with extremely high polymeric PCL concentration (50% w/v PCL), the viscosity must equally be high, affecting the band spacing of birefringence and forming larger spherulites. Birefringence, frequently exhibited on anisotropic crystals, produces colored patterns as distinctively shown in figure 9.

5.1.2. Film Casts of 20% w/v PMMA:PCL = 1:9

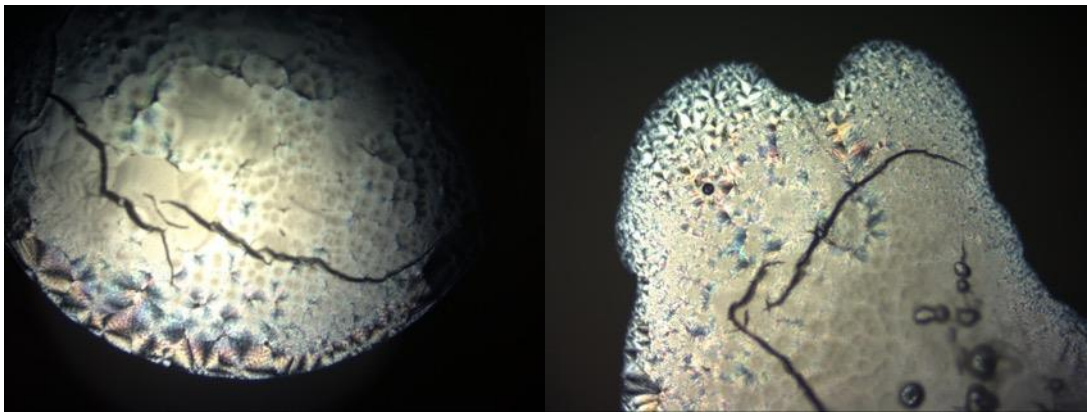

Figure 10. Film Casts of 20% w/v PMMA:PCL = 1:9 at 4x magnification with polarized light

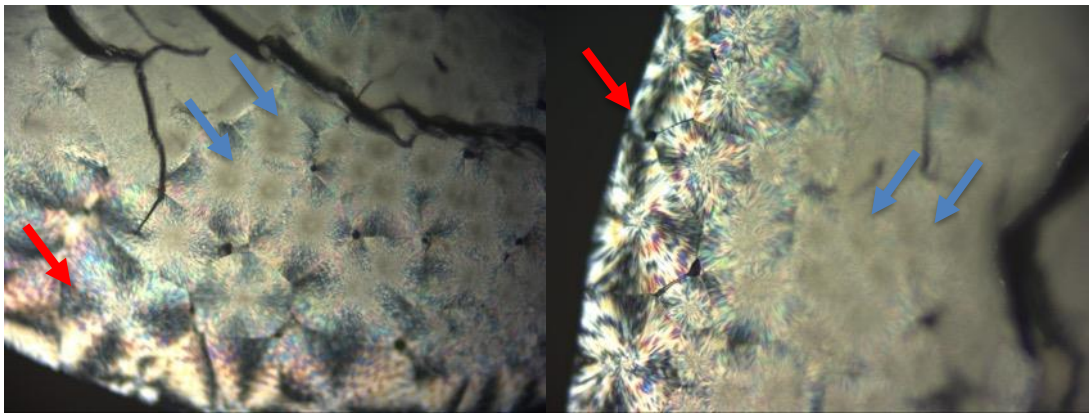

Figure 11. Film Casts of 20% w/v PMMA:PCL = 1:9 at 20x magnification with polarized light

Figure 10 and 11 depict film casts of 20% w/v PMMA:PCL = 1:9. One characteristic to notice is that the higher concentration of PCL allowed the formation of spherulites, which are known to be highly crystalline feature, especially around the edges of the film casts (red arrows, figure 11). The spherulites were evidently surrounding the amorphous regions that seemed to be entrapped more in the middle of the film casts, possibly indicating that the lower concentration of amorphous PMMA could not prevent the crystallization of PCL in higher concentration. However, although the concentration of amorphous PMMA was much lower and was not

exhibited as prevalently as the crystalline structures, there were still presentations of PMMA structures (blue arrow, figure 11).

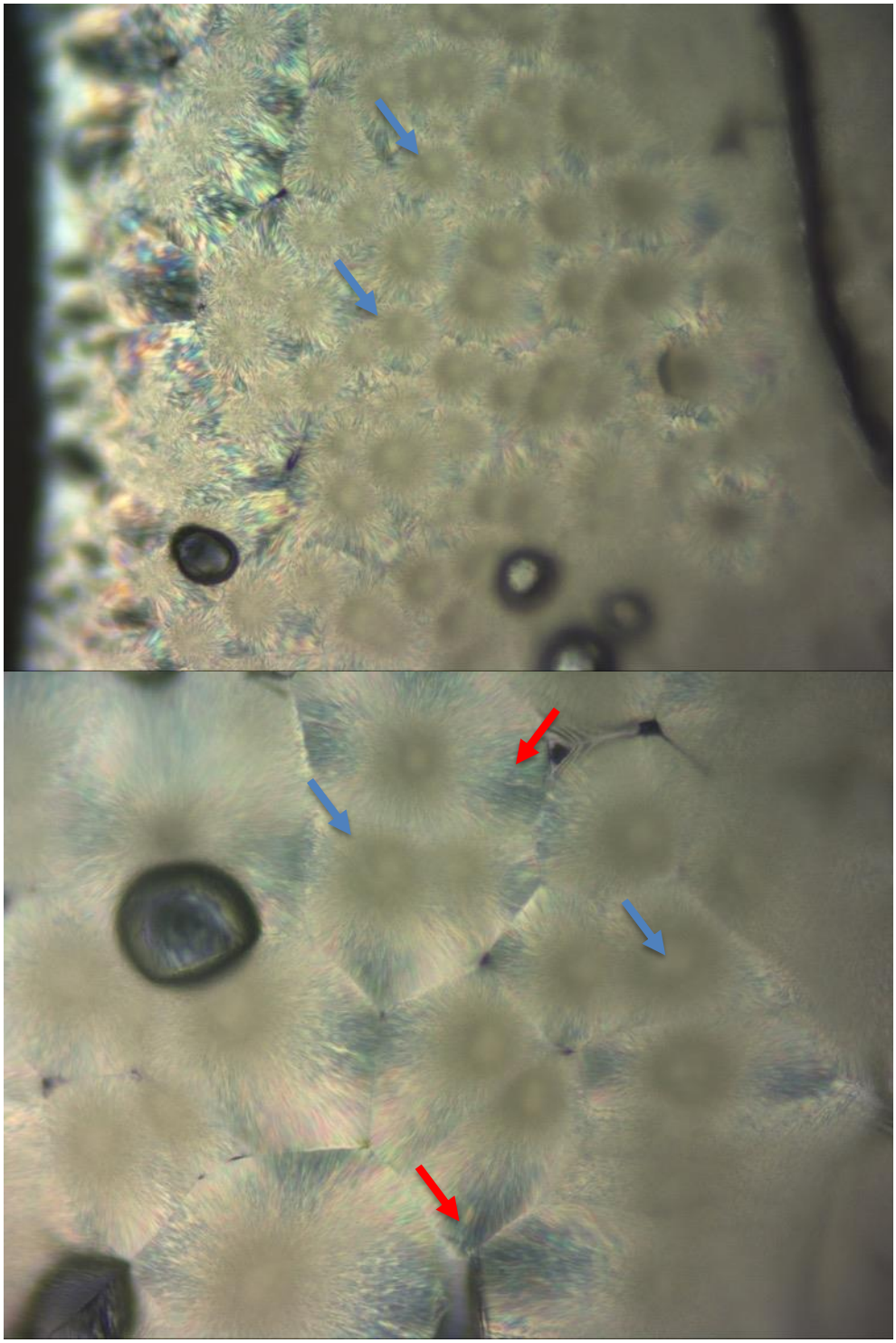

Figure 12. Film Casts of 20% w/v PMMA:PCL = 1:9 at (top) 20x magnification and (bottom) 40x with polarized light

Figure 12 shows the existence of darker round spots in the middle of the spherulites as indicated by the blue arrows. They are assumed to be PMMA polymers that may be interfering with the crystallization of PCL, but spherulites were formed despite the PMMA interference as proven by the radial growth of PCL indicated by the red arrows. Although they were faintly represented, PMMA structures were clearly trying to interfere with the formation of spherulites. Yet, the higher PCL concentration successfully crystallized into higher order structure of crystalline polymer, or the spherulites.

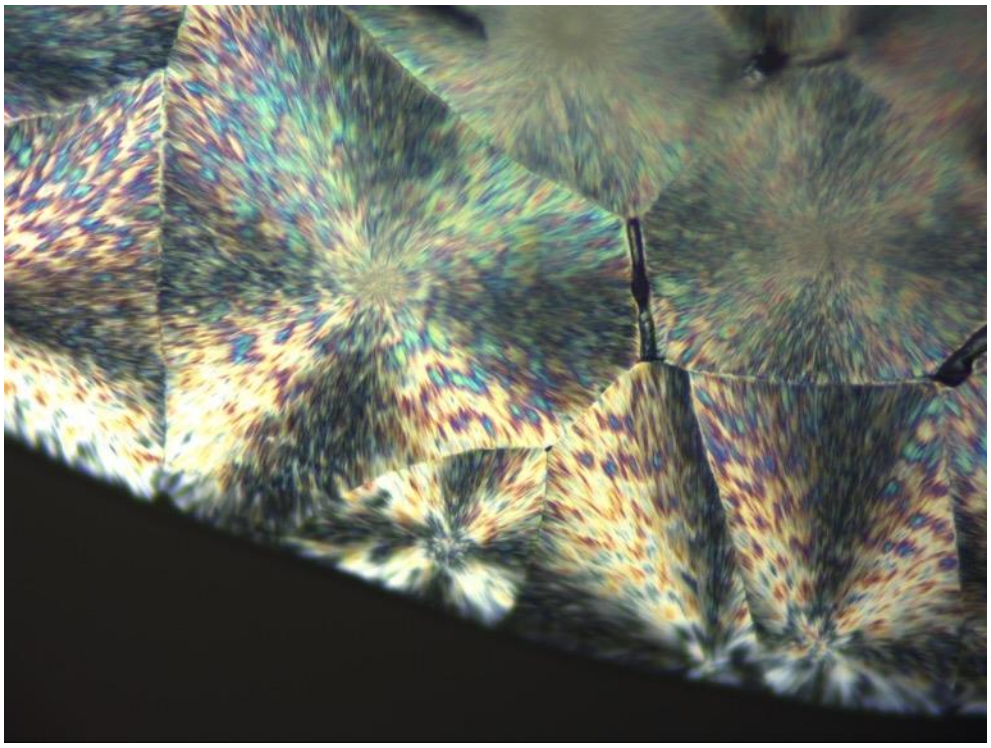

Figure 13. Film Casts of 20% w/v PMMA:PCL = 1:9 at 40x magnification with polarized light

On the other hand, the PCL regions that were not interfered by PMMA shows clear, distinct spherulites. Figure 13 is polarized image of the edges of the 20% w/v PMMA:PCL = 1:9 film cast. Along with the well-defined spherulites formation, color-patterned birefringence, which is also a highly crystalline characteristic, was distinctively exhibited due to higher ratio of crystalline PCL. The presentation of

these apparent spherulites and birefringence supports that PMMA could not overcome crystallization of PCL.

5.1.3. Film casts of 20% w/v PMMA:PCL = 3:7

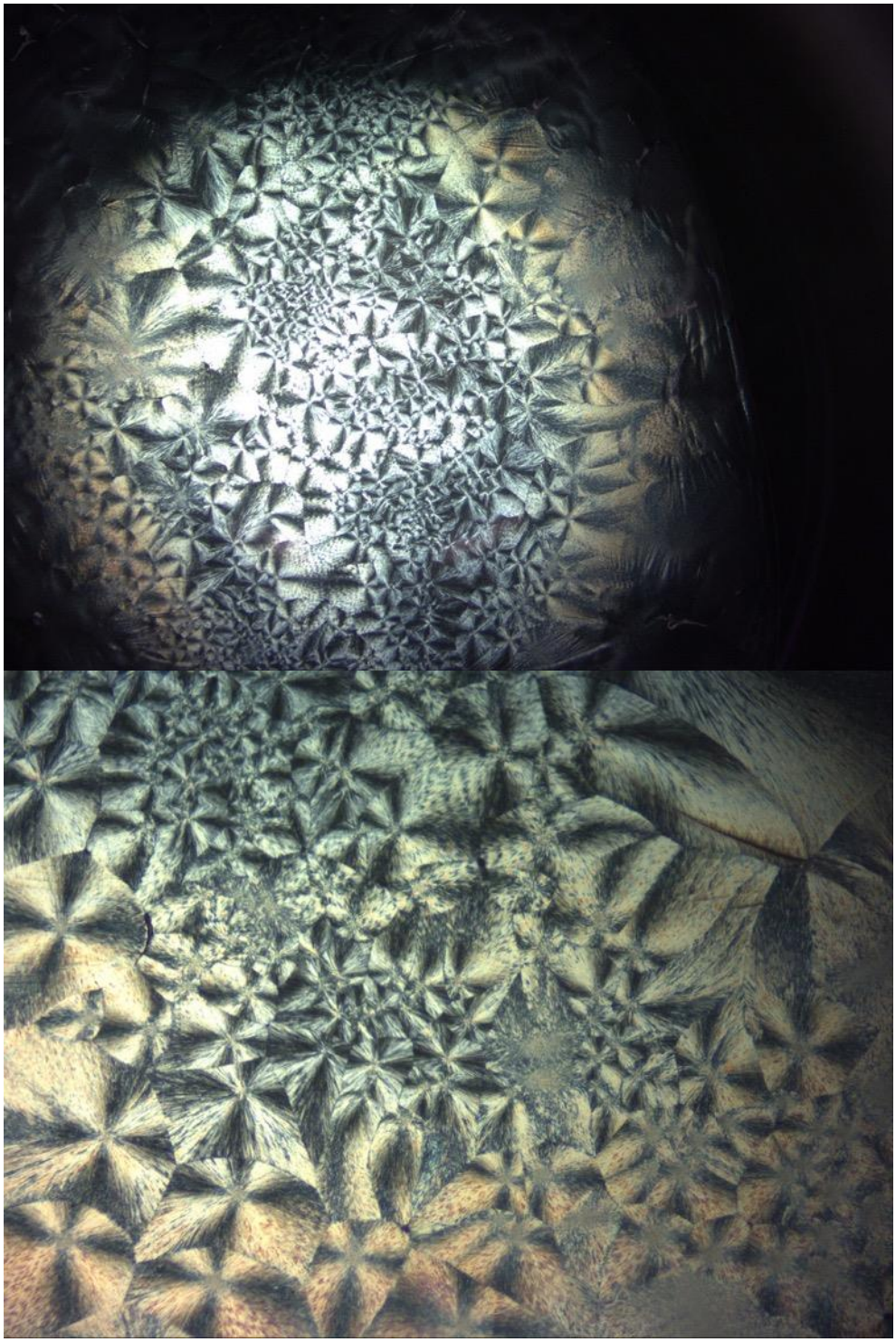

Figure 14. Film Casts of 20% w/v PMMA:PCL = 3:7 at (top) 4x and (bottom) 10x with polarized light

The blend of PMMA and PCL in 3:7 ratio has shown the most homogenous patterns as the film casts (figure 14). The surface of the 20% w/v PMMA:PCL = 3:7 film cast was abundant with spherulites. The size distribution of the spherulites may not be homogenous but the spherulite patterns or shapes were identical and clear as shown by the distinguishable structures of each spherulite. This predominant presentation of spherulites, which is known as the most common highly ordered structure of crystalline polymers, implies that the polymeric solution in the ratio of 3:7 PMMA to PCL is highly crystalline.

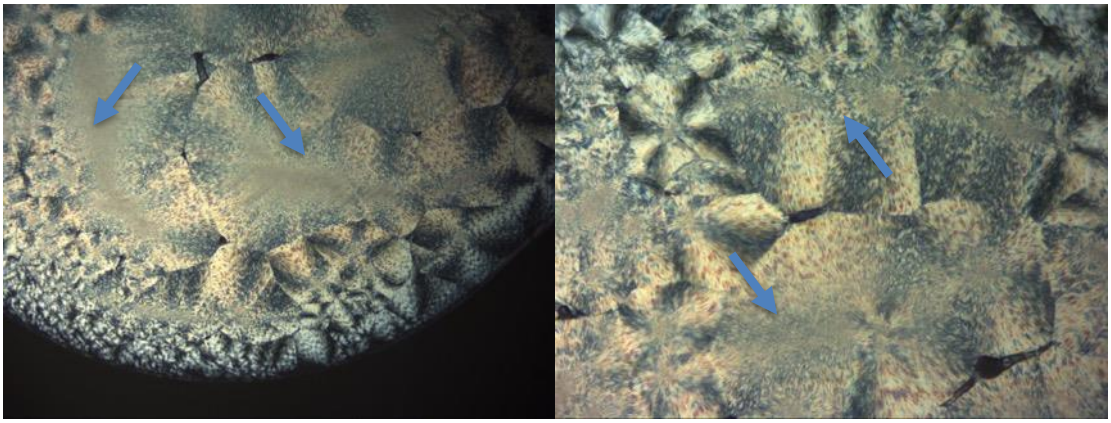

Figure 15. Film Casts of 20% w/v PMMA:PCL = 3:7 at (left)10x and (right) 20x with polarized light

However, there were still signs of amorphous polymer presenting on the film cast as shown by the arrows in figure 15. The arrows pointing to the fainted, darker areas among the apparent spherulites, indicate the possibility of amorphous PMMA trying to interfere with spherulite formations or crystallization of PCL. Nonetheless, it could be assumed that PMMA failed to interfere with PCL crystallization because spherulites were exhibited predominantly on the 20% w/v PMMA:PCL = 3:7 film cast. Additionally, the thickness across the film cast could not be uniform, which could influence the observation.

5.1.4. Film casts of 20% w/v PMMA:PCL = 1:1

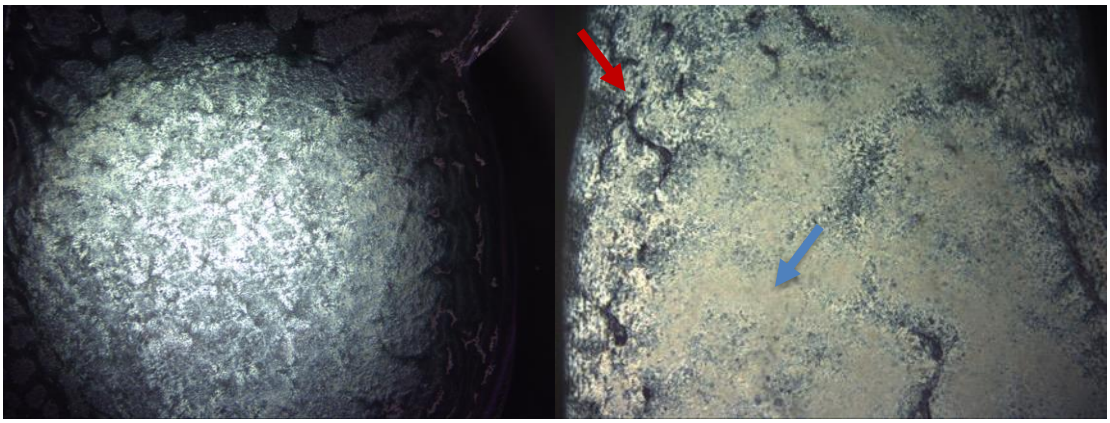

Figure 16. Two different film casts of 20% w/v PMMA:PCL = 1:1 at (left) 4x and (right) 10x magnification with polarized light

Figure 16 shows different film casts of 20% w/v PMMA:PCL = 1:1 at 4x and 10x magnification. For the first film cast (left, figure 16), homogenous distribution of amorphous PMMA and crystalline PCL could be observed as indicated by both dark and light regions. For another film cast of 20% w/v PMMA:PCL = 1:1, two different surface morphologies were observed (right, figure 16). The blue arrow on the micrograph taken at 10x indicates the seemingly smoother and flat surfaces with relatively uniform color whereas the red arrow points to rougher and patch-patterned surfaces that seemed to display both the amorphous and the crystalline structures (right, figure 16). How films are casted onto flat surfaces usually cannot be controlled by manpower and such different film casts of the same polymeric concentration and ratio could be resulted because thickness across the film cast could vary, affecting the rate of evaporation. If some part of the film cast is thicker than the other region, the evaporation rate of the thicker region would be slower, possibly influencing the presence of different surface morphologies.

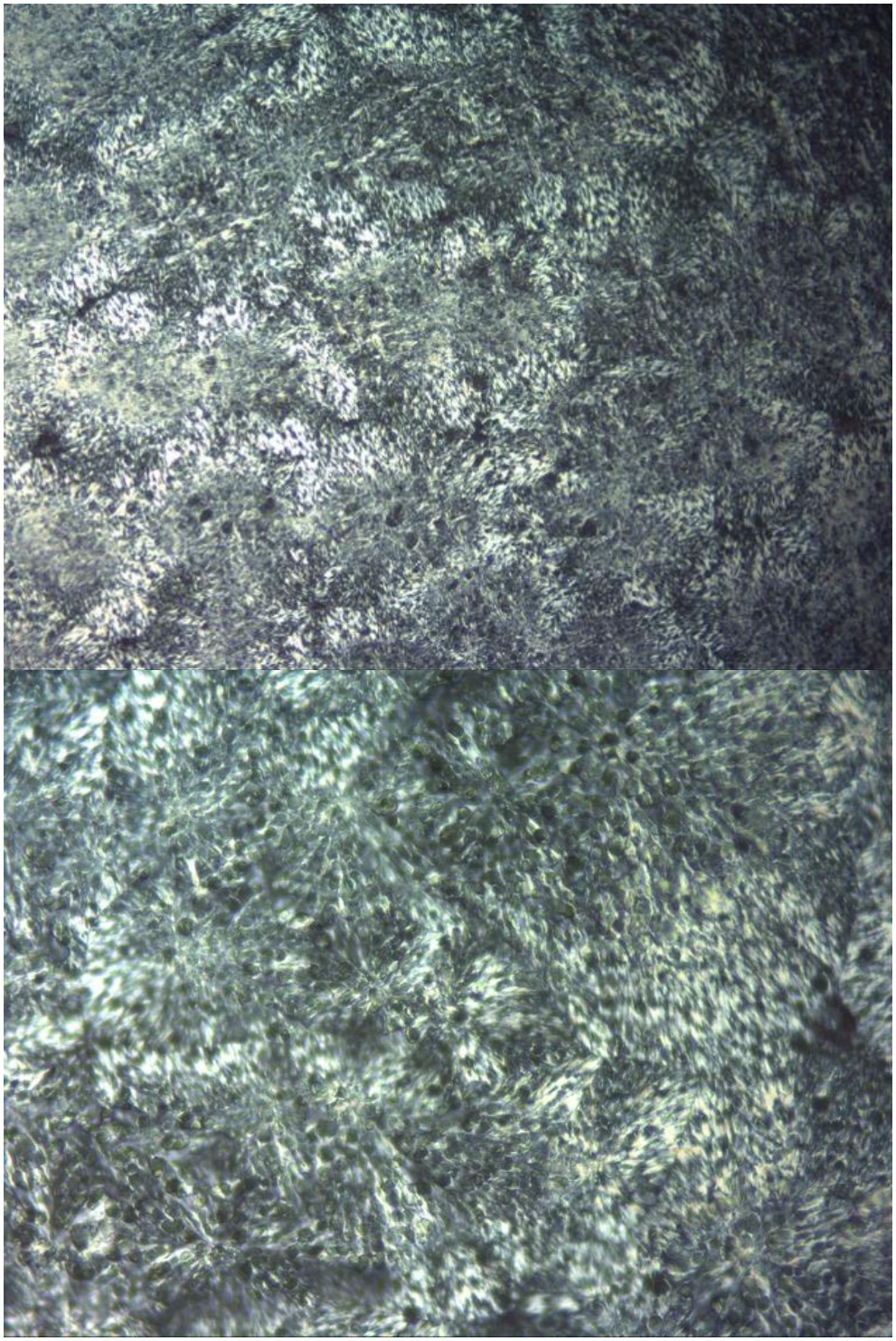

Figure 17. Film Casts of 20% w/v PMMA:PCL = 1:1 at (top) 20x and (bottom) 40x magnification with polarized light

The film cast that showed homogenous distribution of amorphous PMMA and crystalline PCL (left, figure 16) was examined at a much higher magnification, 40x (bottom, figure 17). Unlike 20% w/v PMMA:PCL = 3:7 film casts, there were no

distinguishable structures like the homogenous distribution of spherulites (Figure 14, 15). However, there was still equal distribution of PMMA and PCL observed. The lighter and brighter regions are assumed to be PCL crystalline structures that seemed to radially grow out and crystallize into spherulites. Also present on 20% w/v PMMA:PCL = 1:1 film casts were the darker and round spots, which are assumed to be amorphous PMMA, possibly interfering with PCL crystalline radial growth.

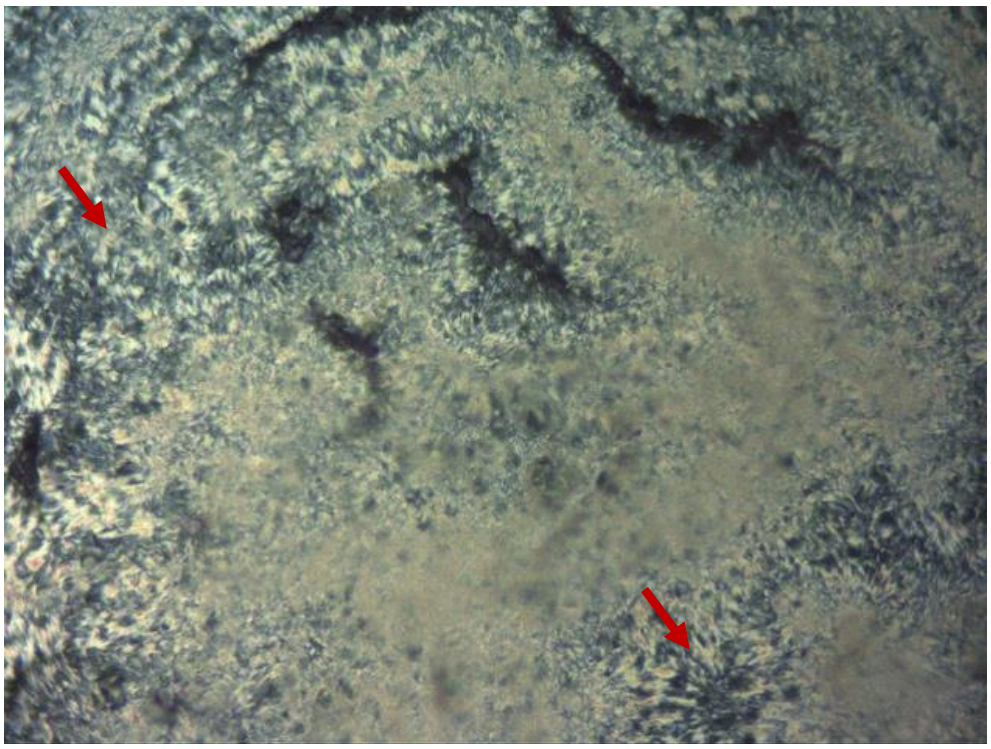

Figure 18. Film Casts of 20% w/v PMMA:PCL = 1:1 at 20x magnification with polarized light

The film cast with two different surface characteristics (right, figure 16) was also examined at higher magnification, 20x. Because the thickness varied across this film cast, it was much difficult to obtain clear image of the film cast at 40x magnification. Even at 20x magnification, especially, around the edges, there were some regions where PMMA and PCL seem to be homogeneously distributed. The red arrows in figure 18 indicates the areas where there were homogenous distributions of

PMMA and PCL and where PCL was trying to crystallize and radially grow while the PMMA dots were interfering PCL crystallization.

In short, although the film casts could have different surface morphologies (figure 17, 18), they seemed to share similar structures containing equal portions of amorphous and crystalline areas. The different morphologies casted were presumably attributed to how the polymeric solutions were film casted, resulting in inconsistent thickness across the film casts.

5.1.5 Film casts of 20% w/v PMMA:PCL = 7:3

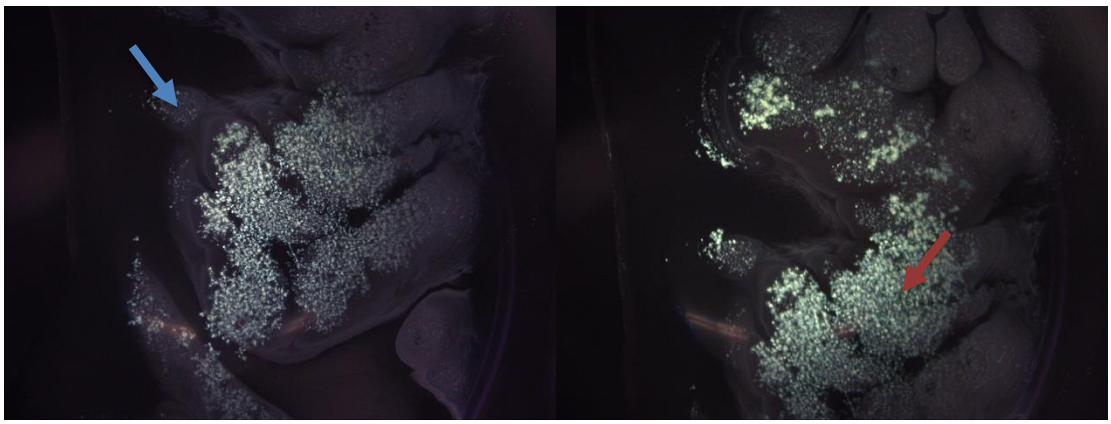

Figure 19. Film Casts of 20% w/v PMMA:PCL = 7:3 at 4x magnification with polarized light

For a film cast of 20% w/v PMMA:PCL = 7:3, crystalline structures were shown to be excessively grouped together with amorphous regions surrounding or encapsulating the brighter crystalline groups as shown in figure 19. The blue arrow indicates the relatively darker regions of predominantly amorphous PMMA, which seemed to be surrounding the groups of crystalline PCL structures indicated by the red arrow (figure 19). From this film cast, higher concentration of PMMA was more dominant in the process of phase separation and thus, able to engulf the smaller concentration of PCL.

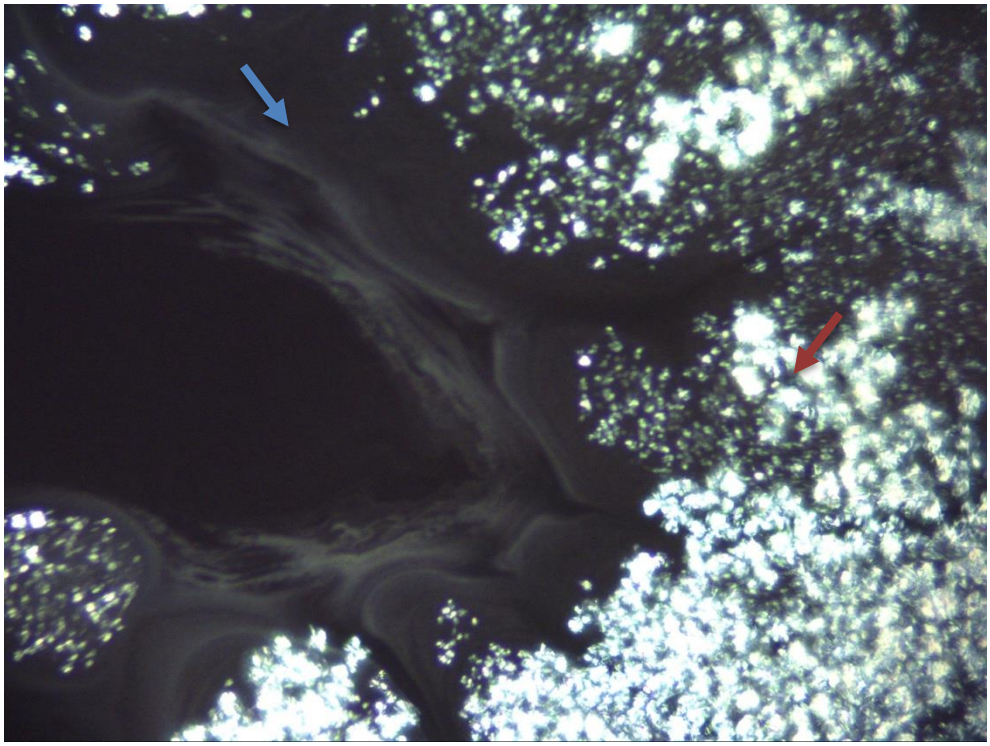

Figure 20. Film Casts of 20% w/v PMMA:PCL = 7:3 at 20x magnification with polarized light

At higher magnification of 20x, crystals accumulated within the PMMA (red arrow, figure 20) seemed much smaller than the crystals from the film casts of 20% w/v PMMA:PCL in the ratios of 1:9 and 3:7 (figure 10-15). Furthermore, as there were no definite spherulite formation, this observation potentially indicates that the higher concentration of amorphous PMMA may be interfering with crystallization of PCL.

5.1.5. Film casts of 20% w/v PMMA:PCL = 9:1

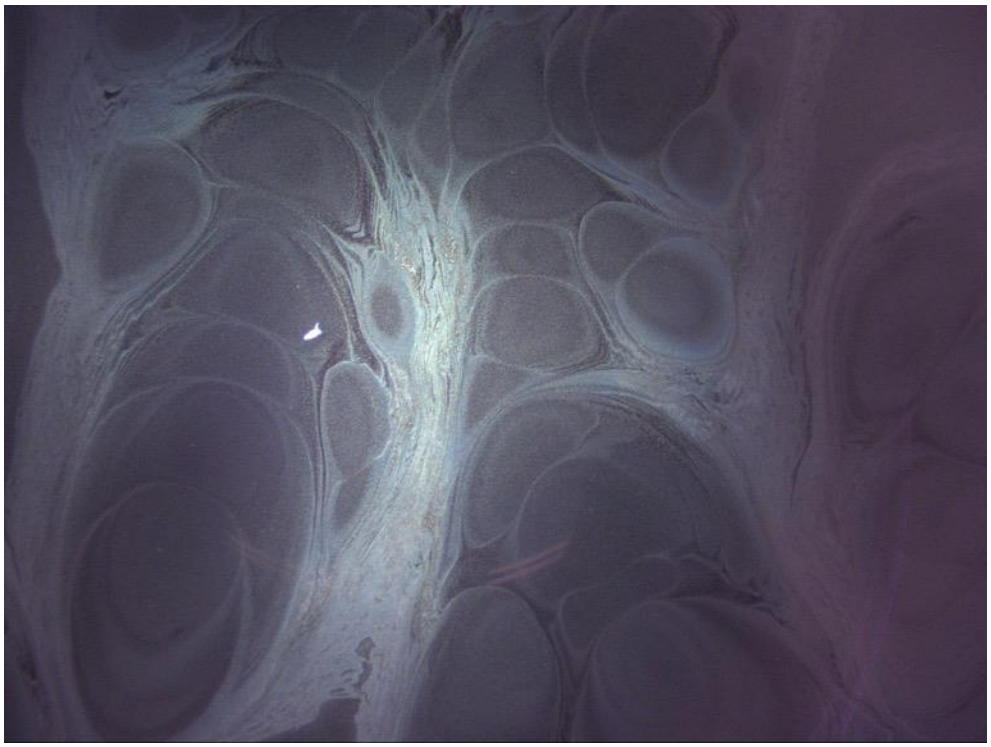

Figure 21. Film Casts of 20% w/v PMMA:PCL = 9:1 at 4x magnification with polarized light

From figure 21, the film cast of 20% w/v PMMA:PCL = 9:1 shows the different phase separation phenomenon and morphologies from 20% w/v PMMA:PCL = 1:9 film casts (figure 10-13) and completely opposite engulfing phenomenon from 20% w/v PMMA:PCL = 7:3 film casts (figure 19, 20). 20% w/v PMMA:PCL = 7:3 film casts shown in figure 19 and 20 showed the higher concentrated amorphous PMMA encapsulating or entrapping the lower concentrated crystalline PCL, as indicated by the bright crystals grouped together (red arrow, figure 20). In comparison, for 20% w/v PMMA:PCL = 9:1 film casts, the higher concentrated amorphous PMMA were presented in forms of large blobs, densely grouped together with lower concentrated crystalline PCL surrounding the PMMA groups. This morphology is assumed that the cast of PMMA was so predominant and

highly dense that the lower concentration of PCL failed to penetrate the assembly of large PMMA globules.

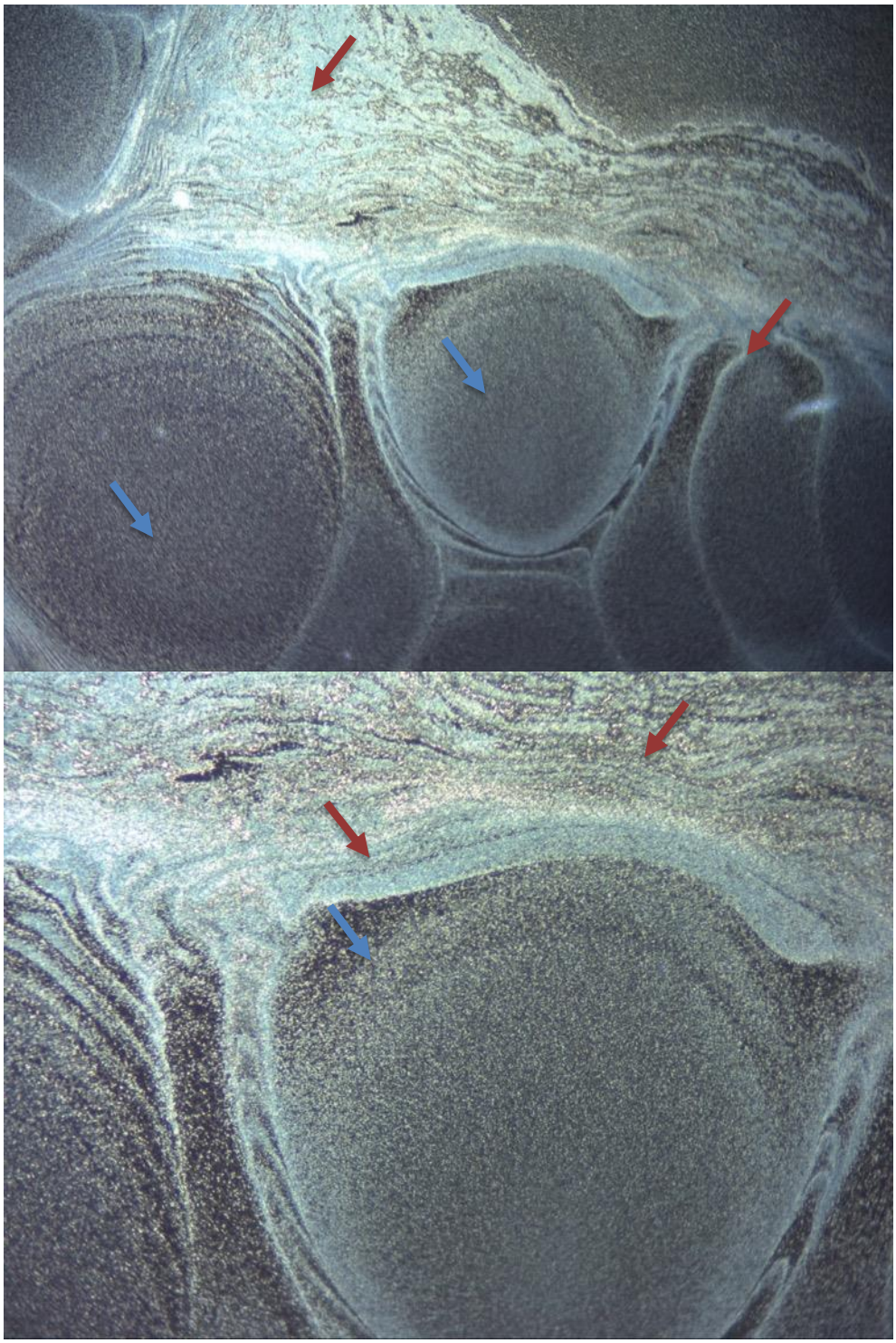

Figure 22. Film Casts of 20% w/v PMMA:PCL = 9:1 at (top) 20x and (bottom) 40x magnification with polarized light

When examined at higher magnification, darker and semi-circular amorphous regions indicated by blue arrows in figure 22 could be observed with brighter crystalline regions confining the perimeter in brighter PCL grains (red arrows, figure 22). From figure 22, the circular amorphous PMMA regions are assumed to be grouped strongly together (blue arrows) that the less concentrated crystalline PCL (red arrows) seems to be failing to enter these circular amorphous regions.

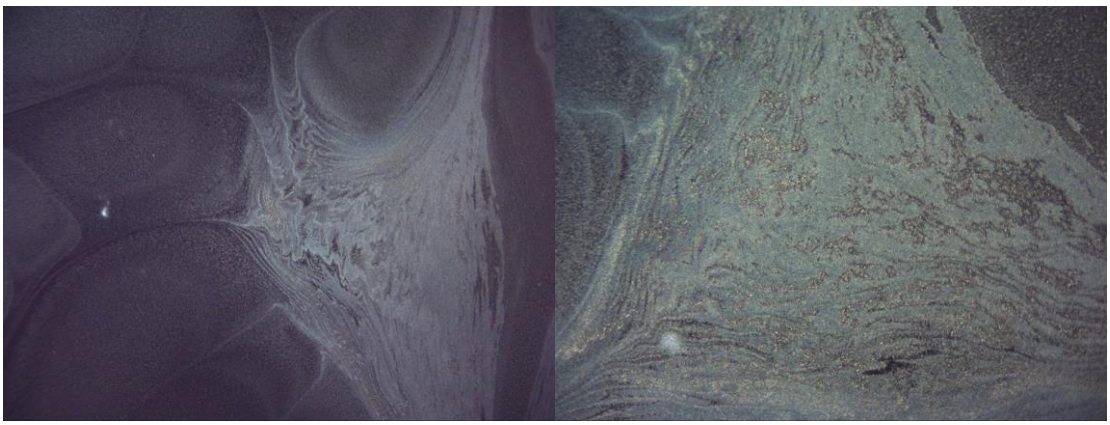

Figure 23. Film Casts of 20% w/v PMMA:PCL = 9:1 at (left) 20x and (right) 40x magnification with polarized light

Another feature of the 20% w/v PMMA:PCL = 9:1 film cast was the small crystal size shown in figure 23, which shows two micrographs of relatively crystalline regions of the film cast at two different magnifications. Even at higher magnifications of 20x and 40x, the crystal size was found much smaller than those formed in spherulite in PMMA/PCL films casted in different ratios (figure 10-15). In fact, there was no presentation of definite spherulites and crystals were presented in grain-like sizes (figure 23). This leads to the same analysis that the higher ratio of PMMA was restricting the crystallization of PCL. With less intensity of cross-polarized light, the comparison between the PMMA and PCL regions is more apparent (appendix 5, 6).

5.2. Surface Morphology of Microspheres

5.2.1. Scanning Electron Microscopy (SEM): 20% w/v PMMA:PCL = 1:1 microspheres prior to cryo-sectioning

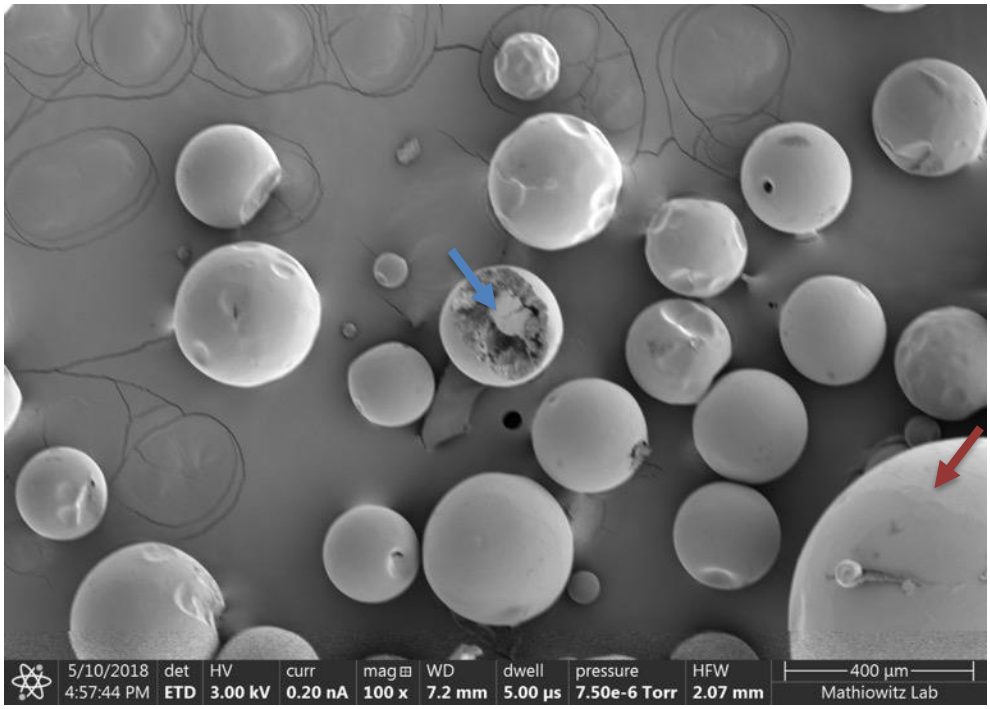

Figure 24. SEM image of 20% w/v PMMA:PCL = 1:1 microspheres formed during 3-hour long solvent evaporation before cryo-sectioning.

Figure 24 shows a scanning electron micrograph (SEM) of 20% w/v PMMA:PCL = 1:1 microspheres. Depending on spreading coefficients and interfacial surfaces, the polymers could configure into three different possible configurations, double-walled completely engulfed, partially engulfed, and non-engulfed as shown in figure 3. By using scanning electron microscope (SEM), which is only used to examine the surface characteristics of subjects of interest, most of the surfaces of PMMA/PCL microspheres were observed to be smooth without any immediate indication of partially or non-engulfed microspheres (figure 24). Figure 24 features a SEM image of 1:1 PMMA-PCL microspheres, which experienced 3 hour-long stirring in 1% PVA, washing, and lyophilization, but prior to cryo-sectioning, so internal morphologies including these configurations could not be obtained. Apparent signs of

double wall formation could not be found, but the blue arrow in figure 24 indicates a microsphere that may have been formed as double wall microsphere formation during solvent evaporation. The white substance shown through the crack is contemplated to be PMMA, which is amorphous. However, whether the inside core is PMMA and the outer layer is PCL cannot be decided through this SEM image unless the microspheres are sectioned for internal morphologies study. Information on the sizes of microspheres could be acquired and the sizes of whole microspheres prior to sectioning seem to vary with the largest over 400 um in diameter. The size variability could be due to insufficient solvent evaporation process which lasted for only 3 hours compared to other microspheres that underwent 24 hours of solvent evaporation. Another possible reason is that when emulsified droplets were generated in the aqueous solution during solvent evaporation process, they were generated in different sizes and uniform size distribution could not be obtained solely in stirring bath of aqueous solution during solvent evaporation process. In such case, there needs to be a rotor-stator homogenizer which is able to draw up the emulsified polymeric droplets into the apparatus by rapidly rotating rotor placed in a stator containing equally sized holes through which the droplets will be dispensed (figure 25). [35]

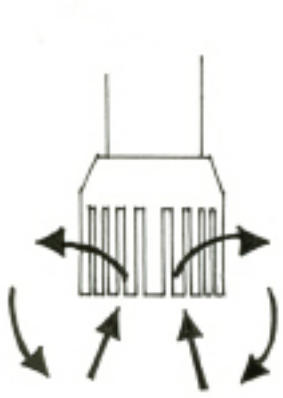

Figure 25. Schematic of rotor-stator homogenizer [35]

Another to note is the ridges on the microspheres indicated by a red arrow in figure 24. This is a possible capture of a polymeric layer encapsulating another layer or core composed of the other polymer. However, identifying which polymers compose of which layers could not be determined solely by an SEM image.

5.2.2. Scanning Electron Microscopy (SEM): Comparison of 5% w/v PMMA:PCL microspheres formed in all ratios prior to cryo-sectioning

In order to examine how different concentrations of polymers solutions (weight per volume, w/v) could affect the formations of microspheres, 5% w/v PMMA:PCL microspheres in different ratios were also formed using 24 hour, 1-step solvent evaporation process. The SEM images do not exhibit significant surface difference between 5% w/v and 20% w/v PMMA:PCL microspheres except 5% w/v PMMA:PCL = 1:9 microspheres (figure 26, 27, Appendix 10).

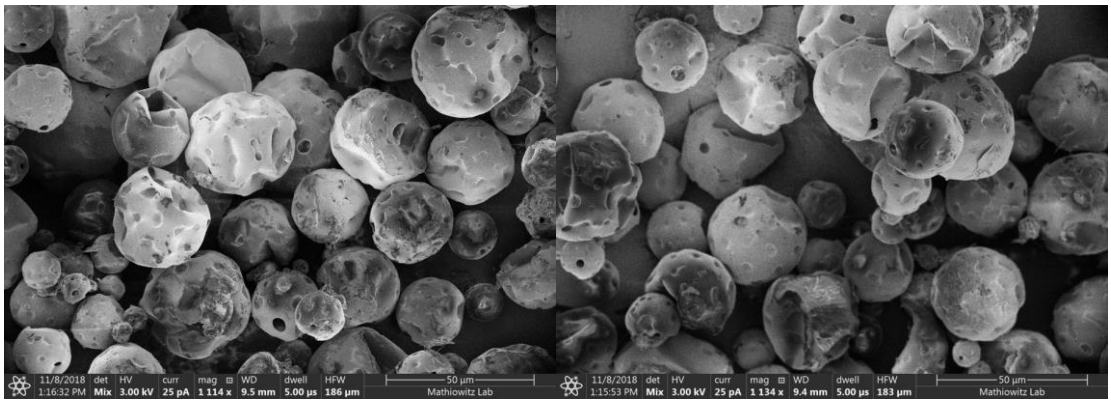

Figure 26. Scanning electron micrographs (SEM) of 5% w/v PMMA:PCL = 1:9

From figure 26, on the surfaces of 5% w/v PMMA:PCL = 1:9 microspheres, presentations of darker spots, presumably dents, could be observed. Yosida et al., although fabricated in different methods using microfluidic system and solvent evaporation process, also created PMMA/poly(4-butyltriphenylamine)(PBTPA) microspheres that had similar dents as shown in figure 26 and suggested that these

were small PMMA domains located on the surface of PBTPA hemisphere (Appendix 11). [36] Likewise, the existence of dents on 5% PMMA:PCL = 1:9 spheres could also suggest that the dents are composed of one polymeric domains that are located on the surface of the spheres composed of the other type of polymer. However, from an SEM image, whether or not if the darker regions are dents composed of one type of polymer or if this morphology was induced from experimental error cannot be determined.

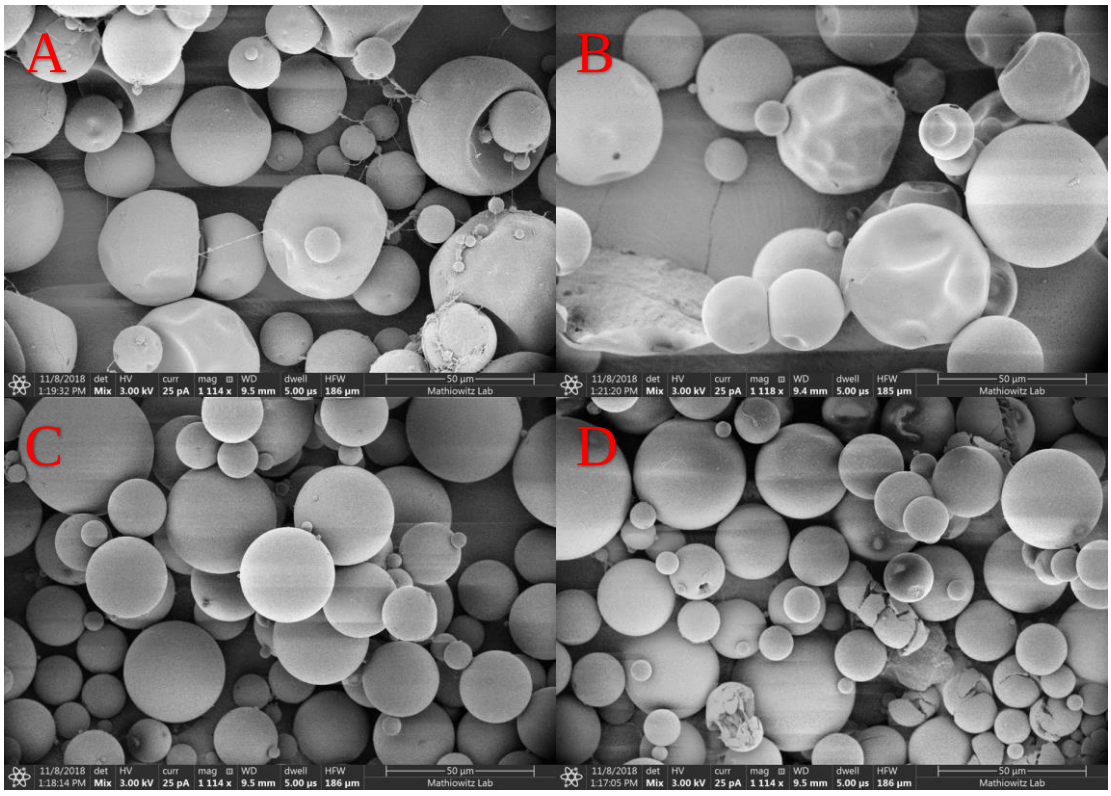

Figure 27. SEM of 5% w/v PMMA:PCL microspheres in different ratios. Ratios of 5% PMMA:PCL are (A) 3:7, (B) 1:1, (C) 7:3, and (D) 9:1.

Except for 5% w/v PMMA:PCL = 1:9 microspheres, there were no significant difference between the surfaces on other microspheres formed in different ratios of PMMA to PCL (figure 24, 26, 27, appendix 10). Figure 27 evidently shows that there is no significant difference in surface morphologies of 5% w/v microspheres formed in ratios of 3:7, 1:1, 7:3, and 9:1 PMMA to PCL (Appendix 10) and between 5% and 20% w/v microspheres.

5.3 Internal Morphology of Microspheres

5.3.1. Scanning Electron Microscopy (SEM) on cryo-sectioned 20% w/v PMMA:PCL = 1:1 microspheres

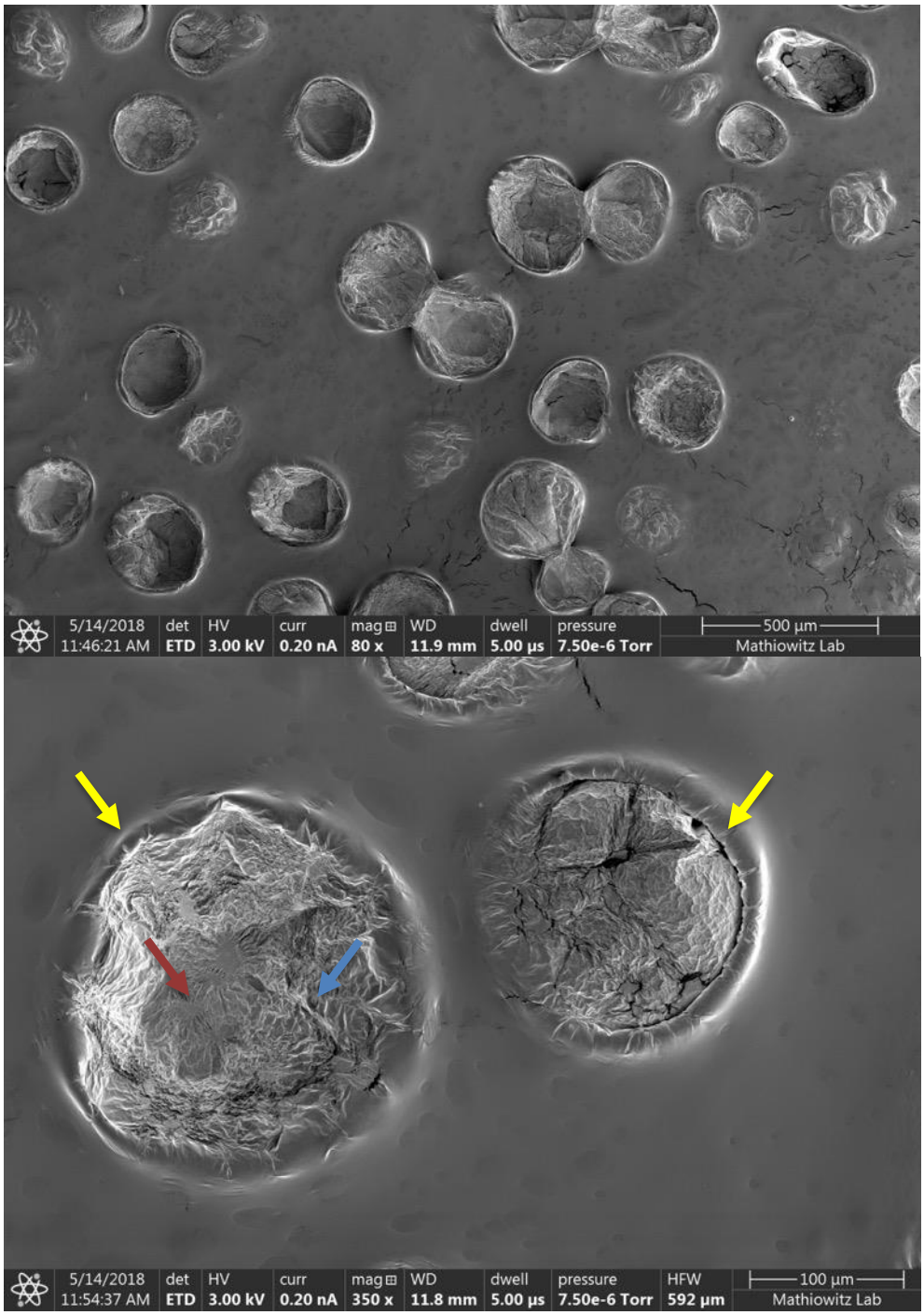

Figure 28. SEM image of cryo-sectioned 20% w/v PMMA:PCL = 1:1 microspheres formed during 3-hour long solvent evaporation process. At different magnifications.

SEM images of the same 20% w/v PMMA:PCL = 1:1 microspheres in figure 28 had been cryo-sectioned and were examined in different magnifications. The sectioned microspheres appeared to have two walls, but it was difficult to confirm that these were double walled microspheres as gold coating used for SEM and/or the OCT embedding material might have completely covered the outer layer, obscuring whether there were double walls present. Sputter coating of gold usually is required for SEM to improve the imaging of samples by inhibiting charges and reducing thermal damages [37], but in this case, embedding medium and/or the gold coating obscured the boundaries of the inner, outer, and the background, complicating the analysis of whether there were double walls or single wall. Even when examined at higher magnification (bottom, figure 28), the outermost layers of the microspheres seemed to be covered by the same material as what covered the background indicated by the yellow arrows in figure 28.

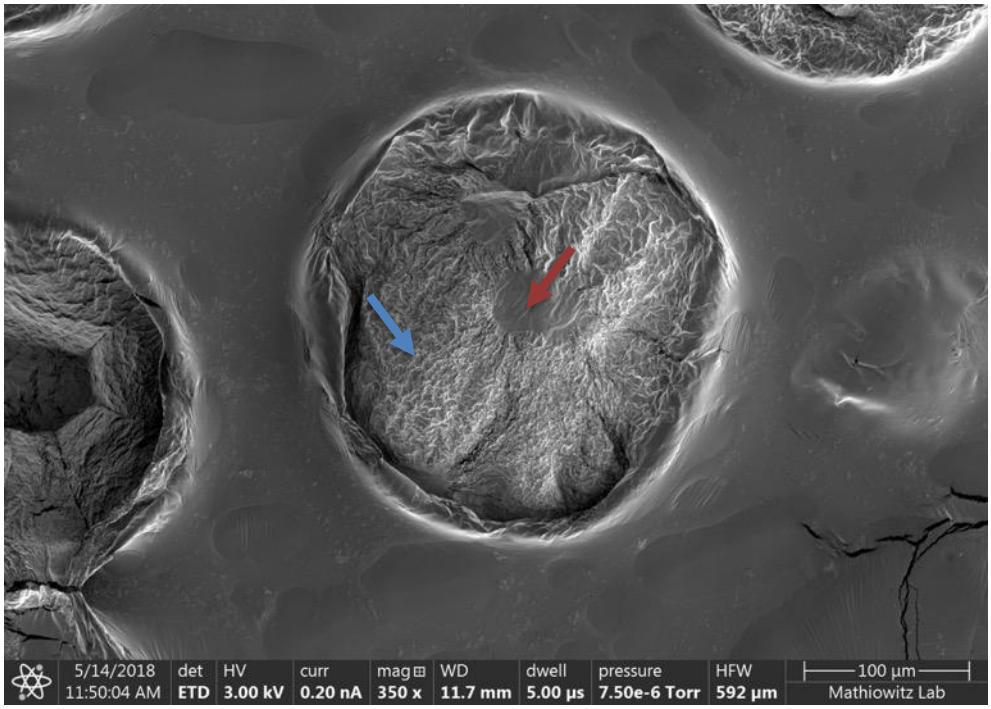

Figure 29. SEM image of cryo-sectioned 20% w/v PMMA:PCL = 1:1 microspheres formed during 3-hour long solvent evaporation process without homogenizer.

However, the inhomogeneity of the cryo-sectioned surfaces could still indicate that these microspheres were formed and precipitated while going through some phase separation. From an SEM image of cryo-sectioned 20% w/v PMMA:PCL = 1:1 microspheres formed during 3-hour long solvent evaporation, two different morphologies or surfaces could be observed indicated by the red and blue arrows (figure 29). It is assumed that the relatively smoother surface indicated by red arrows are the amorphous PMMA and the rougher surfaces indicated by blue arrows is the crystalline PCL.

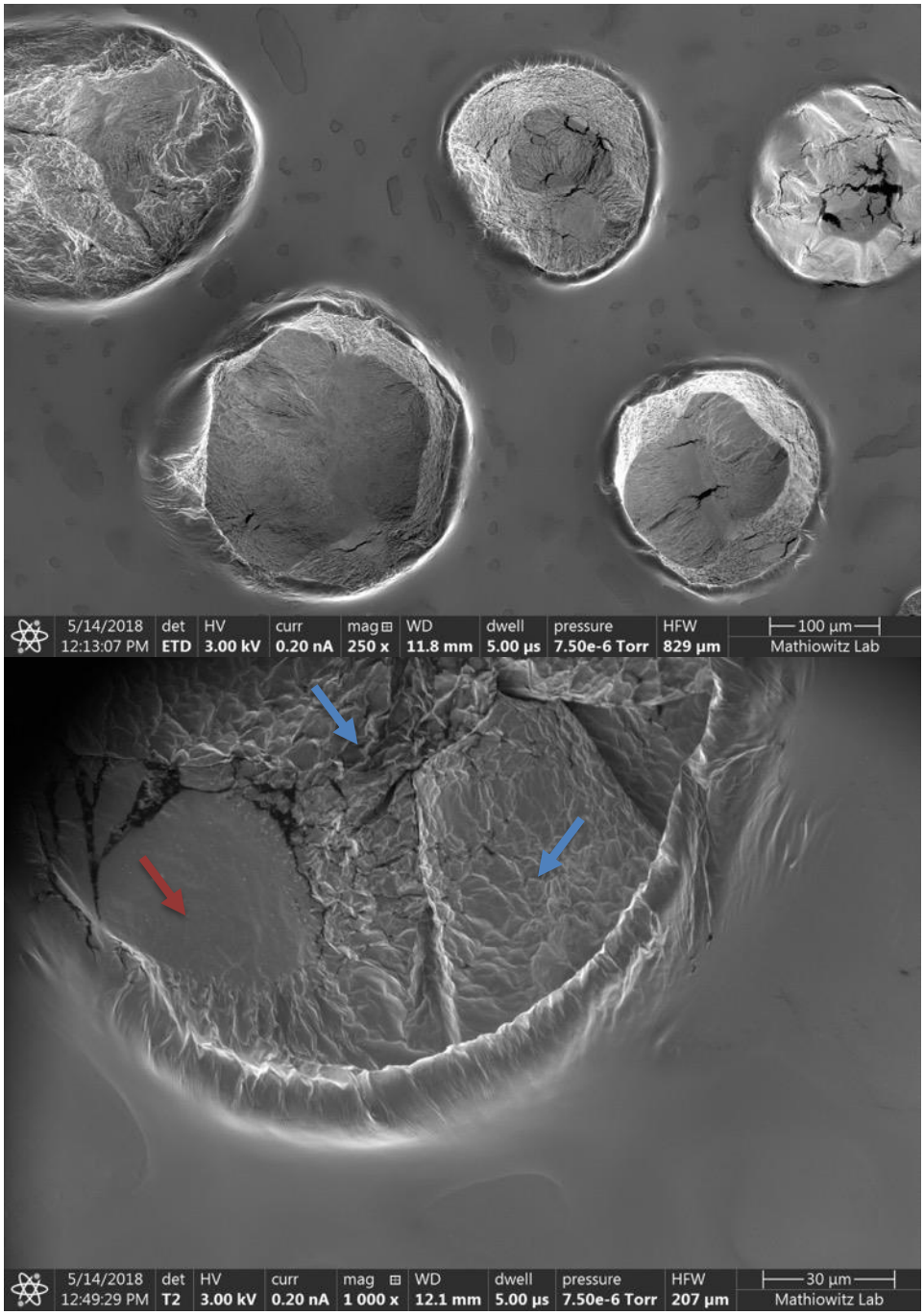

Figure 30. SEM images of cryo-sectioned 20% w/v PMMA:PCL = 1:1 microspheres formed during 24-hour long solvent evaporation process without homogenizer in different magnifications.

Figure 30 shows other SEM images of cryo-cutted 20% w/v PMMA:PCL = 1:1 microspheres that had experienced 24 hours of solvent evaporation process. Although there was no apparent difference between the microspheres that were formed during 3 hour-long and 24 hour-long solvent evaporation processes, it should

be noted that surfaces on microspheres after 24 hours of solvent evaporation were inhomogeneous with two different internal surface characteristics (figure 28-30). The red arrow points to a relatively smoother surface, probably PMMA, and the blue arrow points to a rougher surface, possibly PCL. The fact that the surfaces were not continuous and not homogeneous may indicate that these microspheres might have been still phase separating and that phase separation was incomplete when the sphere precipitated into solid microspheres.

Even though the purpose of SEM is mainly to study the surface characteristics of the subjects of interest, it is still able to provide information on internal morphological characteristics by comparison of smoothness and/or roughness of the surfaces on the cryo-sectioned specimens or samples (figure 28-30).

5.3.2. Characterization of Microspheres with Polarized Light Microscopy

The lyophilized 5% and 20% w/v PMMA/PCL microspheres were placed in cubic embedding molds along with OCT embedding material, frozen, sectioned in 16 – 20um, and placed onto glass slides. These sections were examined with and without polarized light using light microscope, which helps distinguish the amorphous and crystalline regions indicated by the dark and bright regions, respectively.

5.3.2.1. 20% w/v PMMA/PCL microspheres

5.3.2.1.1. 20% w/v PMMA:PCL = 1:9 microspheres

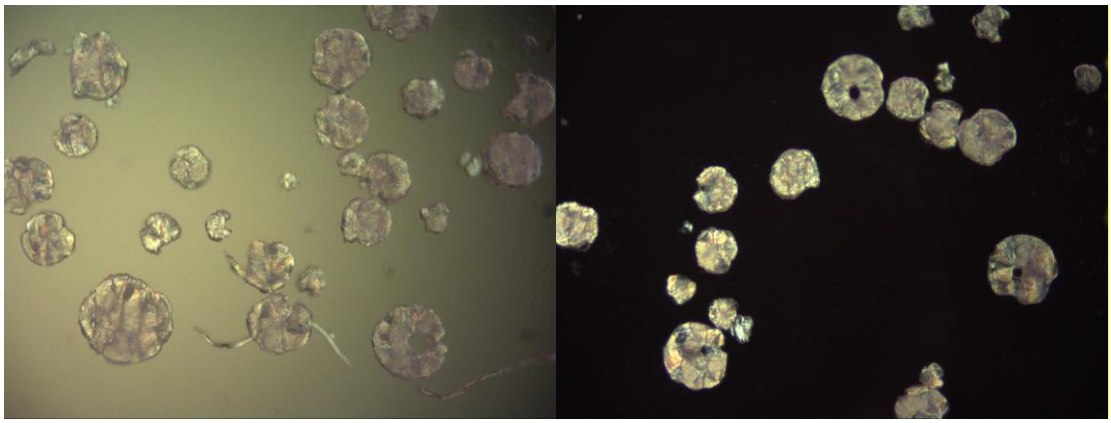

Figure 31. Sections of 20% w/v PMMA:PCL = 1:9 at 10x magnification (left) without and (right) with polarized light

From figure 31, approximately 16 um thin sections of 20% w/v PMMA:PCL = 1:9 are were examined without and with polarized light at 10x magnification. At 10x magnification, there seemed to be no repetitive apparent structures or patterns throughout the whole section, which could also be seen in lower magnification (appendix 12).

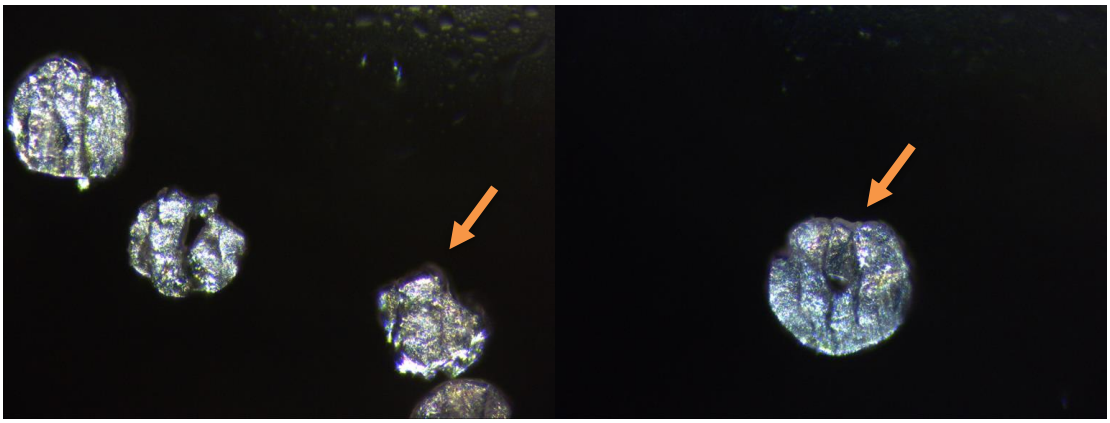

Figure 32. Sections of 20% w/v PMMA:PCL = 1:9 at 20x magnification with polarized light

Because the concentration of PCL was much higher compared to that of PMMA, it was expected for the internal structure to be more crystalline as shown in

figure 32 with polarized light. However, there were still relatively darker or amorphous regions on the section that corresponds to the ratio 1 of PMMA, mostly around the edges of the microspheres indicated by the orange arrows.

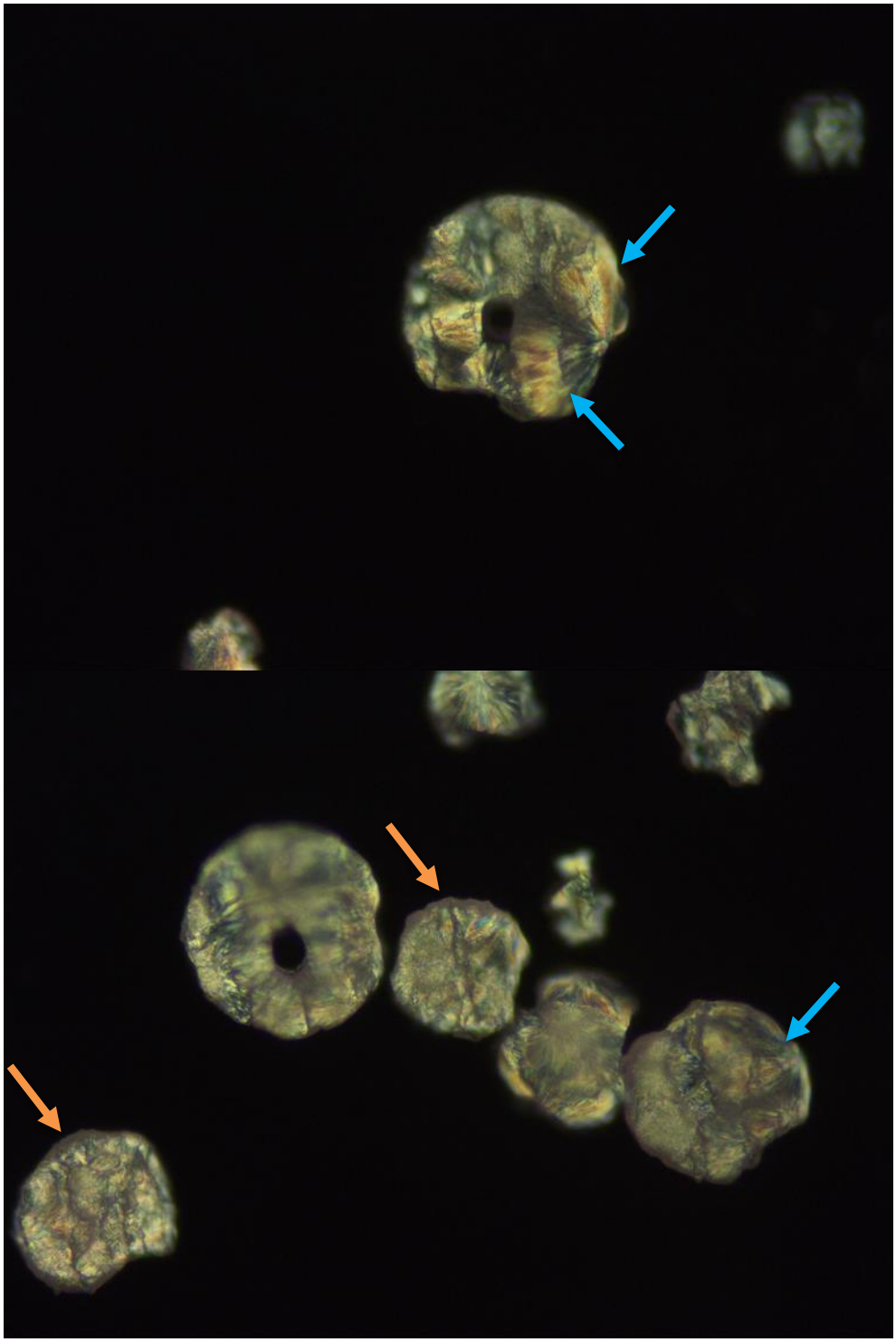

Figure 33. Sections of 20% w/v PMMA:PCL = 1:9 at 40x magnification with polarized light

At higher magnification and with different light settings, birefringence, indicated by the blue arrows, was observed (figure 33). Birefringence which is usually color-patterned, can defined as an optical property of some crystalline materials that exhibit anisotropy due to differences between two refractive rays of light. [38] Usually, polymers that are in completely amorphous states would have molecules that are randomly oriented, exhibiting no birefringence while anisotropic crystals that exhibit different properties in different directions such as non-cubic crystals would display birefringence. Therefore, the presence of birefringence on 20% w/v PMMA:PCL = 1:9 microspheres could indicate that these microspheres have more anisotropic crystalline structures, referring to different properties along difference axes.

These two figures (figure 32 and 33) could explain that 20% w/v PMMA:PCL = 1:9 microspheres show highly crystalline feature, which could intuitively be deduced from higher concentration of crystalline PCL in ratio of 9. They could also imply that these microspheres are more anisotropic crystalline as there were birefringent or colored patterns exhibited on their sections (figure 33). Although there were no apparent presentations of spherulites on these microspheres, the existence of crystalline birefringence could imply that some resemblance between 20% w/v PMMA:PCL = 1:9 microspheres and film casts which display definite spherulites (figure 10-13).

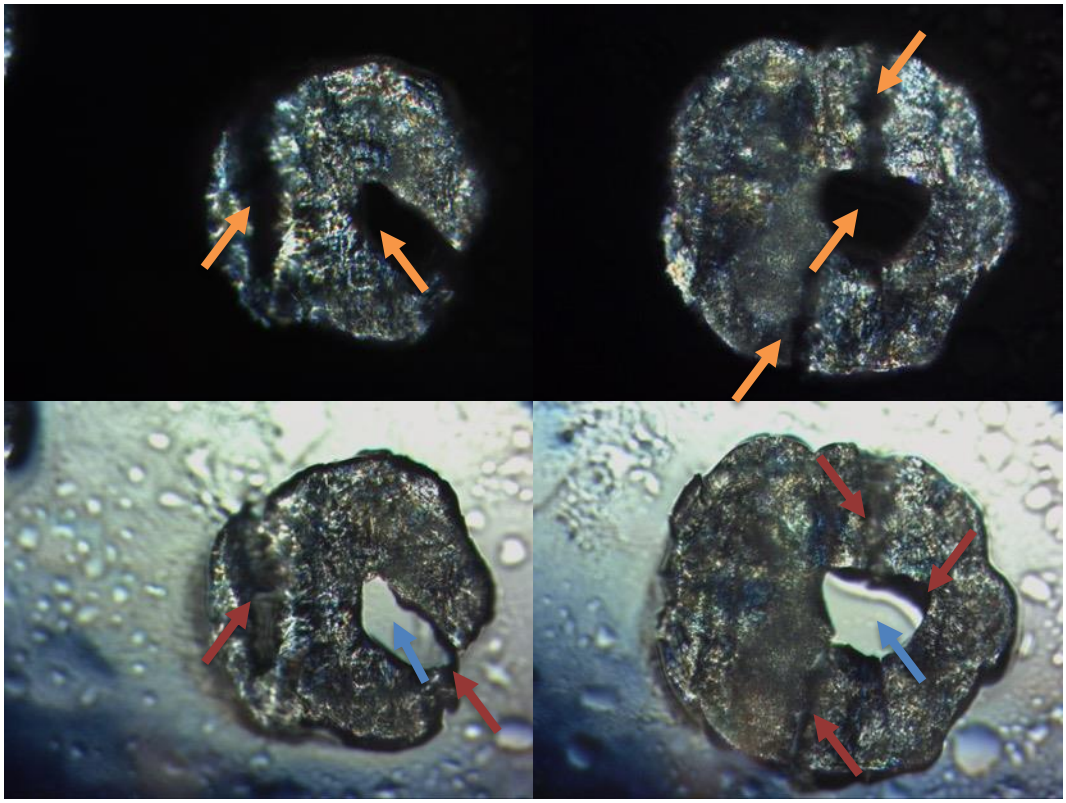

Figure 34. Sections of 20% w/v PMMA:PCL = 1:9 at 40x. (Top) With polarized light and (bottom) without polarized light.

Additionally, there were some microspheres with seemingly hollow holes in middle when 20% w/v PMMA:PCL = 1:9 microspheres were cryo-sectioned and initially examined with only cross-polarized light. From the film casts of 20% w/v PMMA:PCL = 1:9 (figure 10-13), it was easier to distinguish the amorphous and the crystalline with only polarized light because there were less noticeable holes or cracks. However, it was difficult to determine if the darker regions indicated by the orange arrows on top micrographs in figure 34 were actually amorphous or simply holes/cracks when they were not compared to the microspheres examined without the cross-polarized light. Therefore, it was necessary to compare the spheres both with and without the polarized (figure 34). In figure 34, the blue arrows indicate hollow holes as the pointed areas were of same color as the background or transparent to the background. The red arrows, on the other hand, which point to the areas that were

shown dark under polarized light (top, figure 34), were found not transparent when examined with polarized light (bottom, figure 34), implying that these regions were amorphous.

From the analysis on morphologies of cryo-sectioned 20% w/v PMMA:PCL = 1:9 microspheres (figure 31-34), it could be assumed that there were two different types of morphologies; ones with holes in the middle and the others without holes. One common feature of the holed sections was that the circumferences of the holes seemed more amorphous as shown by the red arrows in figure 34. The red arrows pointing to the areas that were not transparent without polarized light but dark with polarized light indicate the amorphous states, but the reason why this morphology was induced is not known. Hypothetically, it could be due to formation of air bubbles within the emulsified droplets during solvent evaporation process. Additionally, whether the sections of the spheres without the holes are simply the sections of the top layers before reaching the point of phase separation and/or their cores could not be determined without further studies on comparing their consecutive sections.

5.3.2.1.2. 20% w/v PMMA:PCL = 3:7 microspheres

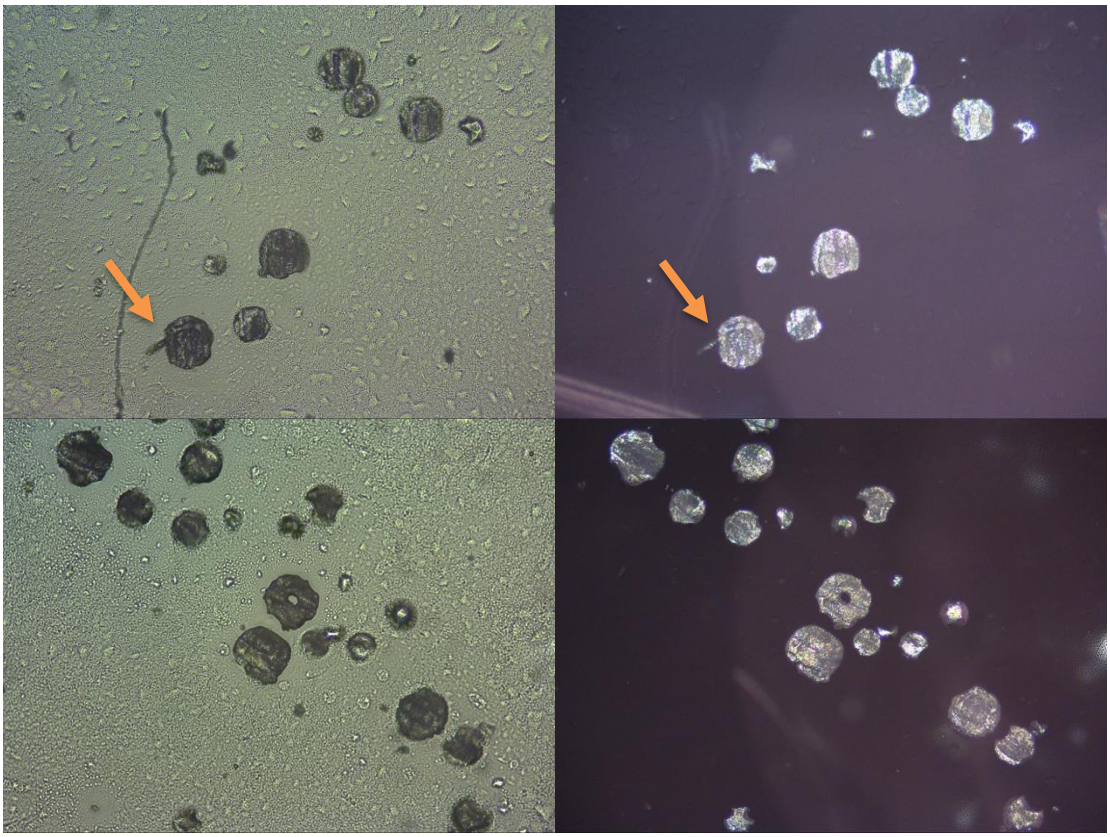

Figure 35. Sections of microspheres of 20% w/v PMMA:PCL = 3:7 (left) without and (right) with polarized light. 10x magnification.

From the film casts of 20% w/v PMMA:PCL = 3:7, there were apparent, homogeneous patterns of spherulites (figure 14, 15) and how these homogenous patterns would be exhibited when the 20% w/v PMMA:PCL = 3:7 polymeric solution was formed into microspheres was particularly of interest. However, despite the evident patterns of spherulites observed on the film casts, there was not any morphological significance shown throughout the sections of the 20% w/v PMMA:PCL = 3:7 microspheres at low magnification (figure 35). Because the concentration of PCL was higher than that of PMMA, all cross-sections seem to be relatively crystalline. Also, there seemed to some double wall microspheres formed indicated by an orange arrow, but there were no presentations of completely engulfed microspheres with one type of polymer inside a layer of the other type of polymer as

shown in 20% w/v PMMA:PCL = 1:1 microspheres (figure 37-39). Instead of distinct layers, the double layers seemed to be composed of a blend of PMMA and PCL, the PMMA/PCL blended outer layer and PMMA/PCL blended inner core. However, whether these spheres are formed of PMMA/PCL blended double walls or simply a homogenous PMMA/PCL single sphere cannot be determined at such low magnification with a basic light microscope.

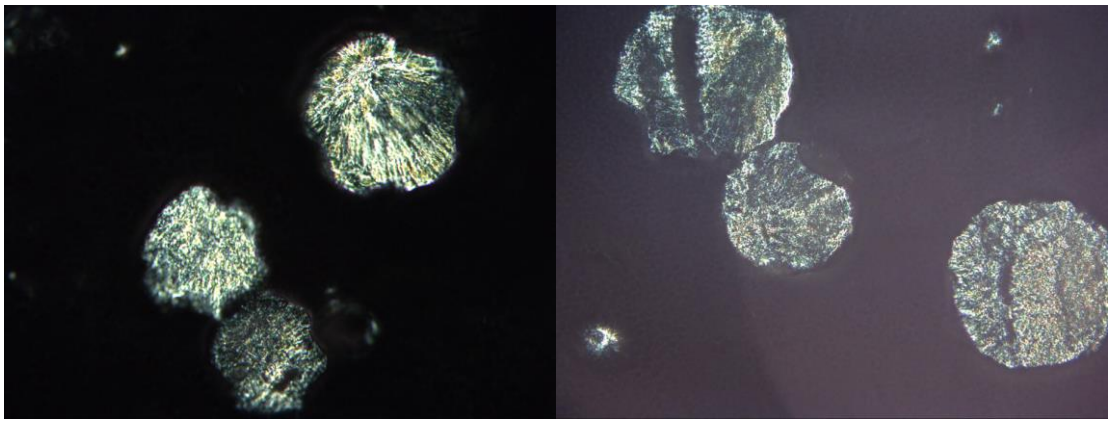

Figure 36. Sections of microspheres of 20% w/v PMMA:PCL = 3:7 with polarized light. 40x magnification.

However, when examined at higher magnification of 40x on different sections of the microspheres, many of the cross-sections were presented with spherulites as shown in figure 36 (appendix 14). The crystalline structure seemed to be radially growing out with little hints of amorphous regions attempting to impede PCL crystallization. However, since the concentration of crystalline PCL is higher in these microspheres, spherulites which are highly crystalline characteristics seemed to be predominant, indicating that lower concentration of amorphous PMMA was not able to overpower the crystalline PCL growth into spherulites. Conclusively, these 20% w/v PMMA:PCL = 3:7 microspheres very closely resemble the film casts of same PMMA:PCL ratio (figure 14, 15).

5.3.2.1.3. 20% w/v PMMA:PCL = 1:1 microspheres

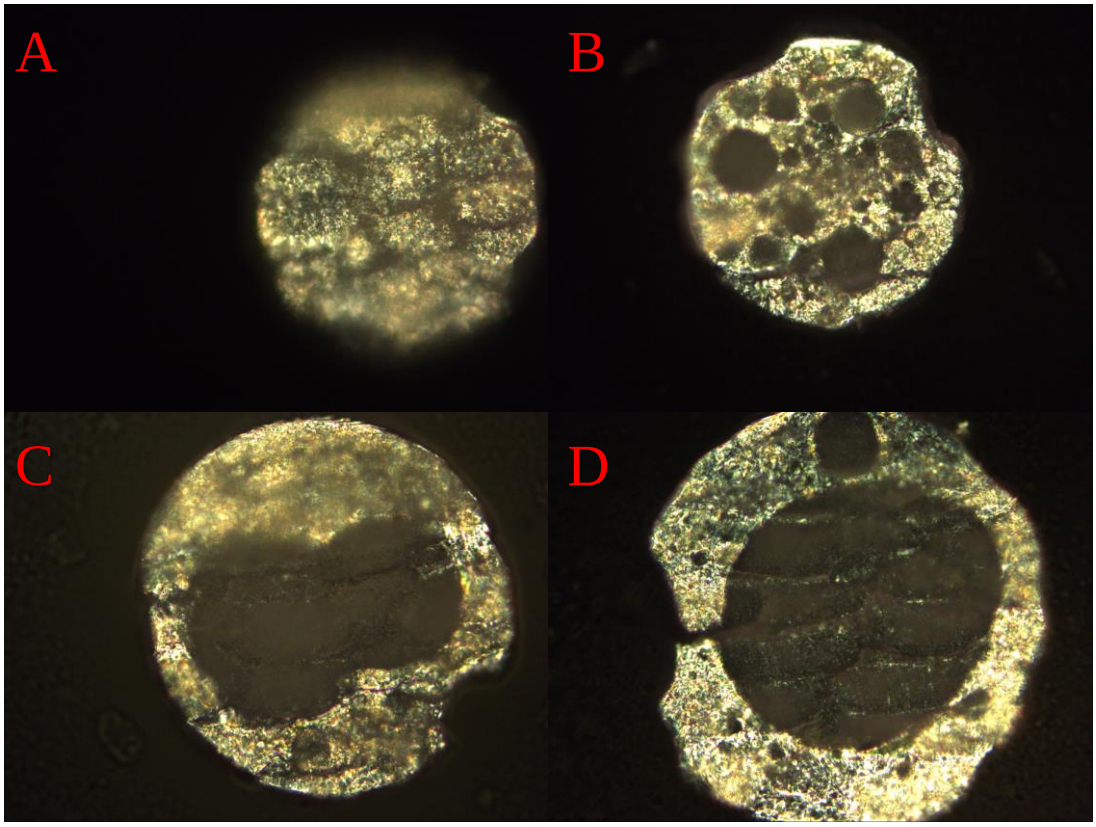

Figure 37. Different Morphologies shown in cross sections of 20% w/v PMMA:PCL = 1:1 microspheres with cross polarized light. 40x magnification.

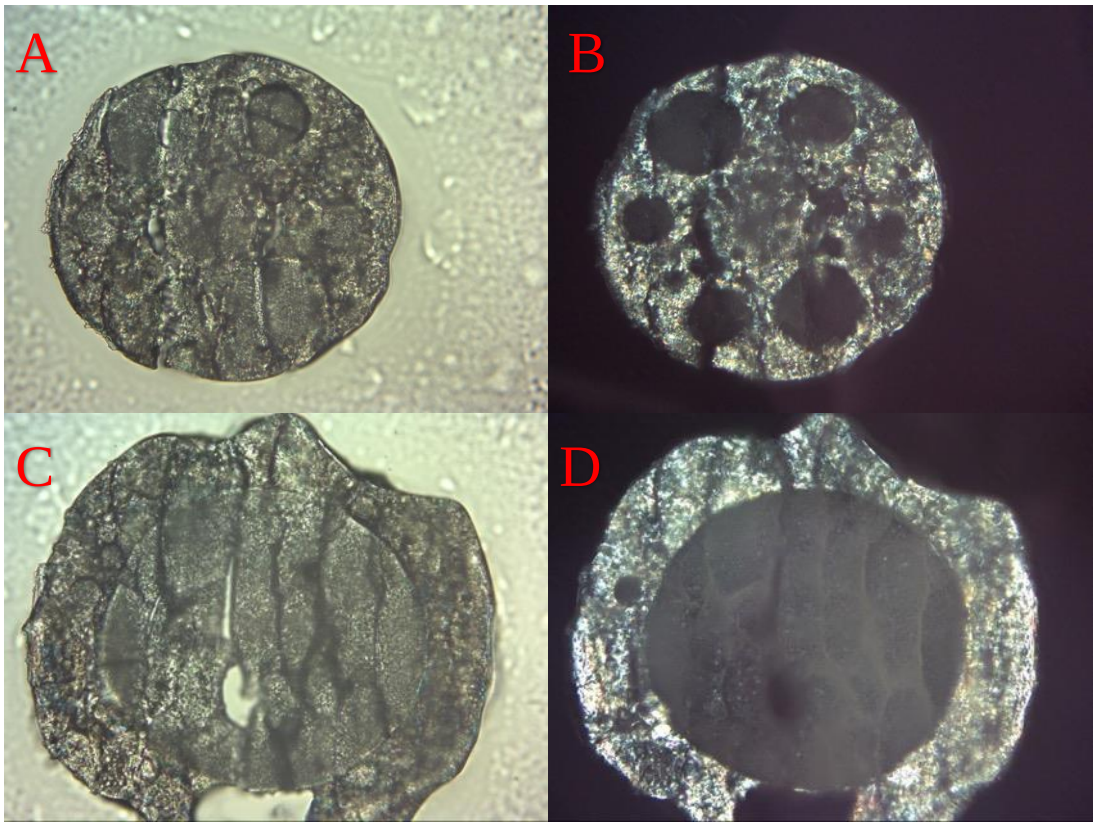

Figure 38. Two prevalent internal morphologies microspheres of 20% w/v PMMA:PCL = 1:1 (left) without and (right) with polarized light. 40x magnification.

Figure 37 and 38 show polarized micrographs of different morphologies observed in cross-sections of 20% w/v PMMA:PCL = 1:1 microspheres, but most interestingly, there were some formations of definite double wall microspheres as shown in figure 37C, 37D, 38C, and 38D. However, there were also configurations that were not in complete engulfment configurations as shown in figure 37A, 37 B, 38A, and 38B. Especially, the micrograph shown in figure 37A is assumed to be a top cross-section where the cryotome had not yet reached the point of phase separation or the layer of complete engulfment. Whether this section was cut at the upper level of the sphere could be determined by further cross-sectioning and examining the consecutive sections of this single microsphere.

Additionally, there was another configuration in which it seemed to be a cross-section of a microsphere that had been undergoing phase separation but without definite double walls (figure 37B, 38A, 38B). In fact, from these cross-sections, there were multiple, focal regions of amorphous PMMA encapsulated within a large, single crystalline sphere. This potentially indicates when this particular microsphere precipitated, it had been experiencing some phase separation. However, evaporation rate of the organic solvent, DCM, might had been faster than the rate of phase separation, unable to provide sufficient time for the microsphere to completely phase separate into two distinct layers as shown in figure 37C, 37D, 38C, and 38D. For further studies, by slowing down the rate of evaporation, possibly by manipulating the temperature in which solvent evaporation process is conducted, whether or not these focal amorphous areas would combine into a uniform core of PMMA that is entrapped by an outer layer of PCL could be a subject of interest.

Furthermore, figure 37C, 37D, 38C, and 38D show completely engulfed double wall PMMA/PCL microspheres with the core composed of mostly amorphous PMMA and the encapsulating outer layer composed of essentially crystalline PCL. Specifically, the microsphere in figure 37C is assumed to be experiencing phase separation during which the amorphous PMMA regions were starting to combine into a homogenous core of PMMA when the spheres hardened. This microsphere could further configure itself into a complete double wall microsphere as shown in figure 37D, 38C, and 38D if evaporation rate was slower and/or sufficient time for complete phase separation was provided.

Figure 38 emphasizes on the two prevalent morphologies discovered on cross-sections of 20% w/v PMMA:PCL = 1:1 microspheres. Micrographs on the top show complete engulfment of one polymer, mostly PMMA, inside the other polymer, mainly PCL while the micrographs on the bottom show several, smaller engulfment of one polymer, the PMMA, inside the other polymer, the PCL. This predominant distribution of the 20% w/v PMMA:PCL = 1:1 microspheres in these specific morphologies could lead to the assumption that 20% w/v PMMA:PCL = 1:1 polymeric solution is almost capable of 100% production efficiency, the percentage of microspheres with completely phase separated double wall configuration compared to the total number of microspheres. To be more specific, partially engulfed microspheres from figure 38A and B are capable of completely phase separating into double wall microspheres when given more time, supporting the possibility of 100% double wall production efficiency.

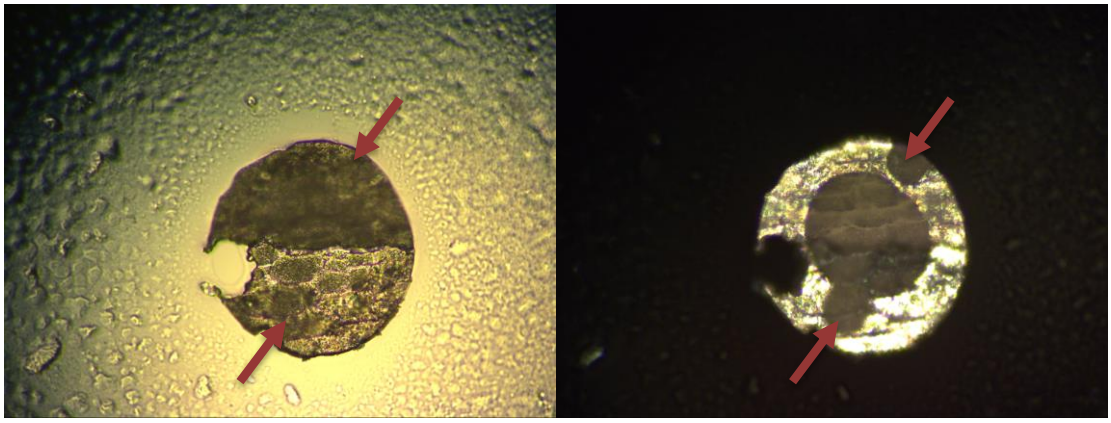
Figure 39. Sections of microspheres of PMMA:PCL = 1:1 (left) without and (right) with polarized light. 40x magnification

Last, it should also be noted that each layer was not composed uniformly of one type of polymer as each layer still had both amorphous and crystalline structures (figure 39, appendix 15). The red arrows in figure 39 indicate the relatively more amorphous regions in the relatively more crystalline outer layer. Although the two polymers were able to phase separate and form distinct double walls, each layer was not composed purely of one type of polymer. The outer layer was relatively crystalline with hints of darker spots indicative of the amorphous regions and the core was relatively amorphous with hints of lighter areas indicative of crystalline regions. As for the core, it seemed to have compartments of amorphous that were slightly confined by minimal amounts of crystalline structures.

5.3.2.1.4. 20% w/v PMMA:PCL = 7:3 microspheres

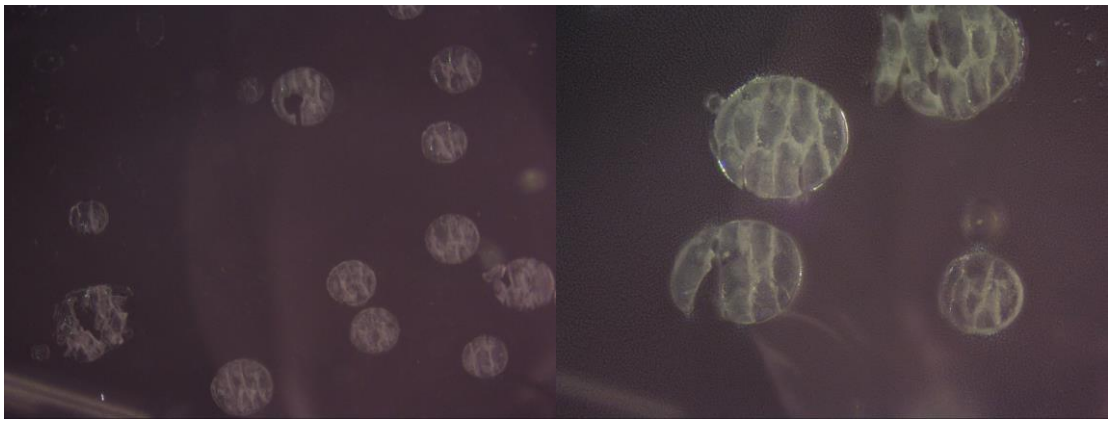

Figure 40. Sections of microspheres of 20% w/v PMMA:PCL = 7:3 with polarized light at (left)10x and (right) 20x magnification.

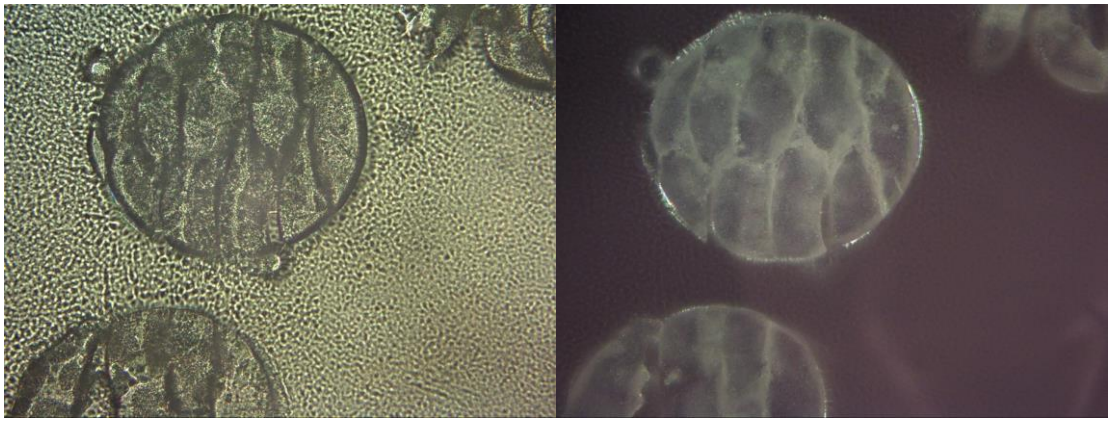

Figure 41. Sections of microspheres of 20% w/v PMMA:PCL = 7:3 (left) without and (right) with polarized light at 40x magnification.

For 20% w/v PMMA:PCL = 7:3 microspheres, the morphologies were highly homogenous across all sections as shown in figure 40 at 10x magnification. Most of the microspheres were observed with compartments of amorphous regions lined by crystalline structures (figure 40, 41, appendix 16).

In partial resemblance to the film cast of 20% w/v PMMA:PCL = 7:3 (figure 19, 20), the size of the crystallites surrounding the amorphous sections on the microspheres seemed small without any indication of crystalline growth, implying that higher concentration of amorphous PMMA could have obstructed PCL crystallization. Also, compared to the film cast exhibiting the amorphous PMMA

seemingly entrapping crystalline PCL, the microsphere cross-sections showed the opposite morphology with small PMMA compartments enclosed by small particles of PCL.

5.3.2.1.5. 20% w/v PMMA:PCL = 9:1 microspheres

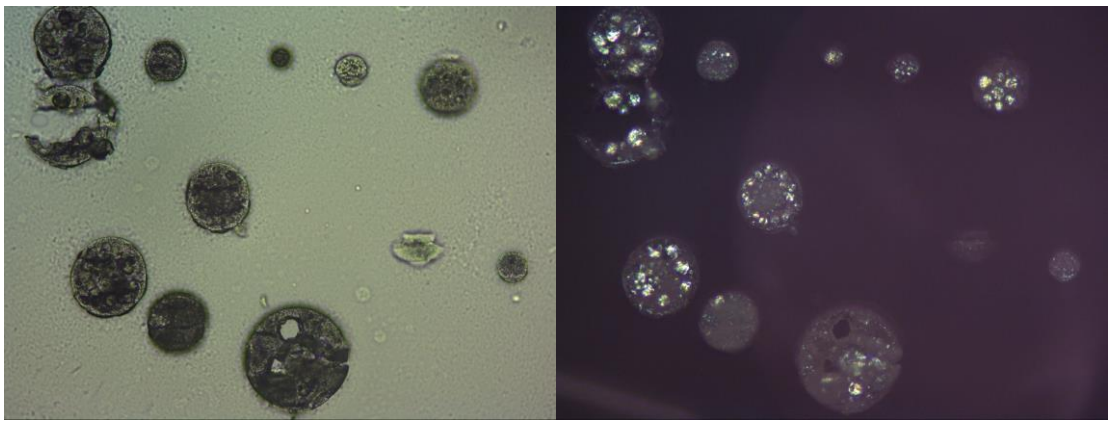

Figure 42. Sections of microspheres of 20% w/v PMMA:PCL = 9:1 (left) without and (right) with polarized light. 20x magnification.

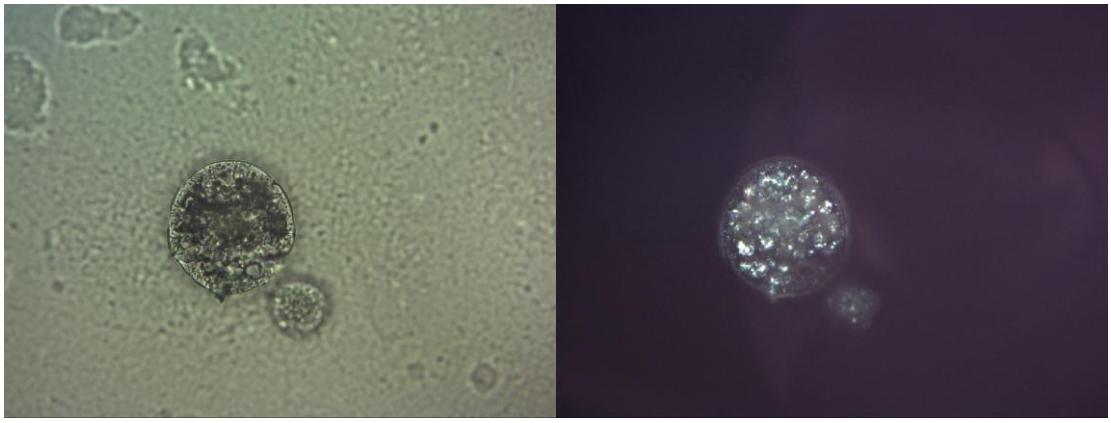

Figure 43. Sections of microspheres of 20% w/v PMMA:PCL = 9:1 (left) without and (right) with polarized light. 40x magnification.

Last for 20% w/v microspheres, cross-sections of 20% w/v PMMA:PCL = 9:1 were examined (figure 42-44). Figure 42 explicitly shows two different morphologies, one that seemed to be in completely amorphous sphere and the other with focal regions of crystalline embedded within a larger amorphous sphere. The morphological variation is probably because embedding the microspheres on the same layer and cryo-sectioning them at the same level was difficult. Therefore, the section that

seemed to be completely amorphous may simply be the top layer of the microsphere that had been cryo-sectioned prior to the point of phase separation. However, it could not be determined if the sphere was completely amorphous or if the section was simply not cryo-cutted at the level of phase separation solely from these images unless consecutive sections of that specific microsphere are acquired.

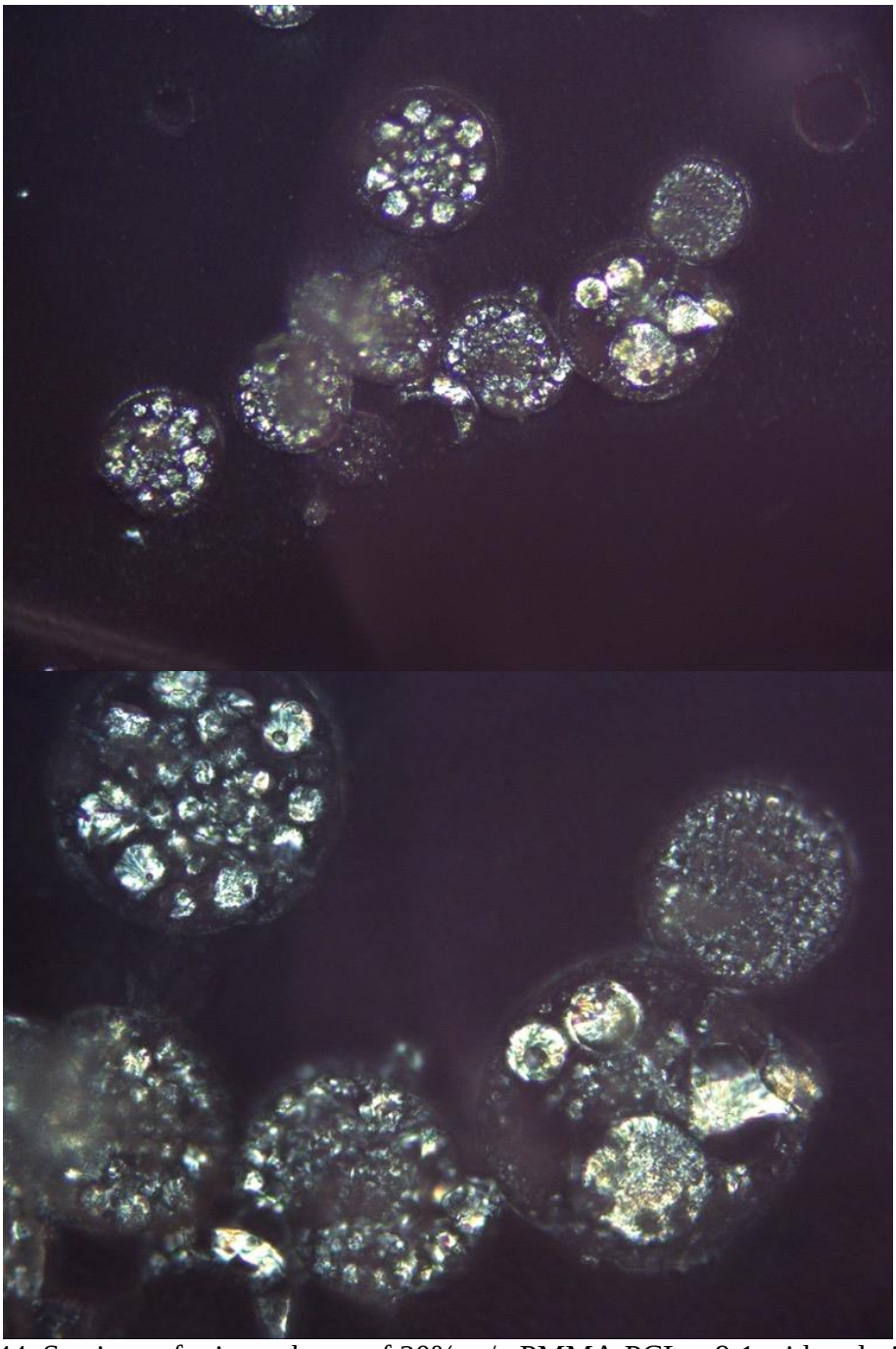

Figure 44. Sections of microspheres of 20% w/v PMMA:PCL = 9:1 with polarized light. (Top) 20x and (Bottom) 40x magnification.

At higher magnification, on 20% w/v PMMA:PCL = 9:1 microspheres, focal regions of concentrated crystalline PCL entrapped within a larger, amorphous PMMA sphere were observed (Figure 44). Compared to the film cast of 20% w/v PMMA:PCL = 9:1 (figure 21-23), in which the crystallization of PCL seemed to be interrupted by the higher concentration of amorphous PMMA, the crystalline regions in the microspheres were profoundly presented, some even exhibiting birefringence and spherulites. Yet, there were still smaller crystals present in the microspheres, possibly implying that rate of crystallization was not homogenous, explaining why the crystal sizes varied. Nonetheless, both the film cast and the microspheres of 20% w/v PMMA:PCL = 9:1 displayed similarity in that the amorphous PMMA grouped in blobs prevalent on the film cast were dominant enough to encapsulate the lower concentration of PCL on the microspheres. In comparison, while the film casts had grouped amorphous blobs surrounded by small particle of crystalline PCL (figure 21-23), the cross-sections of the microspheres seemed to exhibit the opposite morphology with crystalline PCL entrapped within amorphous PMMA.

Lastly, this configuration of 20% w/v PMMA:PCL = 9:1 microspheres is assumed to be incompletely phase separated or in the middle of phase separation when the spheres precipitated. Possibly, by slowing down the evaporation rate by lowering the temperature, whether or not these microspheres will completely phase separate into completely engulfed double wall microspheres could be further tested, allowing optimization of forming double wall microspheres and their production efficiency.

5.3.2.2. 5% w/v PMMA/PCL microspheres

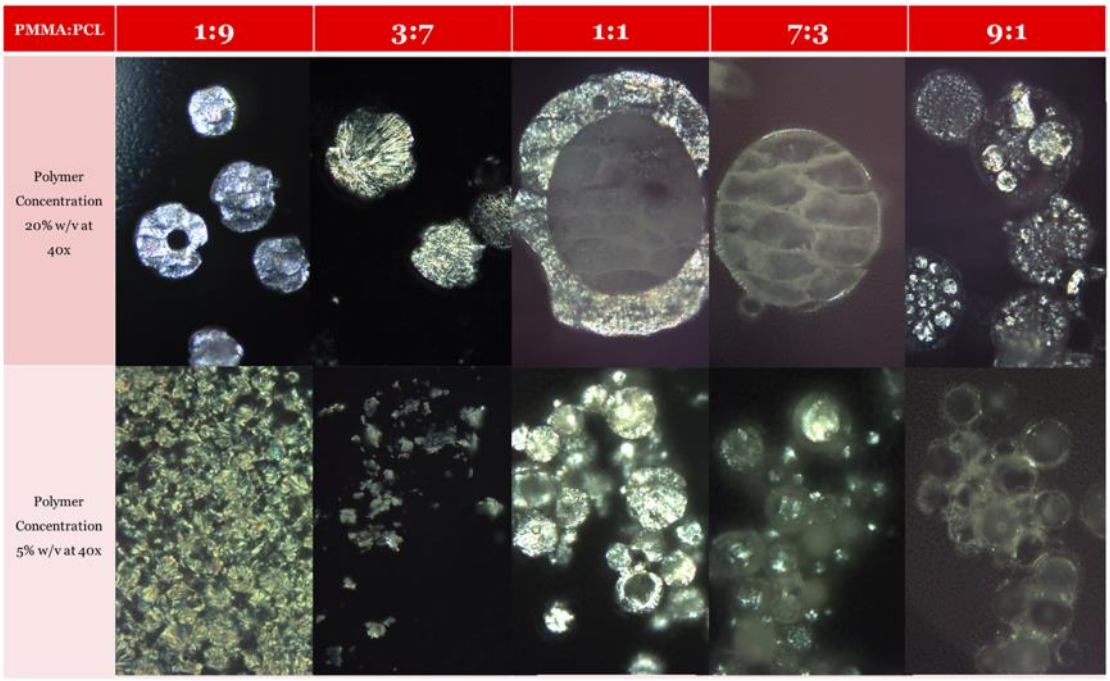

Table 4. Comparison of 5% w/v and 20% w/v PMMA:PCL microspheres

Next, PMMA/PCL microspheres formed in different concentrations, 5% w/v and 20% w/v were compared (table 4). The first noticeable difference between 5% w/v and 20% w/v PMMA/PCL microspheres was the particle size. This could be attributed to a decrease in viscosity with decreasing polymer concentrations, resulting in smaller emulsion droplets during solvent evaporation process and therefore, smaller microspheres. [39]

Second, when comparing the PMMA/PCL microspheres formed in different ratios, especially those formed in ratios of 1:1, 7:3, and 9:1, there seemed to be more double wall microsphere formations for 5% w/v than 20% w/v microspheres. Presumably due to the larger surface areas of smaller 5% w/v microspheres, the evaporation rate of DCM would become slower, allowing the spheres to have adequate amount of time for complete phase separation before precipitation or hardening.

5.3.2.2.1. 5% w/v PMMA:PCL = 1:9 microspheres

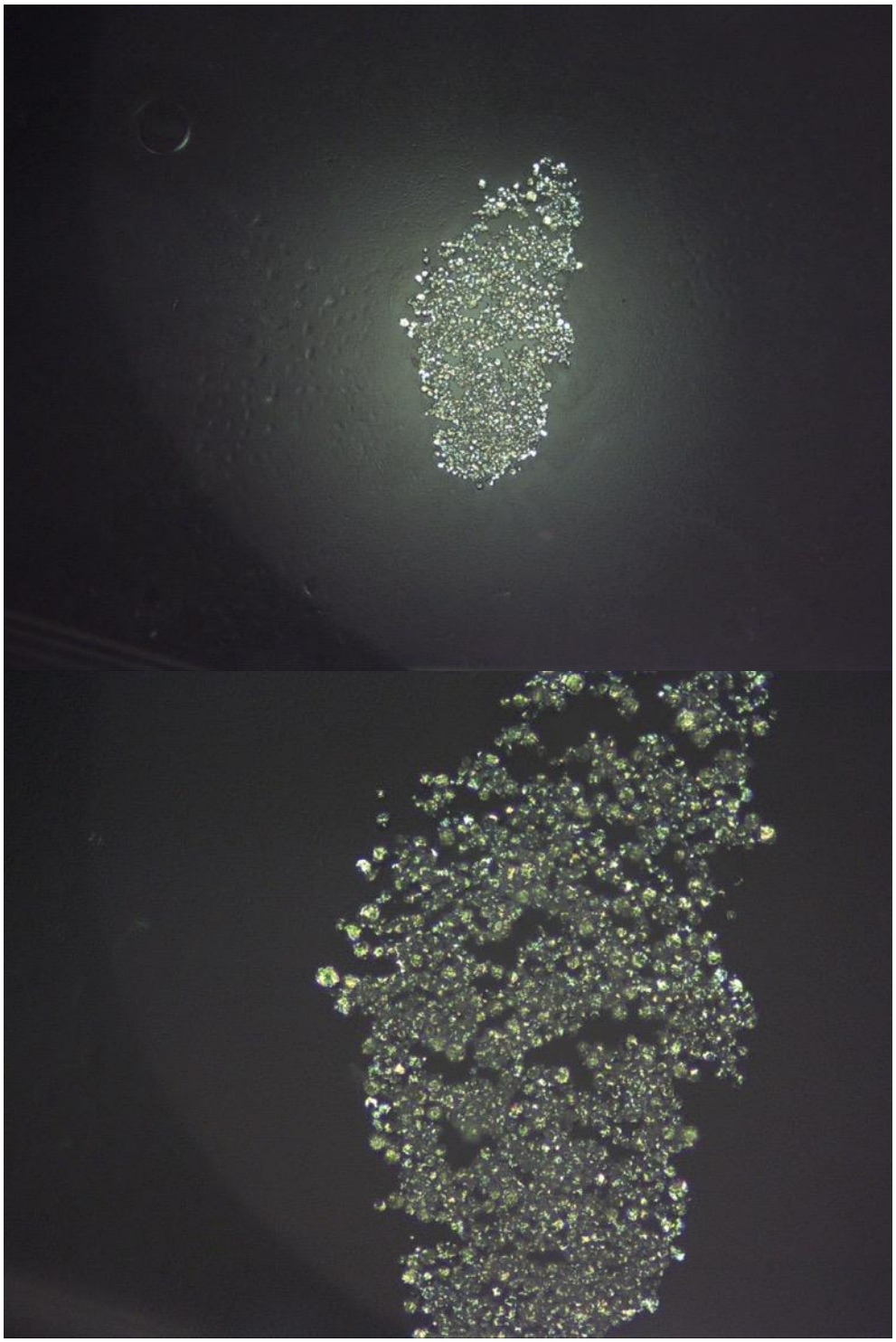

Figure 45. Sections of microspheres of 5% w/v PMMA:PCL = 1:9 with polarized light at (top) 4x and (bottom) 10x magnification

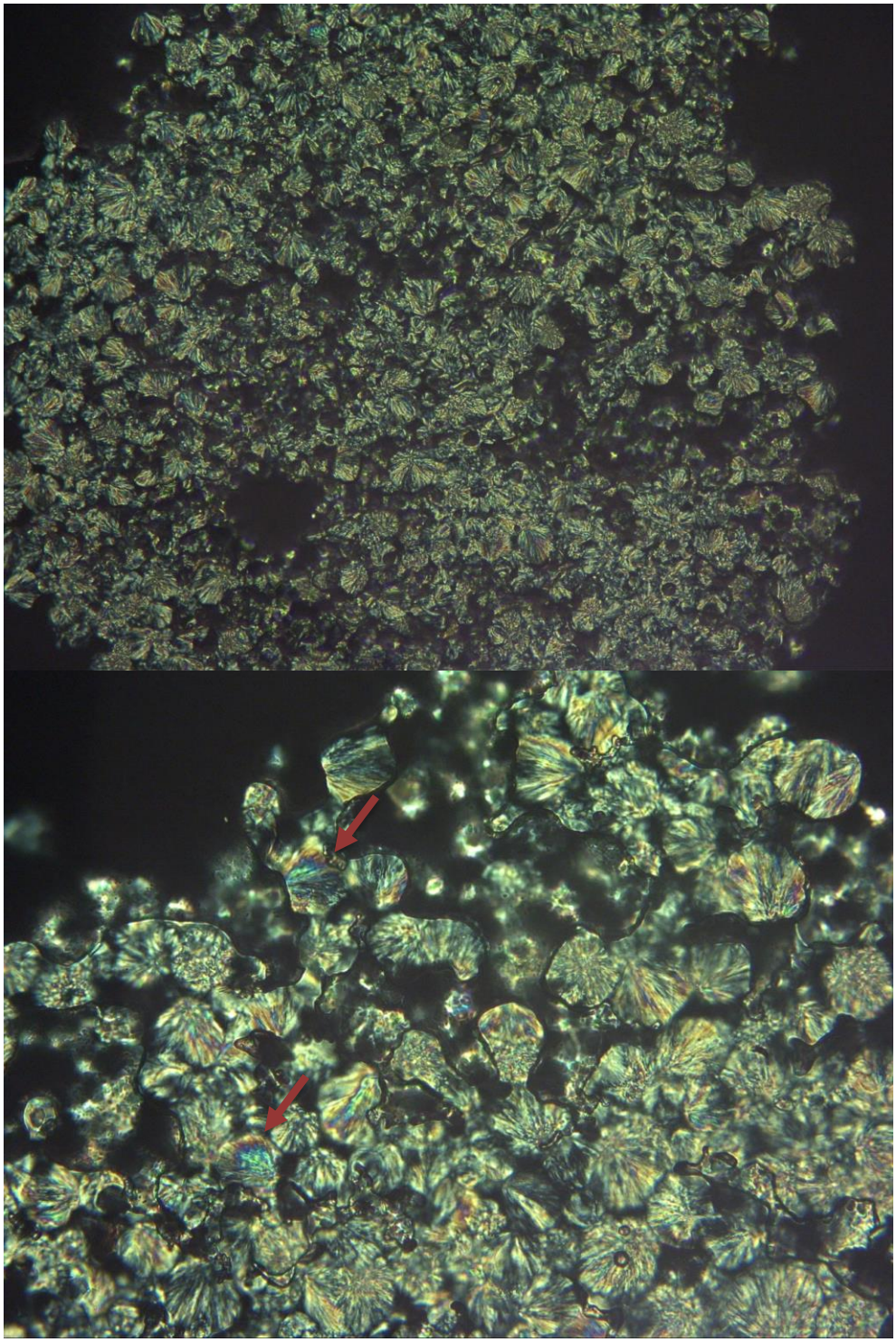

Figure 46. Sections of microspheres of 5% w/v PMMA:PCL = 1:9 with polarized light at (top) 20x and (bottom) 40x magnification

Compared to 20% w/v, 5% w/v PMMA:PCL = 1:9 microspheres were observed in much smaller size largely due to decreased viscosity and smaller emulsified droplets generated during solvent evaporation process (figure 31-33, 45).

Also, as opposed to the cross-sections of 20% w/v PMMA:PCL = 1:9 microspheres (figure 31-33), which could be described as more spherically shaped particles of predominantly crystalline component with negligible amount of birefringence and spherulites, cross-sections of 5% w/v PMMA:PCL = 1:9 microspheres had shown cross-sections of extensively distributed, definite spherulites (figure 46). From the 40x magnification micrograph in figure 46, multicolored and/or birefringent patterns were more identifiable (red arrows) and nearly all sections were in identical spherulitic forms than 20% w/v PMMA:PCL = 1:9 spheres. Although these microspheres were embedded substantially overlapping each other, the morphological characteristics of the microspheres were consistent with most of them projecting radiating arrays of crystalline.

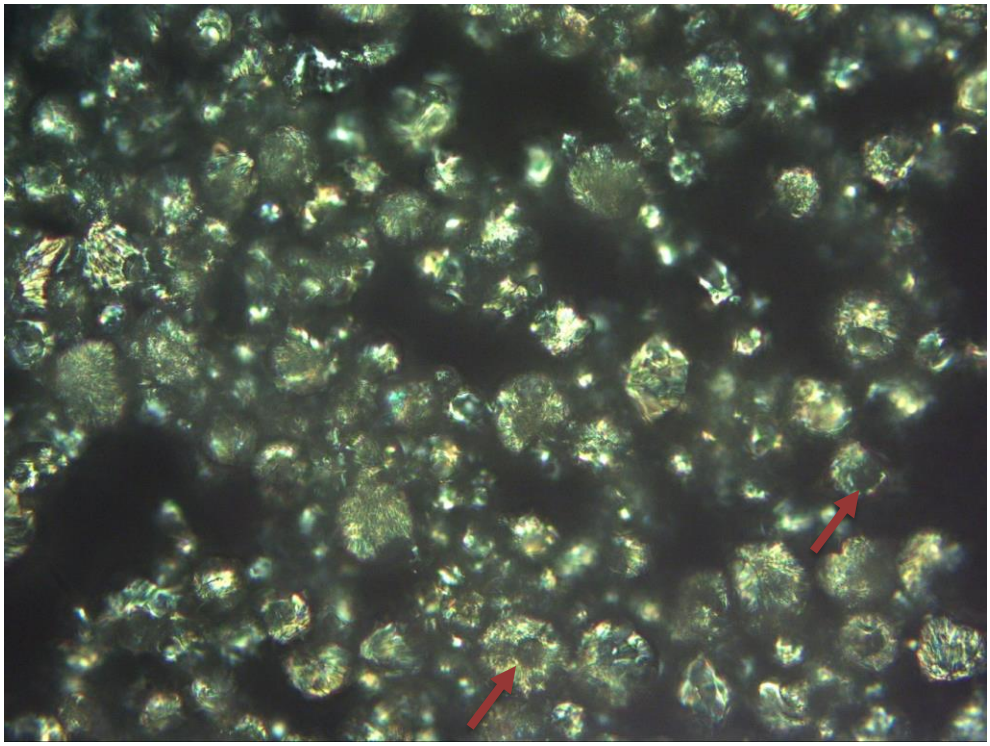

Figure 47. Sections of microspheres of 5% w/v PMMA:PCL = 1:9 with polarized light at 40x magnification

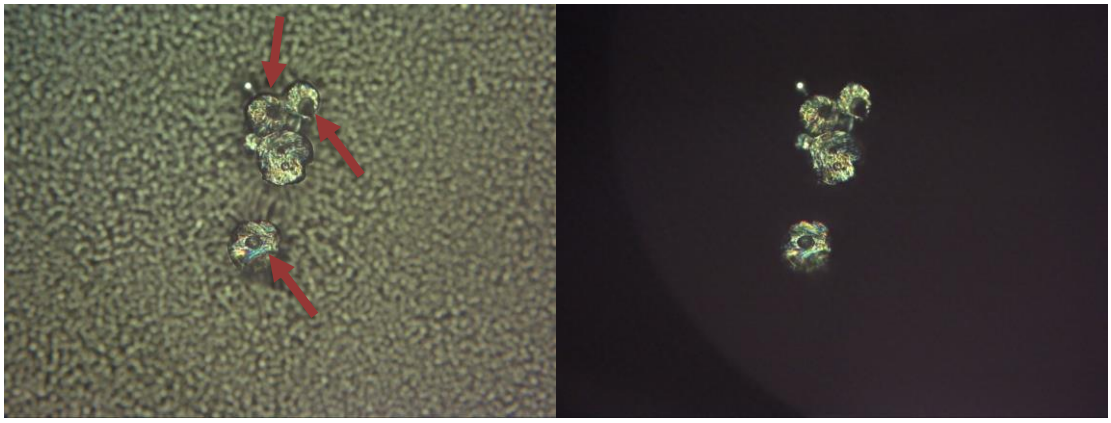
Figure 48. Sections of microspheres of 5% w/v PMMA:PCL = 1:9 (left) without and (right) with polarized light at 40x magnification

Whether or not there were also double wall microspheres was also investigated at higher magnification of 40x (figure 47, 48). As indicated by the red arrows in figure 47 and 48, there were some possible double wall microsphere formation as it could be speculated by darker domains, either representing the amorphous or a cavity. However, it was particularly troublesome to determine whether they were double wall microspheres because they were overspread each other and even at 40x magnification, the particle size was too small to be investigated for their internal morphologies in detail. Nonetheless, there were some definite double wall microspheres formed as shown in figure 48.

5.3.2.2.2. 5% w/v PMMA:PCL = 3:7 microspheres

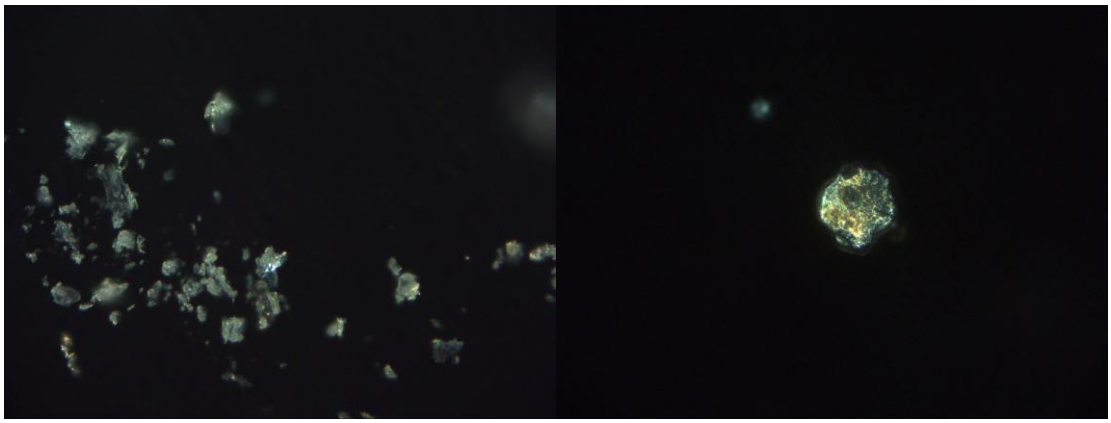

Figure 49. Sections of microspheres of 5% w/v PMMA:PCL = 3:7 with polarized light at 40x magnification

For the cross-sections of 5% w/v PMMA:PCL = 3:7 microspheres, there were not many spherical configurations as shown on the right micrograph in figure 49. The prevailing morphologies were irregularly disfigured (left, figure 49), possibly due to experimental errors and/or rapid precipitation rate. Precipitation kinetics is one of the major factors in determining drug distribution and drug release mechanism, so formulating microspheres in this concentration and in this ratio may not be appropriate for drug encapsulation since it was not able to form spheres. [40] However, this misconfiguration could simply be due to experimental error as all conditions remained identical except for the polymeric concentration (5% w/v, 20% w/v) and the ratios (1:9, 3:7, 1:1, 7:3, 9:1). Still, a few had managed to be configured into a spherical form (right, figure 49), on which spherulite could be observed, a reasonable attribute considering the higher concentration of crystalline PCL. Even the shapeless configurations were shown to be crystalline when examined with cross-polarized light.

5.3.2.2.3. 5% w/v PMMA:PCL = 1:1 microspheres

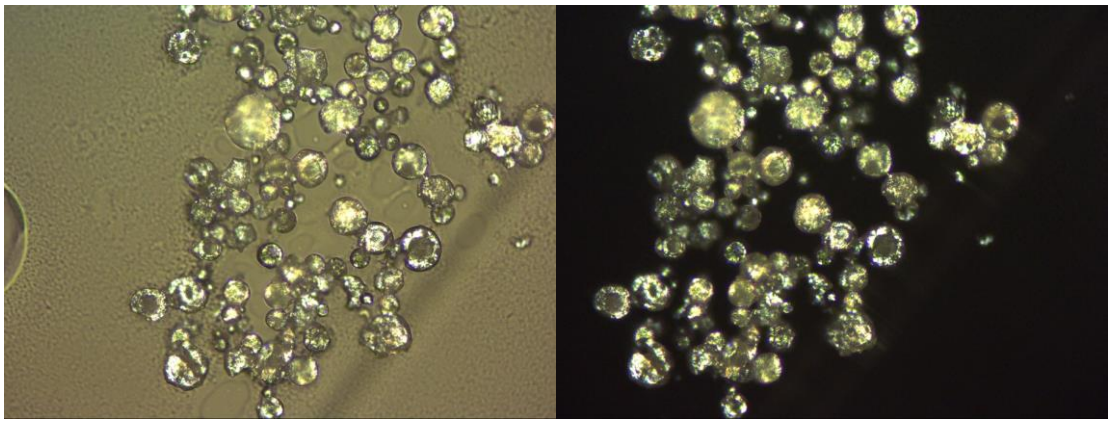

Figure 50. Sections of microspheres of 5% w/v PMMA:PCL = 1:1 (left) without and (right) with polarized light at 20x magnification

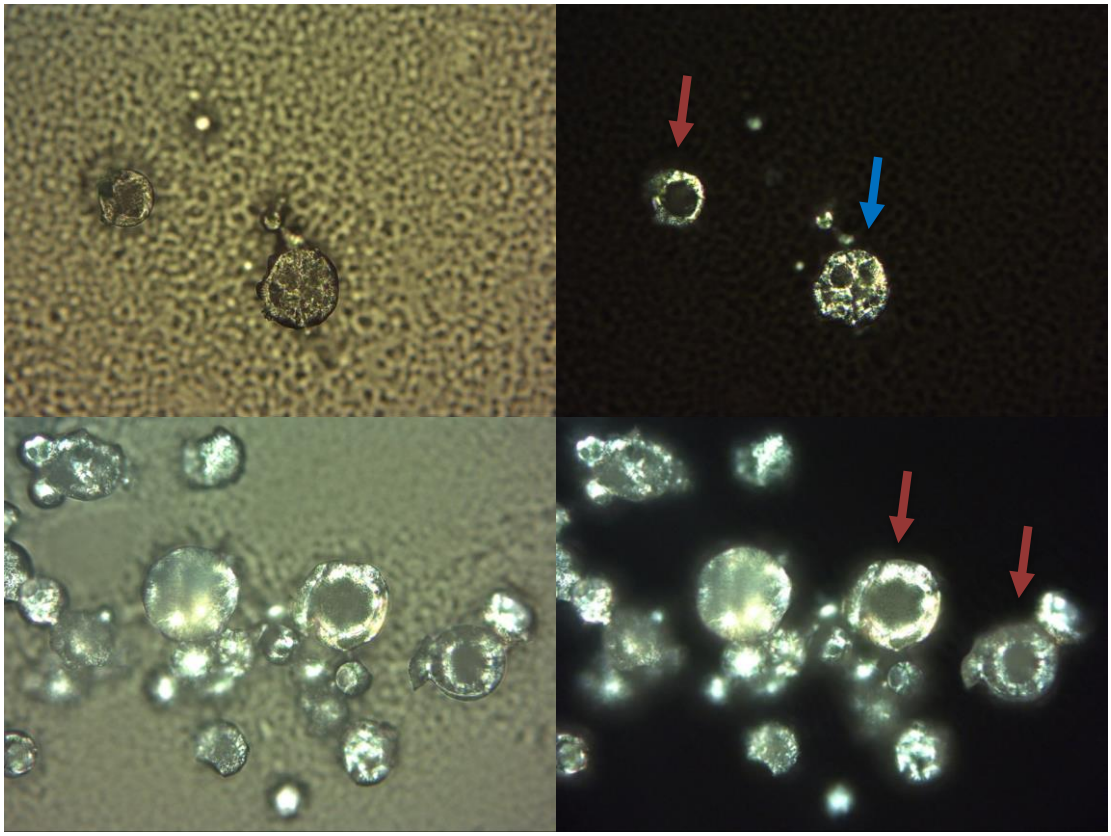

Figure 51. Double wall microspheres of 5% w/v PMMA:PCL = 1:1 (left) without and (right) with polarized light at 40x magnification

Previously, there were different morphologies discovered on the cross-sections of 20% w/v PMMA:PCL = 1:1 with prevalent distribution of completely engulfed double wall microspheres and incompletely engulfed microspheres (figure 37-39).

Likewise, there were both configurations observed from the cross-sections of 5% w/v PMMA:PCL = 1:1 microspheres but in smaller particle size (figure 50, 51). On figure 51, the red arrows indicate completely engulfed microspheres composed of PMMA core and crystalline PCL encapsulating layer and the blue arrows indicate partially phase separated microspheres with focal regions of PCL entrapped within a larger crystalline microsphere.

5.3.2.2.4. 5% w/v PMMA:PCL = 7:3 microspheres

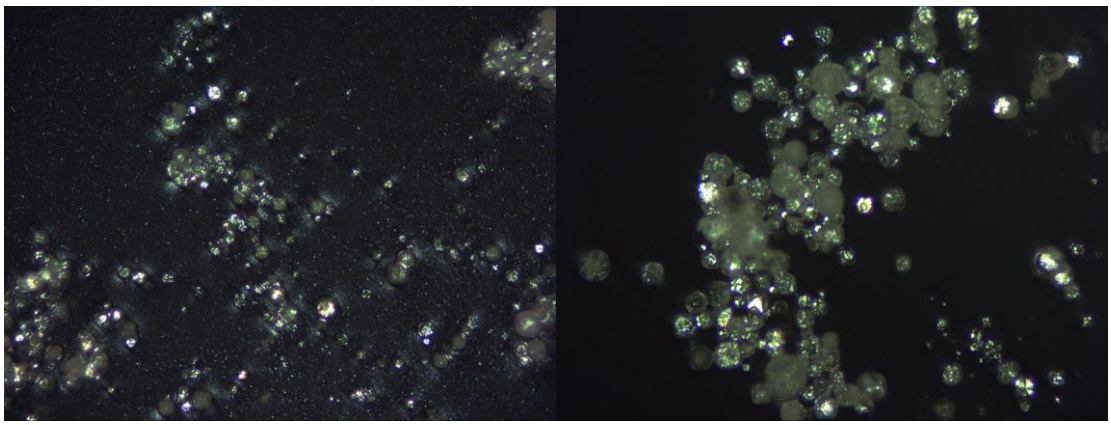

Figure 52. Sections of microspheres of 5% w/v PMMA:PCL = 7:3 with polarized light at (left) 10x and (right) 20x magnification.

Interestingly, the cross-sections of 5% w/v PMMA:PCL = 7:3 microspheres exhibited completely different morphologies from 20% w/v PMMA:PCL = 7:3 microspheres (figure 40, 41, table 4). The microspheres formulated in higher 20% w/v polymeric concentration seemed to compartmentalize amorphous PMMA lined by crystalline PCL structures and the crystal size of PCL was smaller without development of radiating growth of spherulite. However, 10x and 20x micrographs of 5% w/v PMMA:PCL = 7:3 microspheres cross-sections revealed crystalline PCL cores enclosed by distinctive amorphous PMMA outer layers.

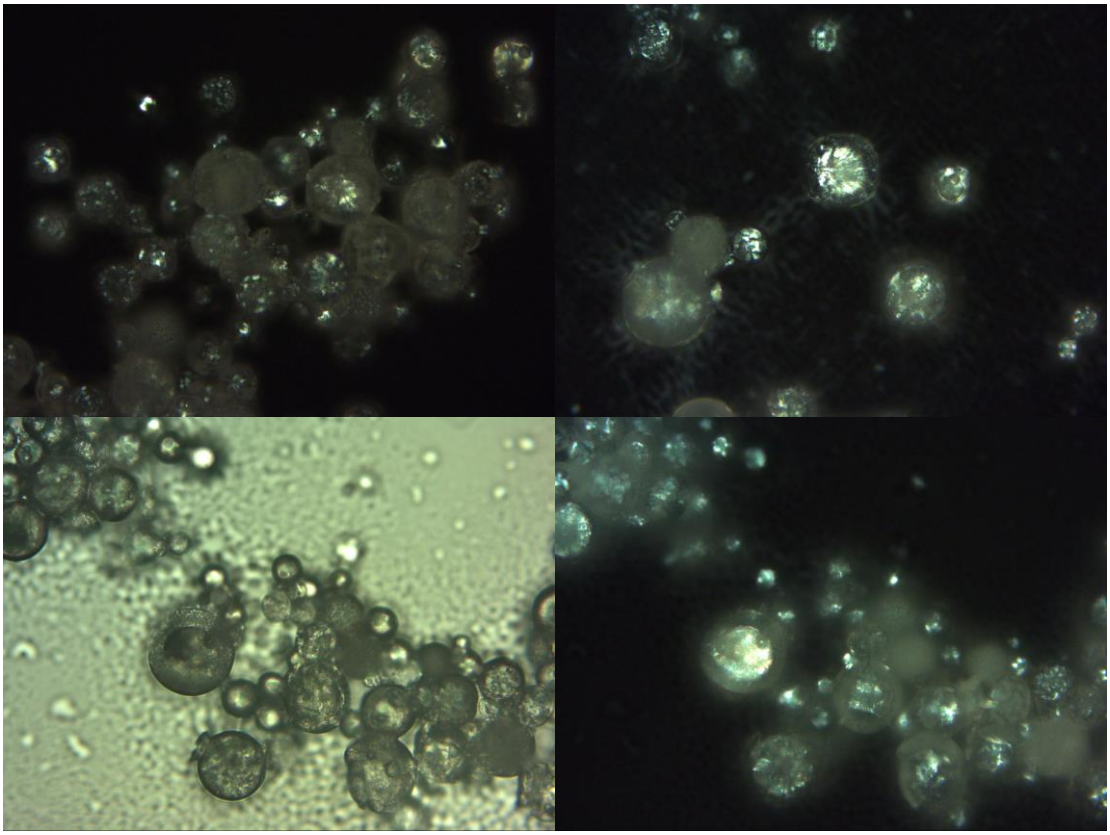

Figure 53. Sections of microspheres of 5% w/v PMMA:PCL = 7:3 with polarized light at 40x magnification.

At higher magnification of 40x, the cores of the 5% w/v PMMA:PCL = 7:3 microspheres cross-sections were highly concentrated in crystalline states (figure 53). This is presumably because of the larger surface areas of smaller 5% w/v microspheres, which slow down the evaporation rate of DCM and allow the spheres sufficient time for complete phase separation into completely engulfed configuration before precipitation or hardening. Also, since microspheres are known to be able to configure themselves into three different configurations depending on the spreading coefficients (figure 3), there could have been changes in the interfacial tensions and energies between PMMA, PCL, and the aqueous solution. [4] There were also completely amorphous cross-sections, potentially the top layers of the microspheres that had not reached the core of complete phase separation and complete engulfment yet.

5.3.2.2.5. 5% w/v PMMA:PCL = 9:1 microspheres

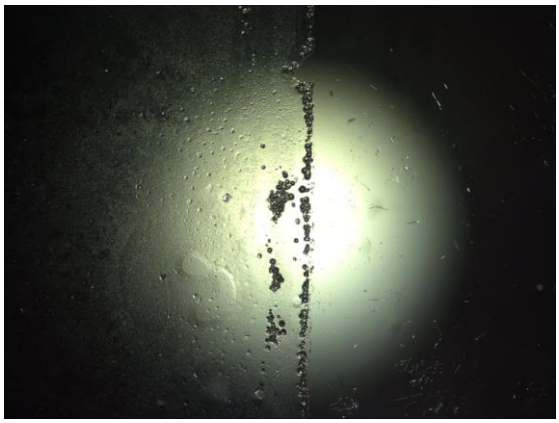

Figure 54. Sections of microspheres of 5% w/v PMMA:PCL = 9:1 with polarized light at 4x magnification.

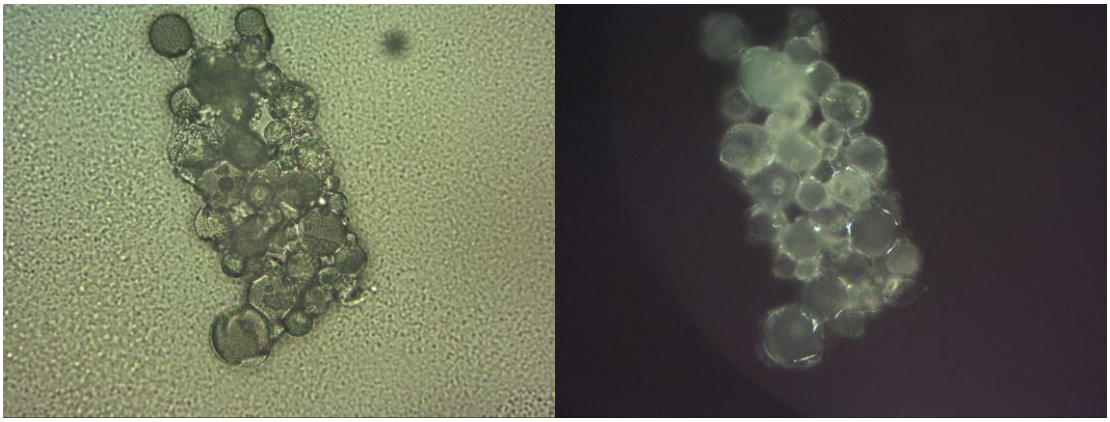

Figure 55. Sections of microspheres of 5% w/v PMMA:PCL = 9:1 (left) without and (right) with polarized light at 40x magnification

Figure 54 shows a micrograph of 5% w/v PMMA:PCL = 9:1 at 4x magnification, demonstrating how smaller the microspheres are compared to the 20% w/v microspheres. Their internal morphologies were also discovered to be in entirely different configurations from those of higher concentration, 20% w/v (figure 42-44). From figure 55, at 40x magnification, the 5% w/v PMMA:PCL = 9:1 microspheres could be identified as completely phase separated and completely engulfed arrangement with relatively amorphous core whereas 20% w/v PMMA:PCL = 9:1 microspheres had several local regions of condensed crystalline PCL (figure 44).

With slower evaporation rate, the focal regions of crystalline in 20% w/v microspheres might have merged into uniform core of PCL encapsulated by PMMA layer. However, 5% w/v microspheres already formed with two distinct components of amorphous core and thin encapsulating crystalline outer layer (figure 55, appendix 17). Thin, slight crystalline layer could be explained by the PMMA:PCL ratio of 9:1 since the ratio of crystalline PCL was much lower. However, how different polymeric concentrations of 5% w/v and 20% w/v of the microsphers of same PMMA:PCL ratio developed into discrete morphologies needs to be further investigated. It was potentially due to changes in interfacial surfaces between the polymers and the organic solvent during solvent evaporation process and how polymeric concentrations could affect interfacial tensions could be a point of further studies.

6. Conclusions

In the work presented here, different blends of 20% w/v 5% w/v PMMA/PCL film casts and microspheres were assessed with cross-polarized light to determine the state of phase separation. By comparing these film casts and microspheres, different polymer concentrations and PMMA:PCL ratios seemed to influence phase separation phenomenon and their internal morphologies. Largely from the film casts, the polymer in higher concentration seemed to be in predominance in the process of phase separation. The film casts with higher concentration of PCL were observed with more crystalline structures and sometimes with formation of spherulites, which represent higher degree of crystallinity. With higher concentration of PMMA, on the other hand, amorphous PMMA seemed to interfere with crystallization of PCL, obstructing the formation of spherulites. Instead, the size of the crystals was smaller and the majority of these film casts had darker amorphous structures. Additionally,

depending on polymer concentrations and ratios, the microspheres were found to be capable of formulating themselves into many different configurations. From the cross-sections of the microspheres, there were two major configurations observed; completely engulfed double wall microspheres and incompletely phase separated, but in neither the partially engulfed nor completely engulfed conformations. To elaborate, there were some formations of completely engulfed double wall microspheres, but there were also configurations with focal regions of one type of polymer entrapped in larger sphere of the other polymer. Presumably, these incomplete configurations had insufficient time for complete phase separation and failed to develop into completely engulfed double wall microspheres. In such cases, evaporation rate of organic solvent is considered to be faster than the rate of phase separation, so slowing down the DCM evaporation could an experiment for future studies. However, it is also essential that the film casts and the microspheres of the same concentrations and ratios do not necessarily correspond to each other although there were still significant similarities between the film casts and the microspheres. This is possibly due to different interfacial tensions caused by disparate formation methods of film casts and microspheres as spreading coefficients and interfacial tensions are major parameters that drive different double wall microsphere configurations. [4]

Additionally, size of the microspheres is also an important factor in micro and nanoparticles in the pharmaceutical fields. Particle size can influence drug encapsulation efficiency, drug release kinetics, and more. [40] However, because fixing microspheres on the equal, parallel layer was unsolvable for the duration of this project, it was unachievable to compare the microspheres of the same polymeric concentrations and ratios at the same horizontal level. Also, from solvent evaporation process, monodisperse particles cannot be acquired because the emulsified droplets

generated during solvent evaporation process are not equal in size as it could be seen from the SEM images (figure 24, 26-27, appendix 10). Therefore, the microspheres created from solvent evaporation process cannot be uniform without an extra instrument called homogenizer with identically sized holes or spherical slots, through which the pre-precipitated droplets are discharged (figure 25).

Thus, future work built on from this project could include developing methods for uniform sized microspheres. Another is to seek methods to form smaller particles in nano-scale such as by increasing the stirring rate and/or shearing rate during solvent evaporation process or any other processes capable of creating polymeric spheres. Jelvehgari et al. proved that the increasing the stirring rate results in high turbulence and decreases the size of the microspheres. [41] Slower stirring rate allows particles to coalesce and aggregate, increasing the overall particle size and all of the microspheres created at the stirring rate of approximately 1,300 rpm for this project were in micrometer (um) range. The 5% w/v microspheres that were created with homogenizer were not cryo-sectioned yet and evaluated, but further studies could include examining and comparing them to the spheres created without the homogenizer. Another factor would be increasing the emulsifier (PVA) concentration, which would stabilize the droplets. [41, 42] With increasing attention and application of nanotechnology in drug development and delivery, nanoparticles could overcome biological barriers such as blood-brain barrier (BBB) and effectively deliver hydrophobic therapeutic agents to preferential target sites such as tumor vasculature. [43-47] However, because nanoparticles are complex multicomponent product with specific arrangement, there still entail many difficulties in nanosphere formation such as formulation stability, reproducibility, biocompatibility, and more, but formulating

PMMA/PCL double wall particle in nano-scale could be conducted for future studies.

[43-48]

References

1. Yujie Xia, Pedro F. Ribeiro, Daniel W. Pack, Controlled protein release from monodisperse biodegradable double-wall microspheres of controllable shell thickness, Journal of Controlled Release, Volume 172, Issue 3, 2013, Pages 707-714, ISSN 0168-3659.

2. Yujie Xia, Qingxing Xu, Chi-hwa Wang, Daniel W. Pack, Protein Encapsulation in and Release from Monodisperse Double-Wall Polymer Microspheres, Journal of Pharmaceutical Sciences, Volume 102, Issue 5, 2013, Pages 1601-1609, ISSN 0022-3549.

3. Qi, F., Wu, J., Li, H. et al. Front. Chem. Sci. Eng. (2019) 13: 14.

4. Kathleen J.Pekarek, Jules S. Jacob, Edith Mathiowitz*. Double-walled polymer microspheres for controlled drug release. (Nature, Vol 367, 20 January 1994).

5. Harvey A J, Kaestner S A, Sutter D E, Harvey N G, Mikszta J A, Pettis R J. Microneedle-based intradermal delivery enables rapid lymphatic uptake and distribution of protein drugs. Pharmaceutical Research, 2011, 28(1): 107–116

6. Okada H. One-and three-month release injectable microspheres of the LH-RH superagonist leuprorelin acetate. Advanced Drug Delivery Reviews, 1997, 28(1): 43–70

7. Han F Y, Thurecht K J, Whittaker A K, Smith M T. Bioerodable PLGA-based microparticles for producing sustained-release drug formulations and strategies for improving drug loading. Frontiers in Pharmacology, 2016, 7: 185

8. James M. Anderson, Matthew S. Shive, Biodegradation and biocompatibility of PLA and PLGA microspheres, Advanced Drug Delivery Reviews, Volume 64, Supplement, 2012, Pages 72-82, ISSN 0169-409X

9. Robinson, J. R.; Lee, V. H. L. *Controlled Drug Delivery: Fundamentals and Applications*; Marcel Dekker: New York, 1987.

10. Burkoth, A. K.; Anseth, K. S. *Biomaterials*2000, 21, 2389.

11. West, B. L.; Kazarian, S. G.; Vincent, M. F.;Brantley, N. H.; Eckert, C. A. *J Appl Polym Sci*1998, 69, 911.

12. Tams, J.; Joziasse, C. A. P.; Bos, R. R. M.;Rozema, F. R.; Grijpma, D. W.; Pennings, A. J.*Biomaterials* 1995, 16, 1049.

13. Domingo, C. , Vega, A. , Fanovich, M. A., Elvira, C. and Subra, P. (2003), Behavior of poly(methyl methacrylate)–based systems in supercritical CO_2 and CO_2 plus cosolvent: Solubility measurements and process assessment. J. Appl. Polym. Sci., 90: 3652-3659.

14. Middleton, J. C. *Biomaterials* 2000, 21,2335.

15. Du, J.; Jasti, B.; Vasavada, R. C. *J Controlled Release* 1997, 43, 223.

16. Lin, W.- J.; Lu, C.- H. *J Membr Sci* 2002, 198109.

17. Hubbell, D. S.; Cooper, S. L. *J Appl Polym Sci* 1977, 21, 3035.

18. Abraham, G. A.; Gallardo, A.; Motta, A.;Migliaresi, C.; San Román, J. *Macromol Mater Eng* 2000, 282, 44.

19. Siripurapu, S.; Gay, Y. J.; Royer, J. R.;DeSimone, J. M.; Khan, S. A.; Spontak, R. J.*Mater Res Soc Symp* 2000, 629, FF991.

20. Domb, A. J., Ed. *Polymeric Site Specific Pharmacotherapy*; Wiley: New York, 1994.

21. Siakumar, M.; Panduranga Rao, K. *React Funct Polym* 2000, 46, 29.

22. Walenkamp, G. H. I. *Biomaterials in Surgery*; Thieme- Verlag Medical Publishers:Stuttgart, Germany, 1998.

23. Kim, H. D.; Valentini, R. F. *Biomaterials*1997, 18, 1175.

24. Shibaev, V. & Lam, L. *Liquid Crystalline and Mesomorphic Polymers*. (1994).

25. Brazel, C. & Rosen, S. *Fundamental Principles of Polymeric Materials*. (Wiley, 2012).

26. Nishida, H. & Tokiwa, Y. Effects of higher-order structure of Poly(3-hydrolxybutyrate) on biodegradation. ll Effects of crystal structure on microbial degradation. *J. Environ. Polym. Degrad.* 1, 65–80 (1993).

27. "Spherulite (Polymer Physics)." *Wikipedia*, Wikimedia Foundation, 19 Mar. 2019, en.wikipedia.org/wiki/Spherulite_(polymer_physics).

28. Keller, A. (1955), The spherulitic structure of crystalline polymers. Part I. Investigations with the polarizing microscope. J. Polym. Sci., 17: 291-308. doi:10.1002/pol.1955.120178414

29. The Gibbs free energy curves of mixing have been calculated with the compressible regular solution free energy model of Ruzette and Mayes[2].

30. Anne-Valerie G. Ruzette and Anne M. Mayes, *Macromolecules* 34, 1894-1907 (2001)

31. The process of nucleation and growth is not limited to polymer blends but has been observed for many other mixtures.

32. L. B. Peppas, “Recent advances on the use of biodegradable microparticles and nanoparticles in controlled drug-delivery,” Int. J. Pharm., vol. 116, no. 1, pp. 1– 9, 1995.

33. K. E. Uhrich, S. M. Cannizzaro, R. S. Langer, and K. M. Shakesheff, “Polymeric Systems for Controlled Drug Release,” Chem. Rev, vol. 99, pp. 3181–3198, 1999.

34. V. P. Torchilin, “Polymer-coated long-circulating microparticulate

35. “The Field of Homogenizing.” *Homogenizers for Mixing, Dispersing, and Emulsifying*, proscientific.com/the-field-of-homogenizing.

36. Yoshida S, Kikuchi S, Kanehashi S, Okamoto K, Ogino K. Microfluidic Fabrication of Morphology-Controlled Polymeric Microspheres of Blends of Poly(4-butyltriphenylamine) and Poly(methyl methacrylate). *Materials (Basel)*. 2018;11(4):582. Published 2018 Apr 10. doi:10.3390/ma11040582

37. Gisela. “Brief Introduction to Coating Technology for Electron Microscopy.” *Learn & Share | Leica Microsystems*, 28 Aug. 2013, www.leica-microsystems.com/science-lab/brief-introduction-to-coating-technology-for-electron-microscopy/.

38. Tagaya A. (2015) Birefringence of Polymer. In: Kobayashi S., Müllen K. (eds) Encyclopedia of Polymeric Nanomaterials. Springer, Berlin, Heidelberg

39. Reddy VR et al., Factors Affecting Microspheres Formation. American Journal of PharmTech Research 2015.

40. Berkland, Cory & Kipper, Matt & Narasimhan, Balaji & Kim, Kyekyoon & Pack, Daniel. (2004). Microsphere size, precipitation kinetics and drug distribution control drug release from biodegradable polyanhydride microspheres. Journal of controlled release : official journal of the Controlled Release Society. 94. 129-41. 10.1016/j.jconrel.2003.09.011.

41. Jelvehgari M, Nokhodchi A, Rezapour M, Valizadeh H. Effect of formulation and processing variables on the characteristics of tolmetin microspheres prepared by double emulsion solvent diffusion method. *Indian J Pharm Sci*. 2010;72(1):72–78. doi:10.4103/0250-474X.62251

42. Perumal D, Dangor CM, Alcock RS, Hurbans N, Moopanar KR. Effect of formulation variables on *in vitro* release and micromeritic properties of modified release ibuprofen microspheres. J Microencapsul. 1999;16:475–87.

43. Desai N. Challenges in development of nanoparticle-based therapeutics. *AAPS J*. 2012;14(2):282–295. doi:10.1208/s12248-012-9339-4

44. Alonso MJ. Nanomedicines for overcoming biological barriers. Biomed Pharmacother Biomed Pharmacother. 2004;58(3):168–172.

45. Silva GA. Nanotechnology approaches to crossing the blood–brain barrier and drug delivery to the CNS. BMC Neurosci. 2008;9(Suppl 3):S4. doi: 10.1186/1471-2202-9-S3-S4.

46. Dong X, Mumper RJ. Nanomedicinal strategies to treat multidrug-resistant tumors: current progress. Nanomedicine (London, England) 2010;5(4):597–615. doi: 10.2217/nnm.10.35.

47. Greish K. Enhanced permeability and retention of macromolecular drugs in solid tumors: a royal gate for targeted anticancer nanomedicines. J Drug Target. 2007;15(7–8):457–464. doi: 10.1080/10611860701539584.

48. De Jong WH, Borm PJ. Drug delivery and nanoparticles:applications and hazards. *Int J Nanomedicine*. 2008;3(2):133–149.

49. Gelperina S, Kisich K, Iseman MD, Heifets L. The potential advantages of nanoparticle drug delivery systems in chemotherapy of tuberculosis. *Am J Respir Crit Care Med*. 2005;172(12):1487–1490. doi:10.1164/rccm.200504-613PP

50. Asanishi, M & Takaki, Tomohiro & Tomita, Yoshihiro. (0002). Polymer Spherulite Growth Simulation during Crystallization by Phase-Field Method. AES-ATEMA International Conference Series - Advances and Trends in Engineering Materials and their Applications. 195-203.

51. Georg Menges, Edmund Haberstroh, Walter Michaeli, Ernst Schmachtenberg: Plastics Materials Science Hanser Verlag, 2002, ISBN 3-446-21257-4

52. Charles E. Carraher; Raymond Benedict Seymour (2003). Seymour/Carraher's polymer chemistry. CRC Press. pp. 44–45. ISBN 0-8247-0806-7.

53. Cornelia Vasile (2000). Handbook of polyolefins. CRC Press. p. 183. ISBN 0-8247-8603-3.

54. Linda C. Sawyer; David T. Grubb; Gregory F. Meyers (2008). Polymer microscopy. Springer. p. 5. ISBN 0-387-72627-6.

55. David I. Bower (2002). An introduction to polymer physics. Cambridge University Press. pp. 133–136. ISBN 0-521-63721-X.

Appendix

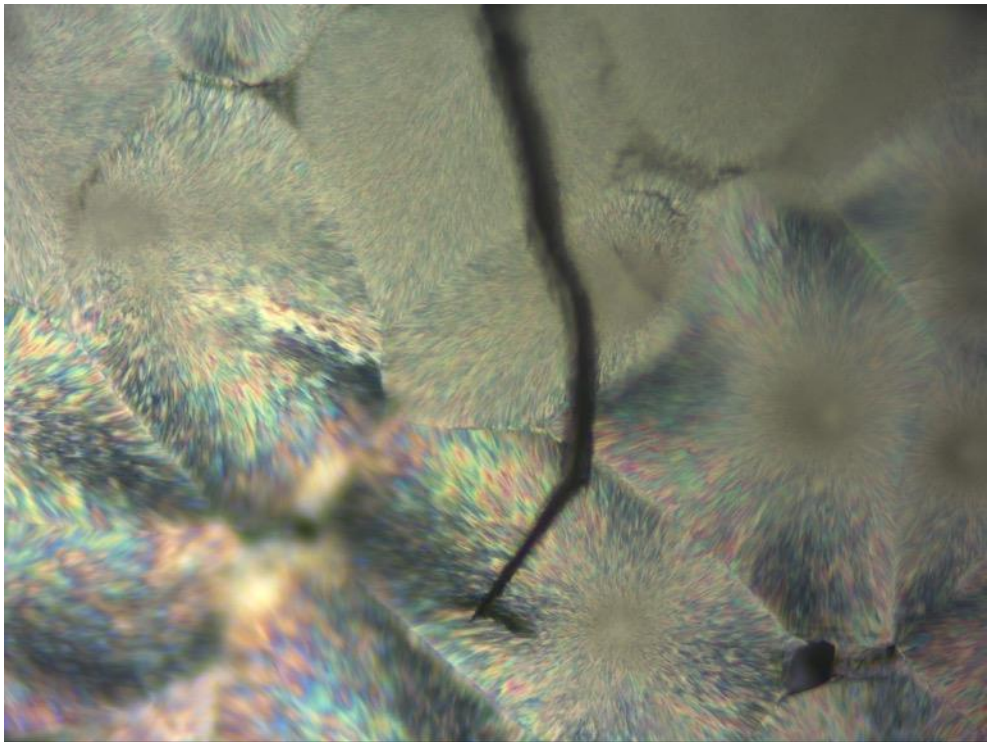

Appendix 1. Film Cast of 20% w/v PMMA:PCL = 1:9 at 40x magnification with polarized light.

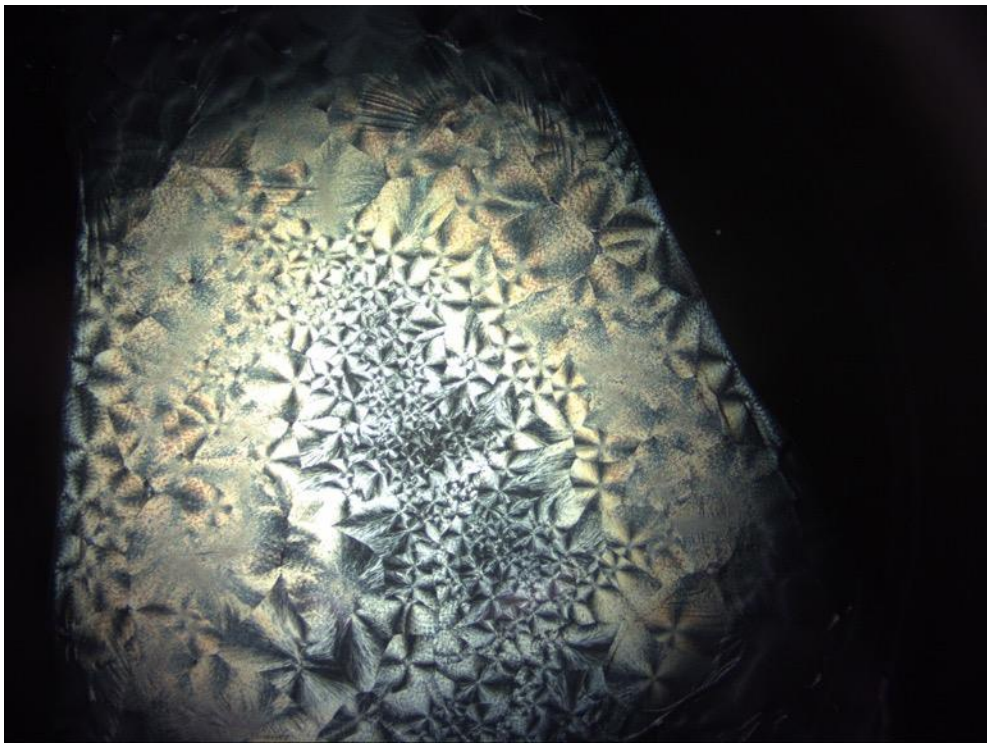

Appendix 2. Film Cast of 20% w/v PMMA:PCL = 3:7 at 4x magnification with polarized light

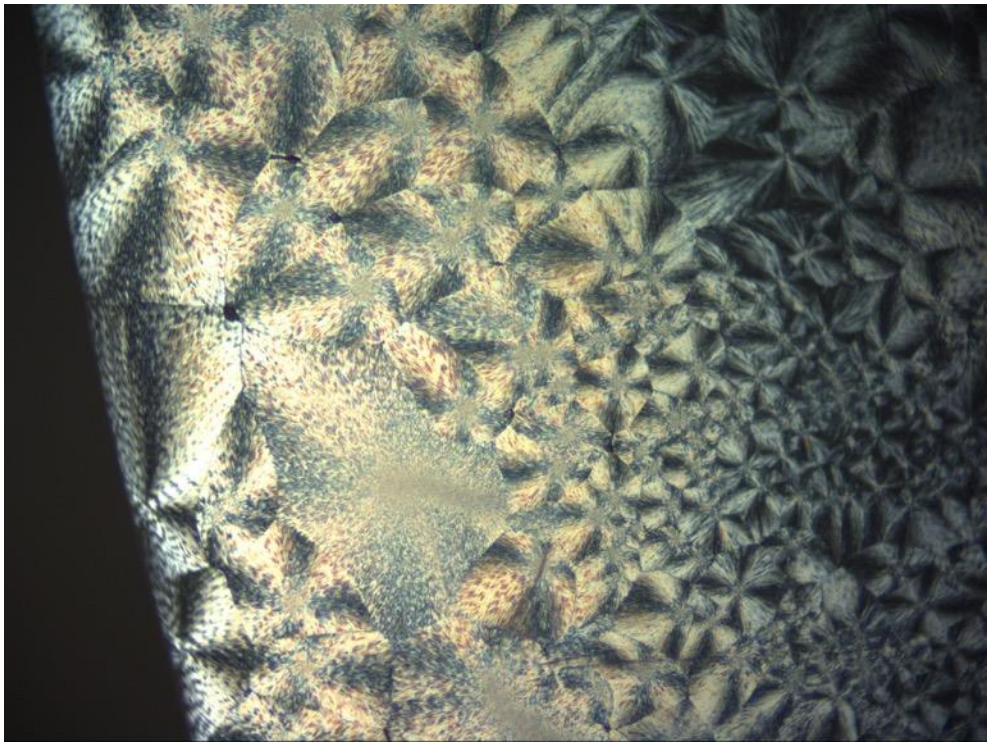

Appendix 3. Film Cast of 20% w/v PMMA:PCL = 3:7 at 10x magnification with polarized light

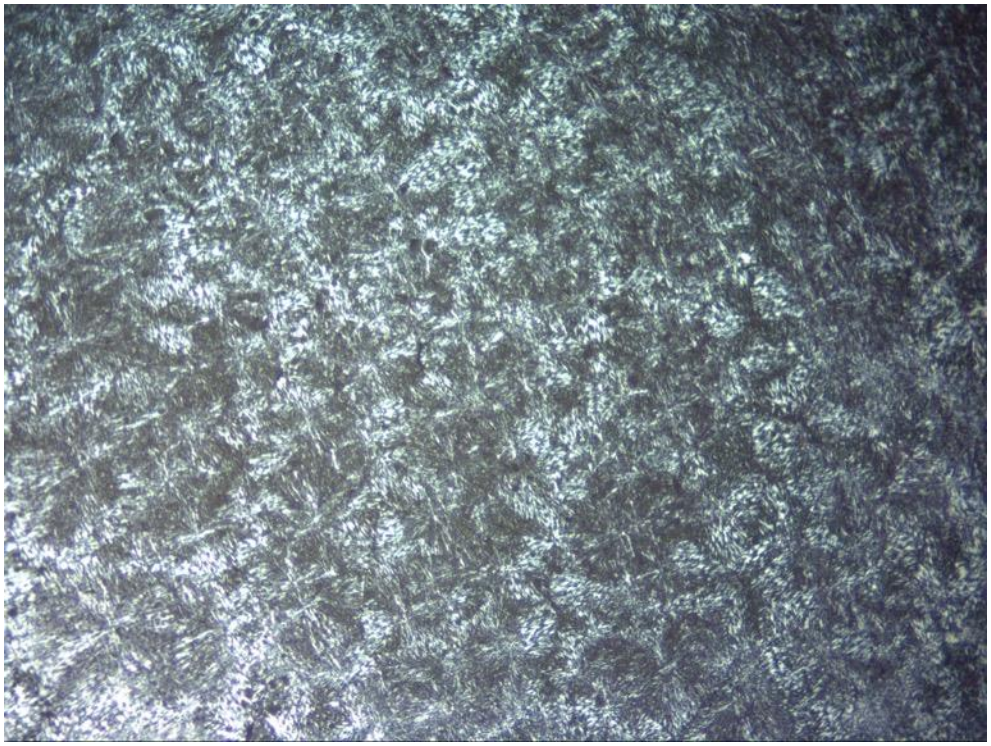

Appendix 4. Film Cast of 20% w/v PMMA:PCL = 1:1 at 20x magnification with polarized light

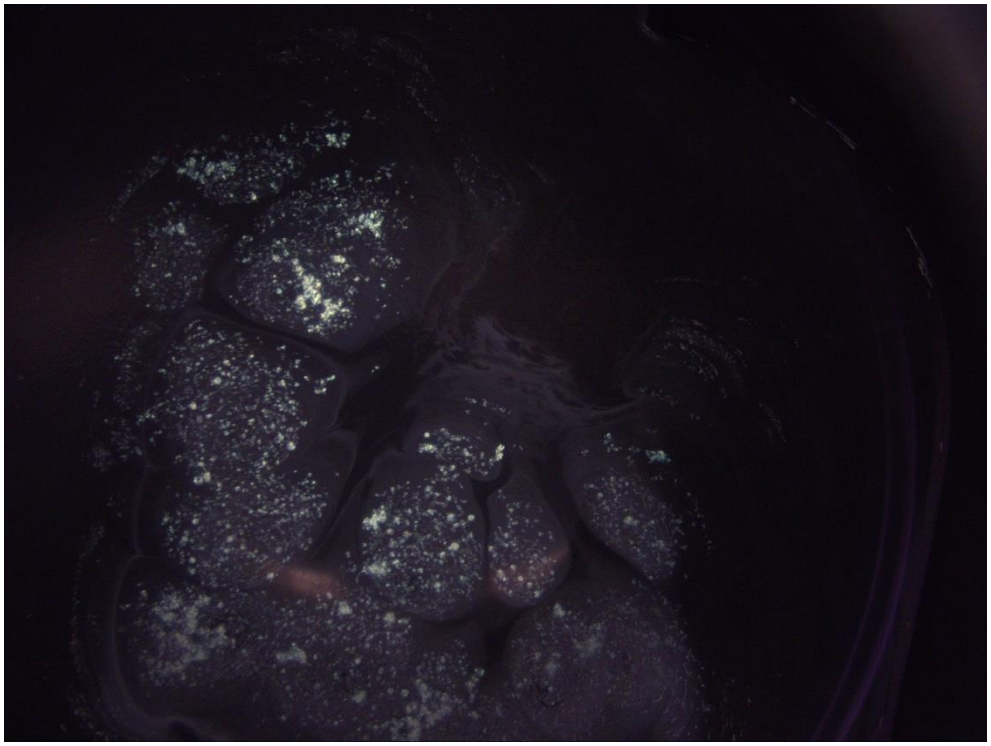

Appendix 5. Film Cast of 20% w/v PMMA:PCL = 7:3 at 4x magnification with polarized light

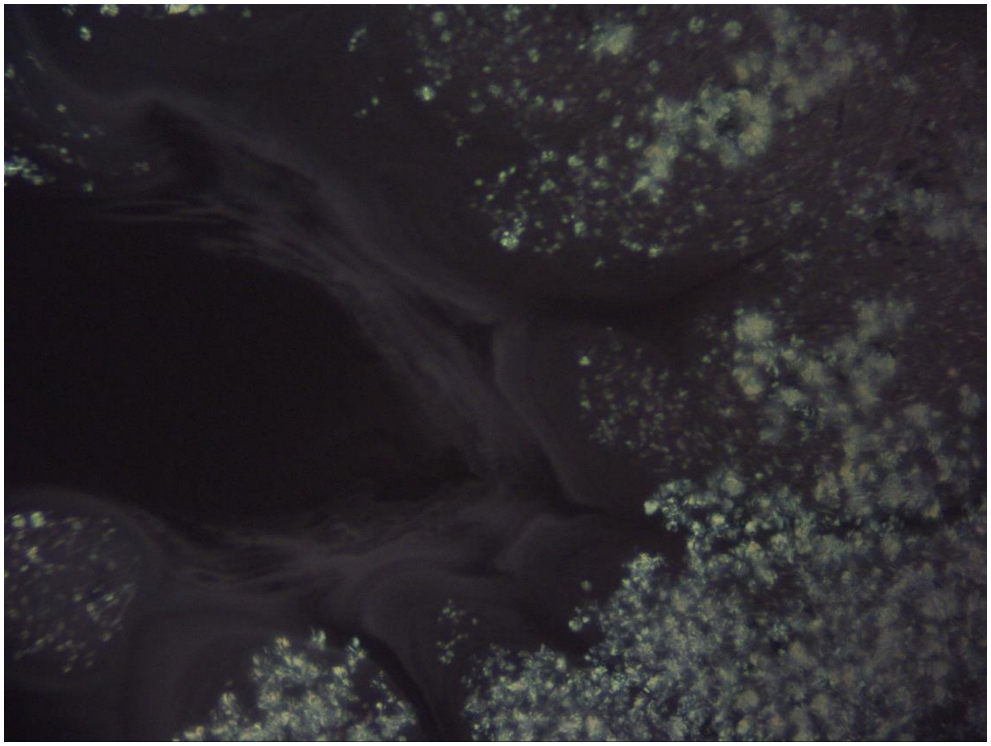

Appendix 6. Film Casts of 20% w/v PMMA:PCL = 7:3 at 20x magnification with polarized light at lower intensity.

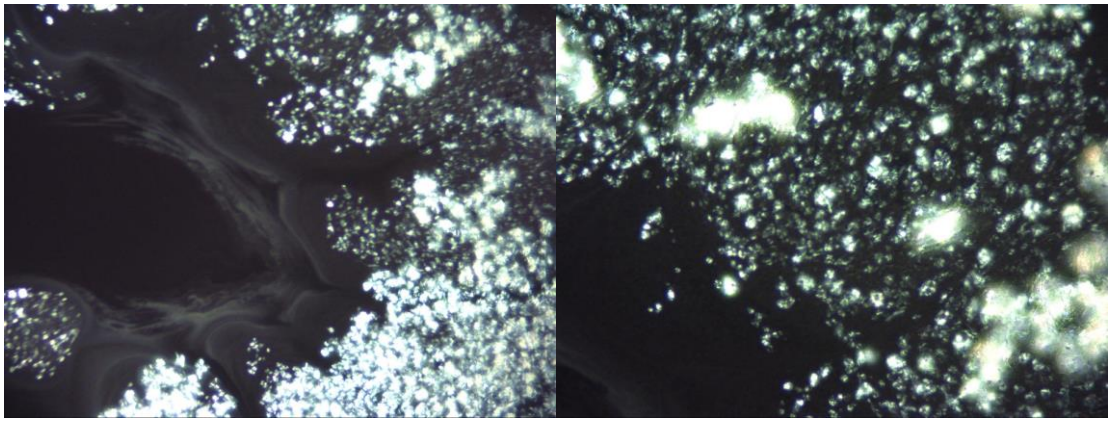

Appendix 7. Film Cast of 20% w/v PMMA:PCL = 7:3 at 20x magnification with polarized light.

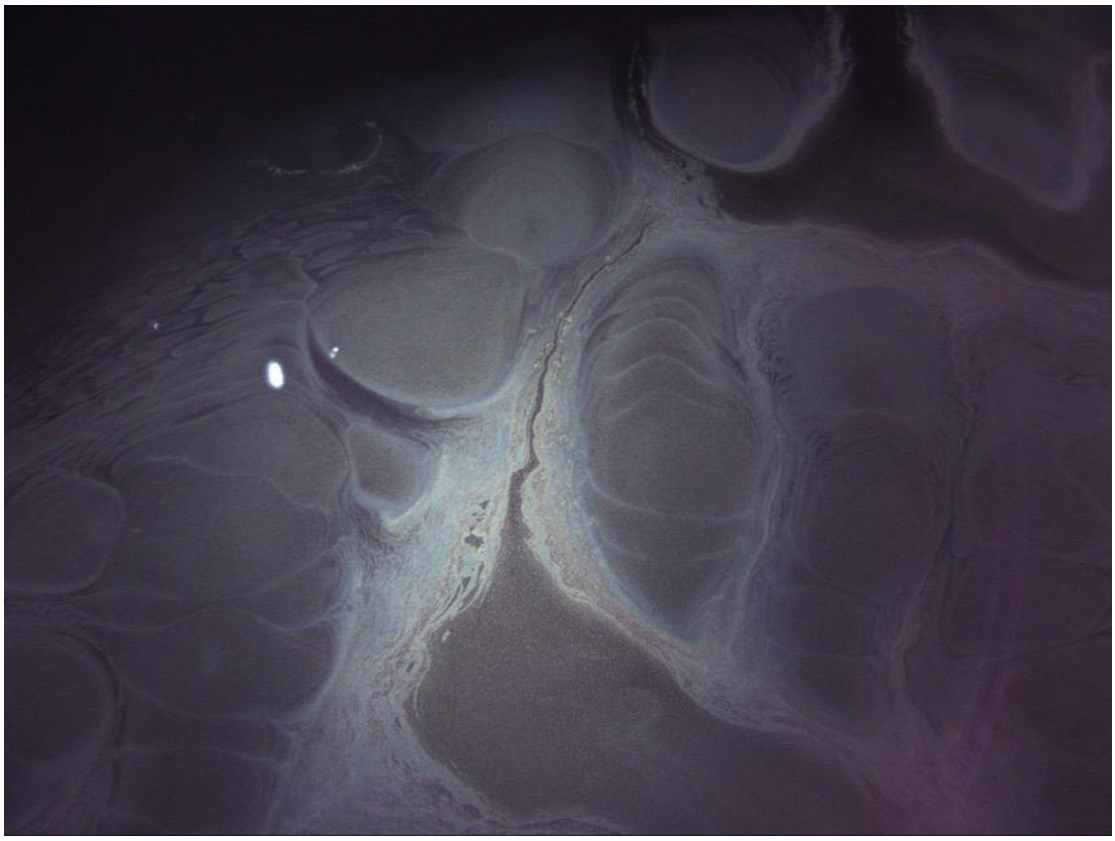

Appendix 8. Film Cast of 20% w/v PMMA:PCL = 9:1 at 4x magnification with polarized light

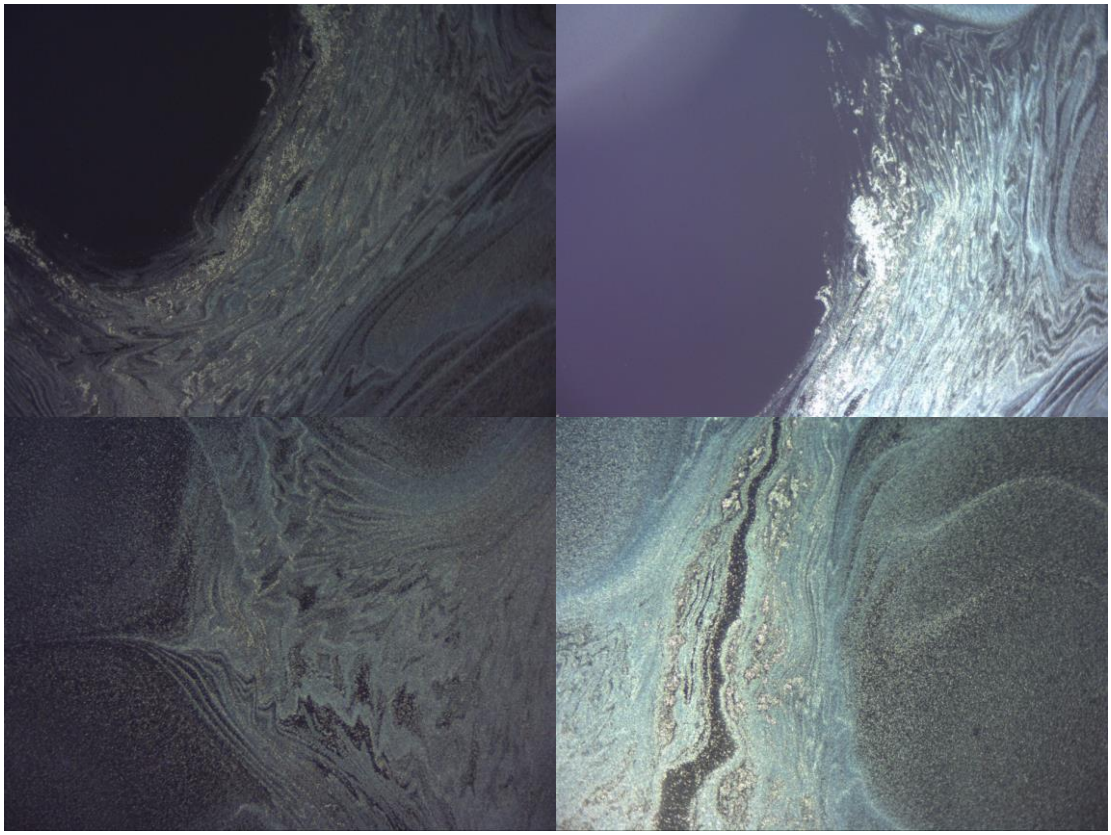

Appendix 9. Film Casts of 20% w/v PMMA:PCL = 9:1 at 40x magnification with polarized light at different light intensities. Focused on crystalline edges.

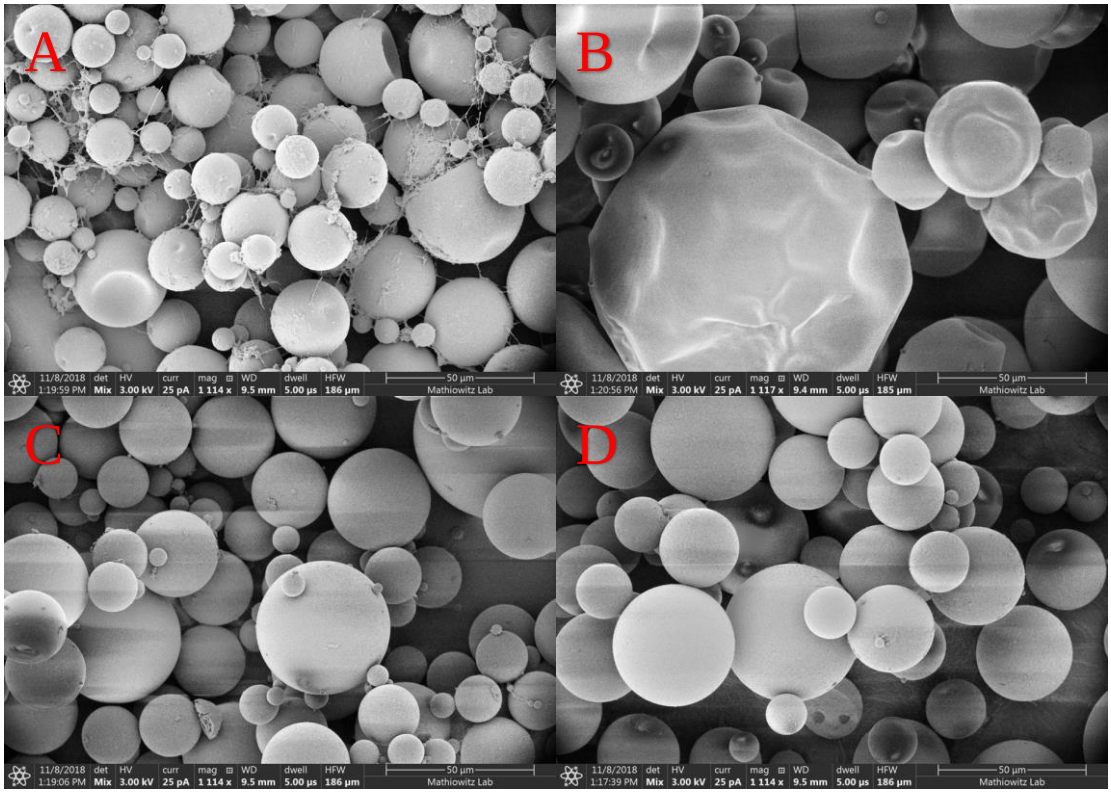

Appendix 10. SEM of 5% w/v PMMA:PCL microspheres. Ratios of 5% PMMA:PCL are (A) 3:7, (B) 1:1, (C) 7:3, and (D) 9:1.

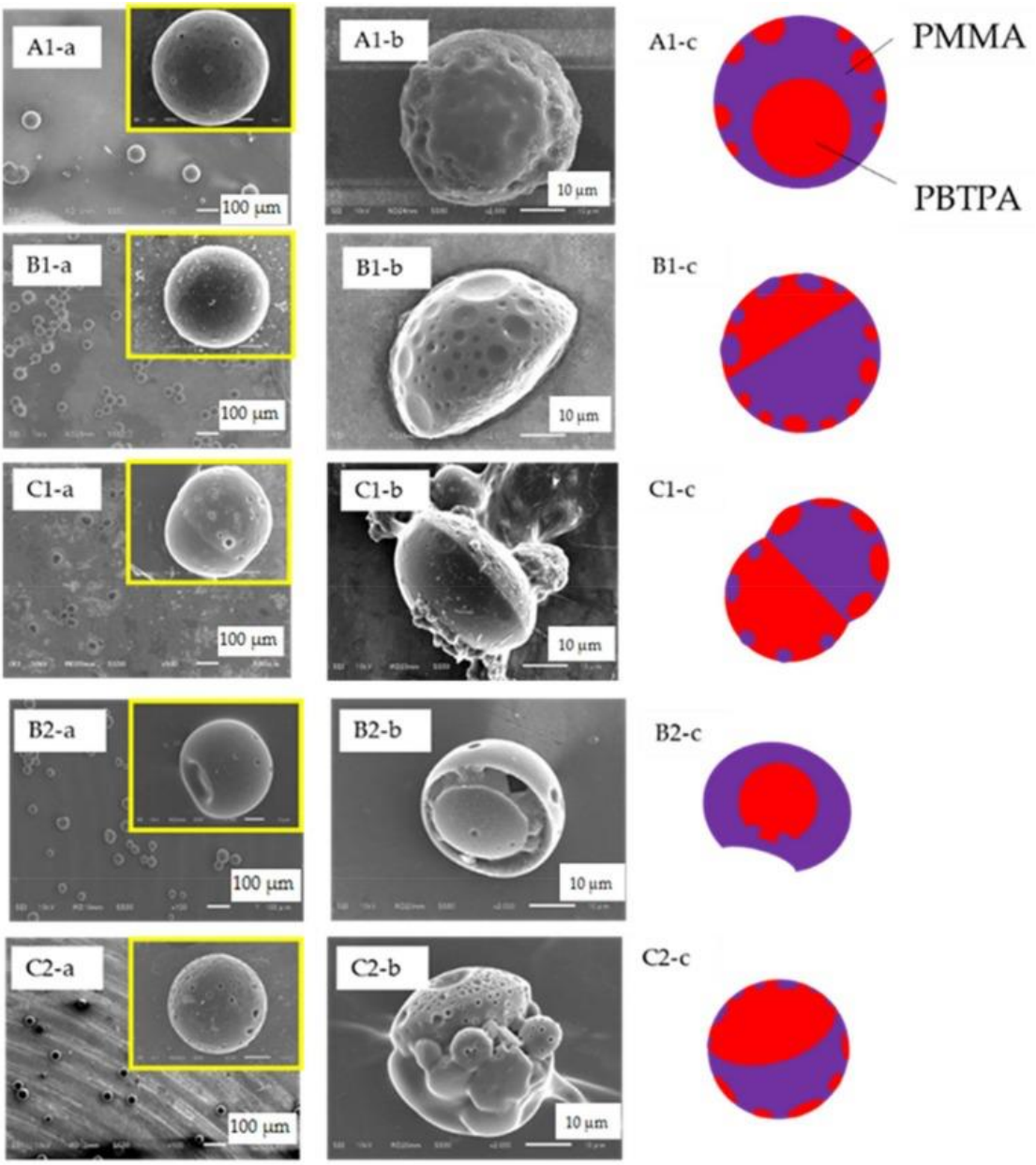

Appendix 11. SEM images of microspheres of PBTPA/PMMA prepared with the conditions listed in Table 1 (A1, B1, B2, C1, and C2), (a) as-prepared, (b) after soaking with acetone, (c) schematic models. [36]

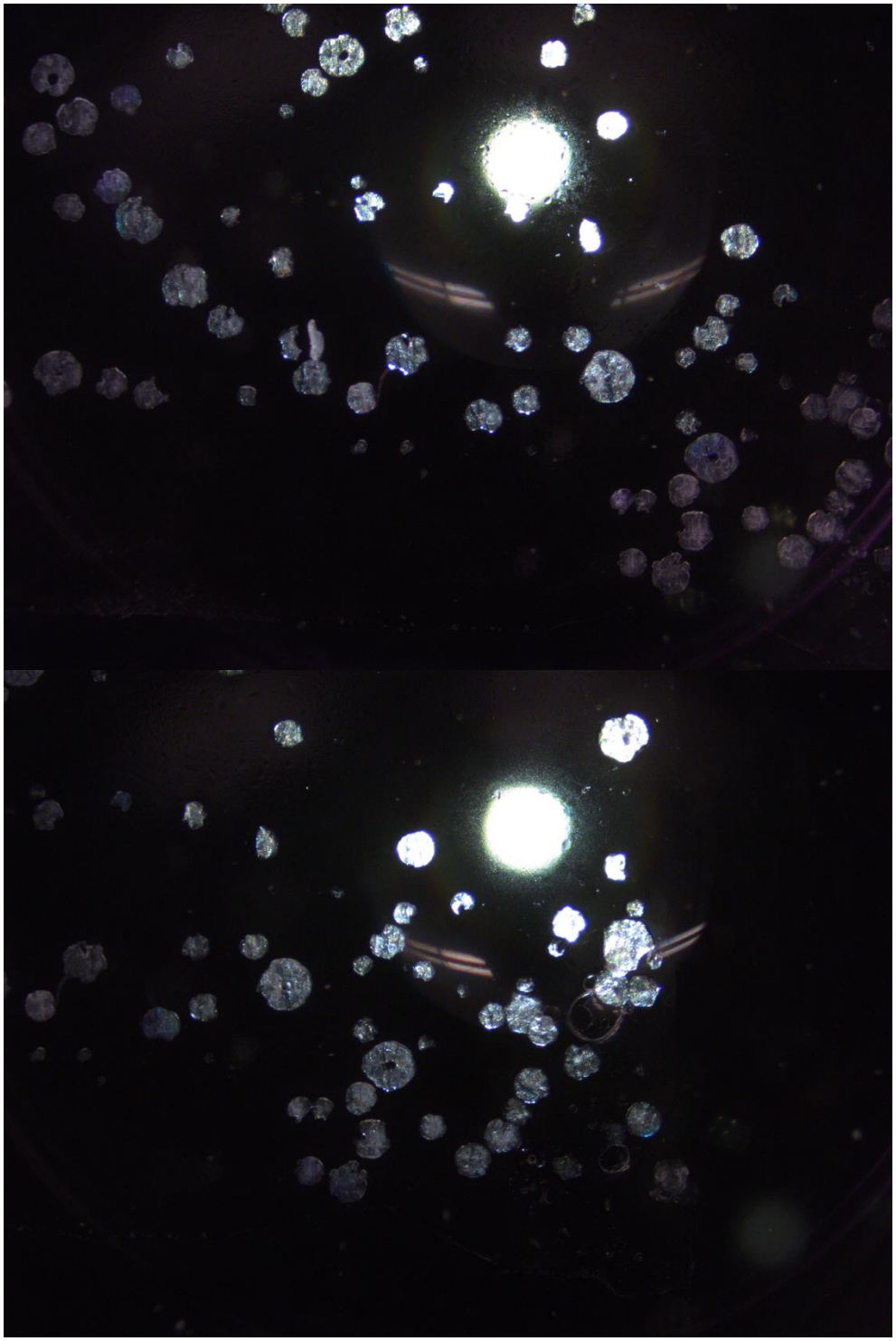

Appendix 12. Sections of 20% w/v PMMA:PCL = 1:9 at 4x magnification with polarized light

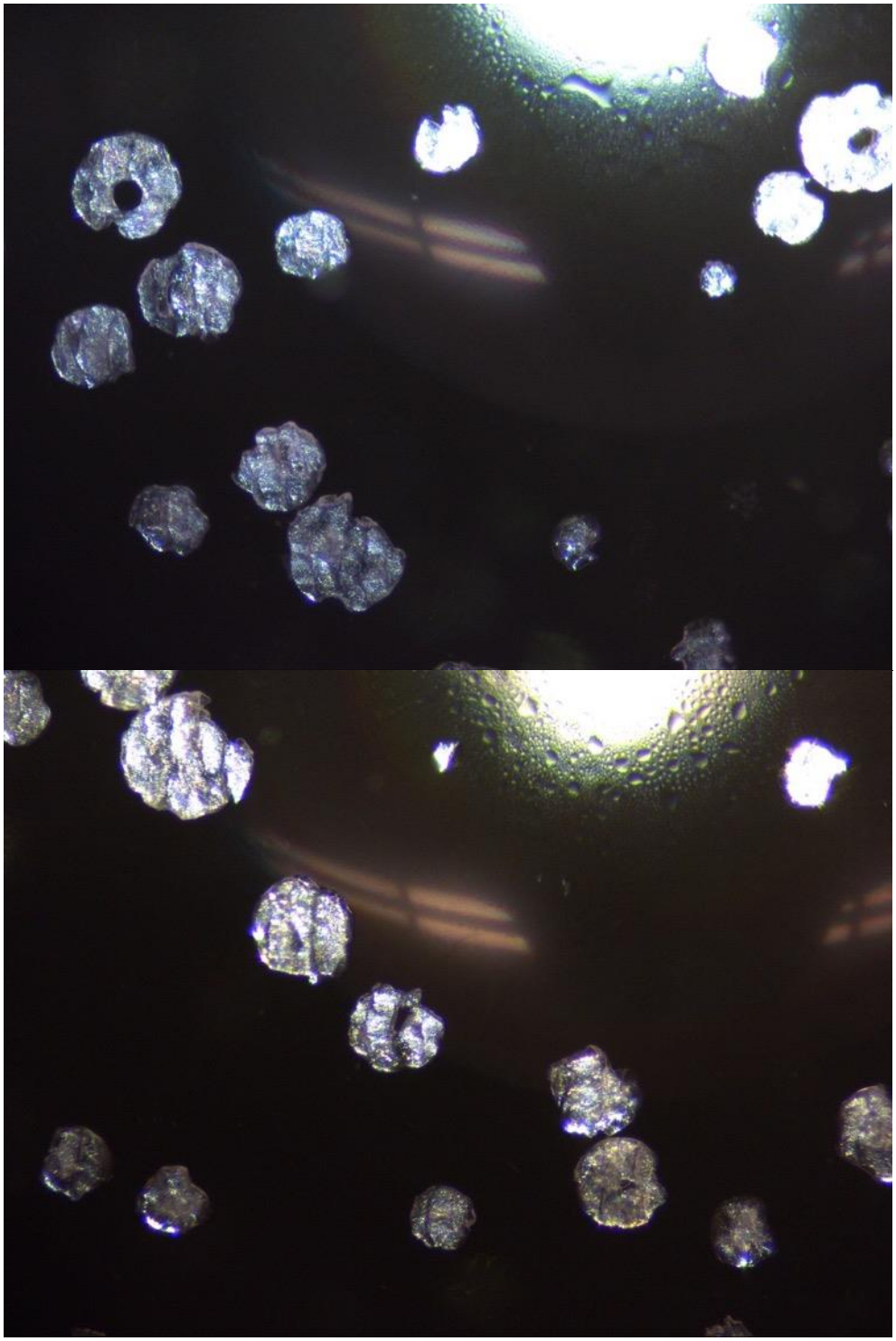

Appendix 12. Sections of 20% w/v PMMA:PCL = 1:9 at 10x magnification with polarized light

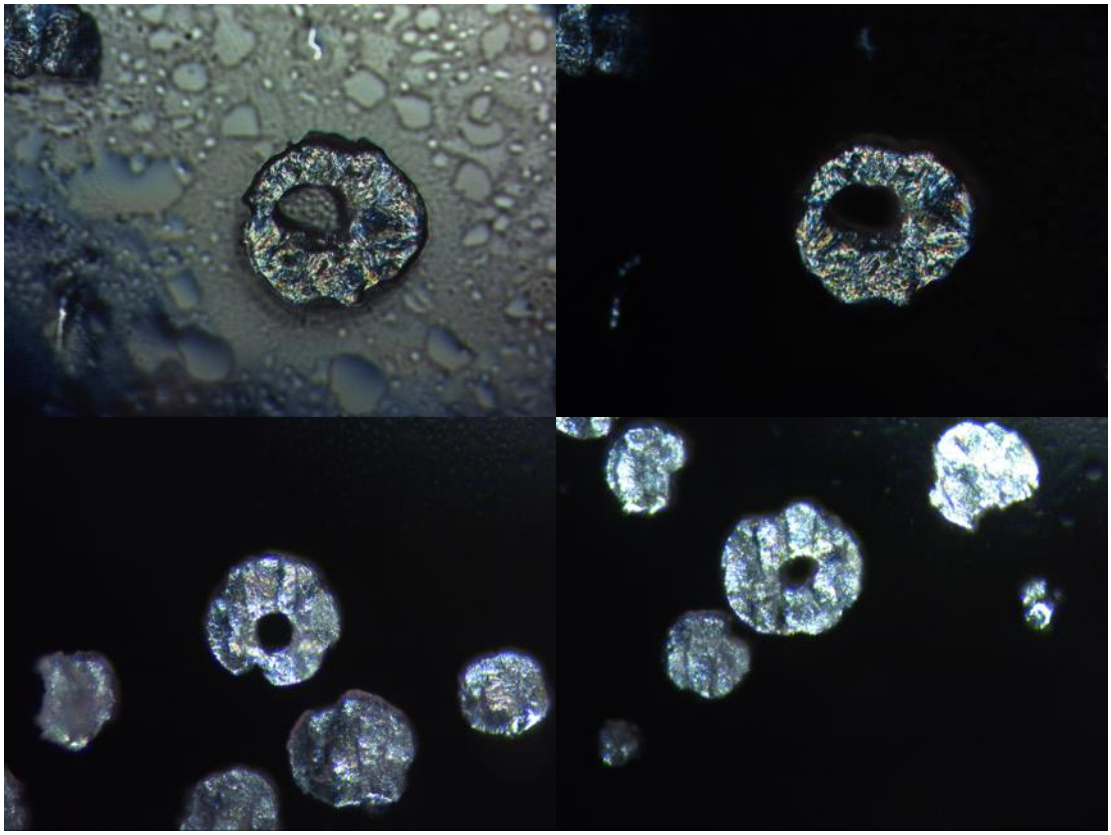

Appendix 13. Sections of 20% w/v PMMA:PCL = 1:9 at 20x manification with polarized light

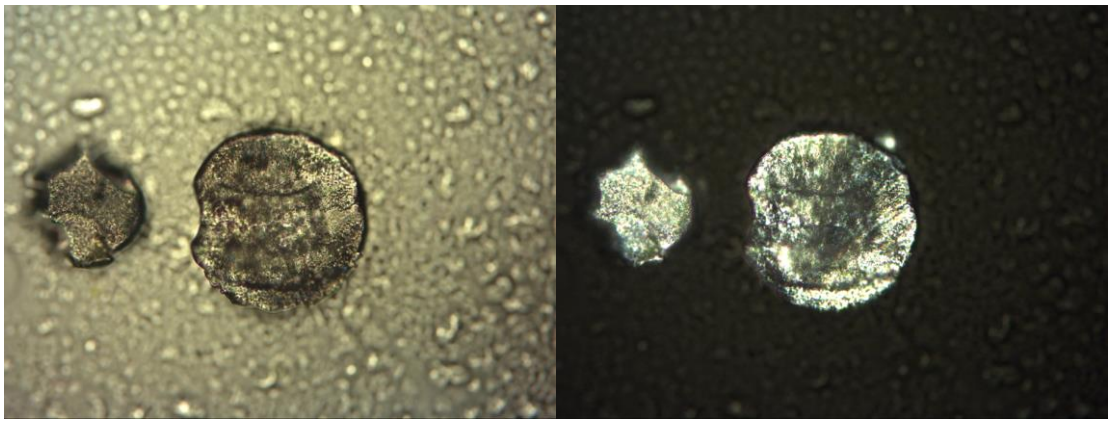

Appendix 14. Spherulites observed on sections of microspheres of 20% w/v PMMA:PCL = 3:7 (top) without and (bottom) with polarized light at 40x magnification.

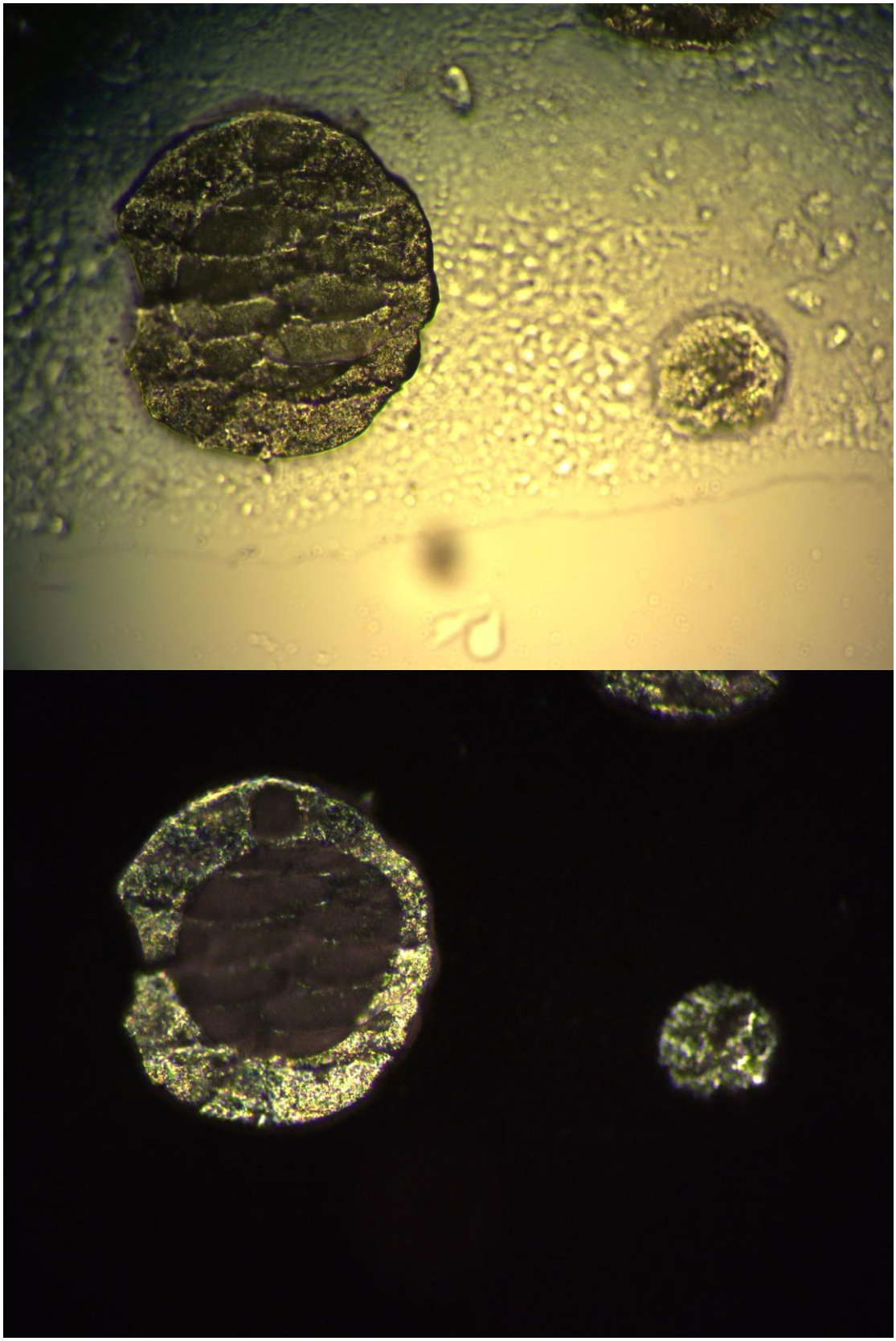

Appendix 15. Inhomogeneous composition of each layers of 20% w/v PMMA:PCL = 1:1 microspheres (top) without and (bottom) with polarized light at 40x magnification.

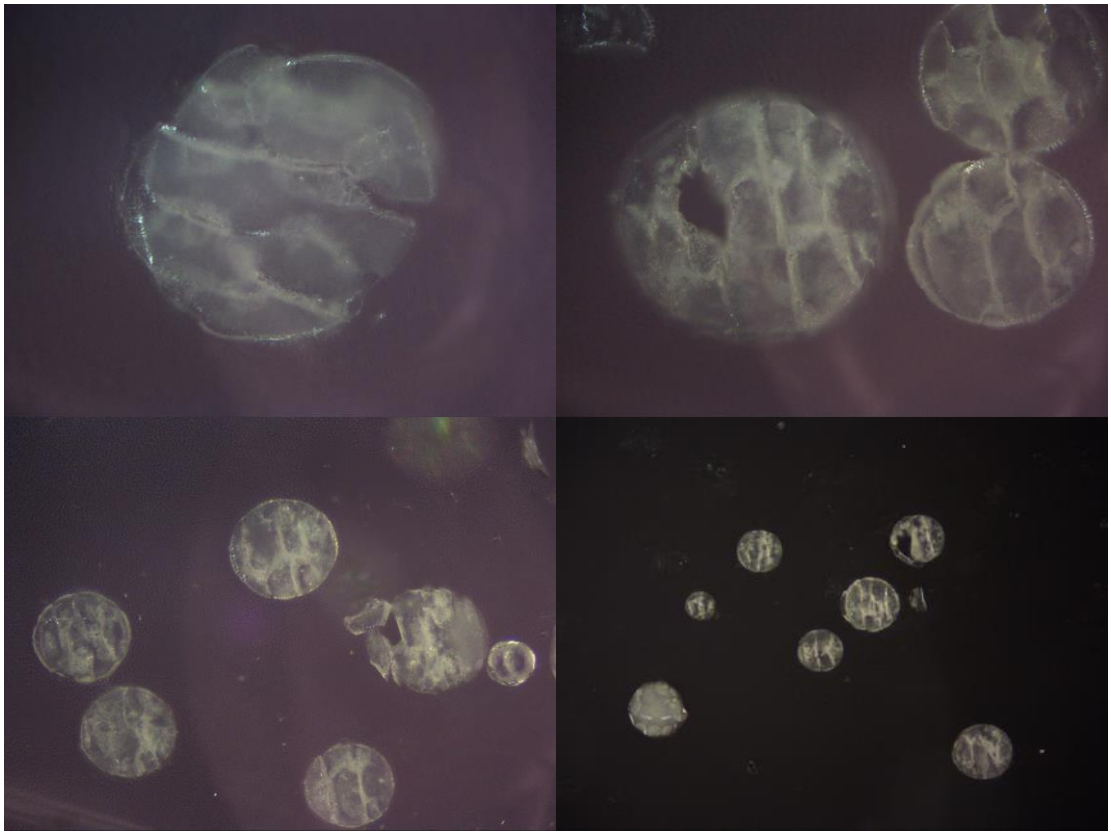

Appendix 16. Homogenous distribution of morphology of 20% w/v PMMA:PCL = 7:3 microspheres with polarized light at different magnifications.

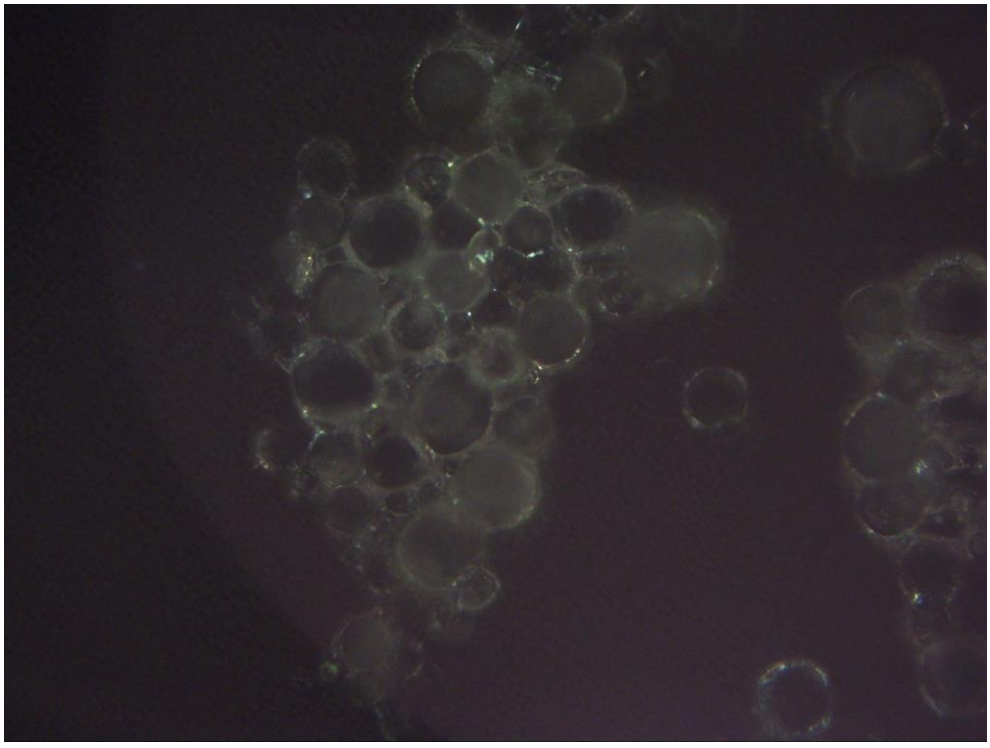

Appendix 17. Sections of microspheres of 5% w/v PMMA:PCL = 9:1 with polarized light at 40x magnification